

DUST STORMS IN THE EASTERN GREAT BASIN
OF UTAH, U.S.A.

by

Maura Hahnenberger

A dissertation submitted to the faculty of
The University of Utah
in partial fulfillment of the degree of

Doctor of Philosophy

Department of Atmospheric Sciences

The University of Utah

May 2014

Copyright © Maura Hahnenberger 2014

All Rights Reserved

The University of Utah Graduate School

STATEMENT OF DISSERTATION APPROVAL

The dissertation of **Maura Hahnenberger**
has been approved by the following supervisory committee members:

<u>Kevin D. Perry</u>	, Chair	<u>4/25/2013</u> <small>Date Approved</small>
------------------------------	---------	---

<u>Thomas E. Gill</u>	, Member	<u>4/25/2013</u> <small>Date Approved</small>
------------------------------	----------	---

<u>Steven K. Krueger</u>	, Member	<u>4/25/2013</u> <small>Date Approved</small>
---------------------------------	----------	---

<u>Kathleen Nicoll</u>	, Member	<u>4/25/2013</u> <small>Date Approved</small>
-------------------------------	----------	---

<u>Courtenay Strong</u>	, Member	<u>4/25/2013</u> <small>Date Approved</small>
--------------------------------	----------	---

and by **Kevin D. Perry**, Chair of
the Department of **Atmospheric Sciences**

and by David B Kieda, Dean of The Graduate School.

ABSTRACT

This study provides a holistic view of dust storms and transport in the eastern Great Basin, and is the first to analyze the meteorological, source, and chemical characteristics of dust production in this region. First, the climatology of dust storm events affecting Salt Lake City, Utah (SLC) was assessed, and the controls on atmospheric dust generation and transport documented. Records indicate seasonal and diurnal patterns, with dust storms typically occurring in spring months during the afternoon. Since 1930, SLC had 379 dust event days (DEDs), averaging 4.7 per year, with elevated PM_{10} exceeding National Ambient Air Quality Standards (NAAQS) on 16 days since 1993, or 0.9 per year. Strengthening cyclonic systems are the primary producer of these dust storms.

Next anthropogenically disturbed areas and barren playa surfaces were identified as the primary dust source types contributing to dust storms in the region. Moderate Resolution Imaging Spectroradiometer (MODIS) satellite imagery during DEDs was analyzed to identify dust plumes, and assess the characteristics of dust source areas, which produce dust during the spring and fall and during drought. Most plumes originate from playas, classified as Barren land cover, with a silty clay soils; they often have anthropogenic disturbances, including military operations and water withdrawal. Disturbance is necessary to produce dust from vegetated landscapes in the region,

evidenced by the new dust source active from 2008-2010 in the 2007 Milford Flat Fire scar, which underwent postfire land treatments.

Finally, the elemental composition of dust in the region was characterized. Dust and surface soil samples were collected, resuspended, and analyzed with Synchrotron X-Ray Fluorescence (SXRF). Dust and soil from the eastern Great Basin are distinctly different, and identifiable. Within the dust and soil groups, however, large differences are not seen and individual samples cannot be identified by their elemental composition. Dust and soil from the eastern Great Basin tends to not be enriched in most major soil elements, excepting a large enrichment of Na in dust samples. Trace elements, however, show very large enrichment values for both dust and soil. The enrichment of dust samples has notable importance for ecosystem functioning and human health.

TABLE OF CONTENTS

ABSTRACT.....	iii
LIST OF TABLES.....	vii
ACKNOWLEDGEMENTS.....	viii
Chapter	
1 INTRODUCTION.....	1
1.1. Introduction: environmental problem and goal.....	1
1.2. Previous research.....	6
1.3. Summary.....	8
1.4. References.....	12
2 METEOROLOGICAL CHARACTERISTICS OF DUST STORM EVENTS IN THE EASTERN GREAT BASIN OF UTAH, U.S.A.....	17
2.1 Abstract.....	17
2.2. Introduction.....	18
2.3. Methods and materials.....	20
2.4. Results.....	23
2.5. Discussion	29
2.6. Conclusions.....	31
2.7. Acknowledgements.....	33
2.8. References.....	52
3 GEOMORPHIC AND LAND COVER IDENTIFICATION OF DUST SOURCES IN THE EASTERN GREAT BASIN OF UTAH, U.S.A.....	59
3.1 Abstract.....	59
3.2. Introduction.....	60
3.3. Regional setting of study area.....	65
3.4. Methods and datasets.....	69
3.5. Results.....	73

3.6. Discussion.....	80
3.7. Conclusions and implications.....	89
3.8. References.....	102
4 CHEMICAL COMPARISON OF DUST AND SOIL FROM THE SEVIER DRY LAKE, UT, USA	111
4.1 Abstract.....	111
4.2. Introduction.....	112
4.3. Methods and materials.....	114
4.4. Results.....	119
4.5. Discussion.....	120
4.6. Conclusions.....	123
4.7. References.....	132
5 CONCLUSIONS.....	135
APPENDIX: TABLE OF DUST SOURCE LOCATIONS.....	139

LIST OF TABLES

Table	Page
2.1. Meteorological data station information.....	34
2.2. Utah Air Monitoring Network station information.....	35
2.3. Summary of PM ₁₀ and PM _{2.5} data during DEDs.....	36
3.1. Meteorological and air quality station data.....	92
3.2. Air quality and wind data for all DEDs with analyzed plumes. Twenty four hour particulate matter (PM) values are reported in µg/m ³ , for both PM ₁₀ and PM _{2.5} . Winds are the maximum speed and direction recorded between the times of the Aqua and Terra satellite overpasses (1000-1500 MST), with wind speed reported in m/s. For station abbreviations, see Table 3.1.....	93
3.3. Observed plume regions. For geographic location of each region see Figure 3.2. Number and percent of plumes based off all plumes identified from 2004-2010 (n=168). Elevation ranges were estimated using Google Earth™. Geomorphic features were identified from MODIS satellite data, Google Earth™, and personal field experience. Land cover was identified using the National Land Cover Database 2006. Soil texture was identified using the NRCS Soil Survey Geographic (SSURGO) Database.....	94
4.1. Site information for dust and soil samples.....	124
4.2. Statistical results (p-values) from the Wilcoxon-Mann-Whitney rank-sum test for dust and soil samples. Results in bold indicate statistically significant result to the 5% confidence level (p<0.05). PM ₁₀ indicates particle sizes less than 10 µm. Coarse indicates particle sizes from 2.5 to 10 µm. Fine indicates particle sizes less than 2.5 µm.....	125

ACKNOWLEDGEMENTS

I would like to thank my advisor, Dr. Kevin D. Perry, for his support and encouragement throughout my academic career. Special thanks to Dr. Kathleen Nicoll for her engaging research collaborations and mentorship. I would like to acknowledge the support received from the Water, the Environment, Science and Teaching (WEST) and Think Globally, Learn Locally (TGLL) fellowship programs. Further, I would like to thank Dr. Holly Godsey for her leadership and positivity while in these programs. I would like to thank my friends and colleagues in the Department of Atmospheric Sciences for their never ending entertainment and stimulating conversation.

Finally, I would like to acknowledge my family for all they have done. I would like to thank my parents for their unending support and inspiration, Ben for his love and adventure, and Rosco for his joy of hiking and snuggling. Finally, I would like to thank my family for their help with field work that contained long drives, bumpy and treacherous roads, muddy clothes, endeavors into the middle of nowhere, some sheep, and, hopefully, quite a bit of fun.

CHAPTER 1

INTRODUCTION

1.1. Introduction: environmental problem and goal

1.1.1 Effects of dust

Dust transport from arid regions has a nonnegligible impact on the global climate, hydrological, biological, and human systems. On the local scale, dust transport into populated regions can lead to high levels of particulate matter, above internationally recommended levels, negatively impacting human health (e.g., Brunekreef and Forsberg, 2005; Ozer et al., 2006; Goudie, 2009). Dust can transport bacteria and fungi, as well as high levels of trace metals such as arsenic (As) and mercury (Hg) (Reheis et al., 2002; Carling et al., 2012). Dust storms have also been shown to be a risk factor for increased respiratory and cardiovascular complaints (Meng and Lu, 2007). Significant dust storms can reduce visibility, limiting ground and air transportation, and causing highway deaths in severe cases (e.g., Pauley et al., 1996). Dust deposition on seasonal snowpack has been shown to increase melt rates, cause an earlier “snow-free” date of up to a month, and cause earlier and higher peak streamflows (Painter et al., 2007; Painter et al., 2010) (Figure 1.1). This has a larger impact on regions which rely on seasonal snowpack for their main water supply, which are often arid regions with adjacent mountains, such as

the intermountain west.

1.1.2 Environmental problem

While some research has been done to identify general regions of dust transport, research is lacking in identification of specific dust sources that impact local areas in an acute way. Arid regions are becoming increasingly populated making the impact of dust transport more important moving into the future. In the western United States some research has been completed in the deserts of California and the Southern High Plains. However, little research is published on dust transport in Nevada and Utah, which are partly in the Great Basin Desert (Reheis et al., 2002; Lee et al., 2008). Utah, particularly, has its largest population center directly downwind of numerous dust source areas, namely, ephemeral terminal lakes known as playas, which are remnants of ancient Lake Bonneville (Figure 1.2).

Records since 1930 indicate that Salt Lake City, UT had 379 dust event days, an average of 4.7 per year (Hahnenberger and Nicoll, 2012). Air quality station data from the more populated regions of Utah, available since 1993, indicate that dust events have produced elevated PM_{10} , exceeding NAAQS, on 16 days over the past 18 years, or 0.9 per year. On most dust event days PM_{10} values were elevated above background levels indicating a potential health impact on residents, especially sensitive groups such as the elderly and children.

Looking into the future, the western U.S., including Utah, is expected to become warmer and drier due to climate change (Cook et al., 2009; Giles, 2005). Further, development, agriculture, grazing, renewable energy development, and recreational use

on these arid lands will also likely increase due to increased population. These activities will result in larger areas of disturbed soil, which is more prone to dust transport (Belnap and Gillette, 1998). Therefore, it is important to identify current dust sources impacting this region, and determine what management steps could be taken in the future to mitigate this problem if deemed necessary.

1.1.3 Goal of research

The overarching objective of this project is to determine the meteorological and physical characteristics of dust transport to the Salt Lake City Metropolitan area of Utah. The geochemistry, magnitude, and frequency of the flux of the dust leaving the source regions and depositing in the Wasatch Front have not been directly measured previously. Further, the impact of these dust storms on air quality in the Salt Lake City Metropolitan has not been previously quantified. This research is aimed at creating a tool for decision makers in this region to better understand dust transport in this area, how it impacts the populations of Utah, and what possibilities lie in the future for forecasting, control, and mitigation of this impact.

This study identifies the primary dust source regions and transport pathways that affect the Salt Lake City metropolitan area, and characterizes the meteorological conditions that lead to the entrainment and transport of dust in specific case studies. This detailed analysis of source areas and dust transport pathways is the first to demonstrate how the eastern Great Basin region produces a significant magnitude of dust that has measurable regional impacts. Identifying the synoptic conditions of dust transport in this region will assist in forecasting and monitoring these events, which pose concerns to a

large population of Utah residents.

Broader impacts of this research come on multiple scales. On the local spatial and short temporal scales, this research will aid in the forecasting and warning of these dust events, which allows citizens and municipalities to prepare and avoid the worst repercussions to health and transportation. Looking into the future, an understanding of how the dust flux varies under different climatic conditions can give us clues as to how this flux may change in the future, dependent on what climate regime changes are predicted for Utah from downscaled Global Circulation Models (GCMs). This change in future dust flux could have large impacts regionally, including changes in snowmelt rates and streamflows as well as human health impacts. This study will also analyze how disturbance events, such as wildfire, grazing, and water use, modulate dust flux, which can have implications for land management practices. Further, climatic and water use changes could impact levels of the Great Salt Lake (GSL), which could create a large new dust source that would impact the Wasatch Front. This could be of particular concern, as the sediments of the GSL have been shown to have large concentrations of methylated mercury (CH_3Hg) (Naftz et. al., 2008), which if lofted and transported with dust could have significant health impacts on the Wasatch Front and beyond.

1.1.4 Motivation

Numerous studies assessing regional and global production and transport of mineral dust have identified the semiarid eastern Great Basin region as a significant dust source in North America (e.g., Engelstaedter and Washington, 2007; Goudie, 1983, 2009; Prospero et al., 2002; Reheis, 2006). Dust transport modeling suggests that this source

region is globally important (e.g., Ginoux et al., 2001; Tanaka and Chiba, 2006; Woodward, 2001; Zender et al., 2003). However, dust storm events in the Great Basin have not been very well characterized. Recent concerns have escalated over how dust may influence the water supplies derived from snowpack (Painter et al., 2007; Painter et al., 2010) (Figure 1.1), human health effects (Derbyshire, 2007; Malek et al., 2006; Roberts and Martin, 2006; Hashizume et al., 2010), transport of bacteria and fungi (Griffin, 2007; Hallar et al., 2011), as well as the effects of haze and reduced visibility on transportation and crops (e.g., Brough et al., 1987). Despite its importance, limited research has been conducted to identify and describe the controls on dust mobilization and transport within the eastern Great Basin region.

Air quality and the health effects related to elevated airborne particulate matter levels (e.g., Pope III, 1991; Johnston et al., 2011; Sandstrom and Forsberg, 2008) are growing concerns in the Salt Lake City, UT metropolitan area (SLC), which is located on the eastern edge of the Great Basin physiographic province. SLC is currently one of the most densely populated urban corridors in the intermountain west (U.S. Census Bureau, 2010). In addition to dust produced within city limits, large amounts of particulate matter are contributed to the region via both natural processes (e.g., wind erosion) and human activities (e.g., disturbance events such as cultivation and fires, e.g., Neff et al., 2008). Thus far, only local-scale controls on aerosols in the Salt Lake Valley have been assessed (Alexandrova et al., 2003; Shaw, 2008), with emphasis on transportation and industrial produced aerosols at the urban scale (e.g., Hanna et al., 2003; Long et al., 2003; Princevac and Venkatram, 2007). The degree to which regional dust transport influences aerosol concentrations in SLC has not been studied. Therefore, it is important to

determine the synoptic and mesoscale controls on regional dust transport and the magnitude to which these events impact this population center.

1.2. Previous research

It has been established that three factors are necessary for effective regional dust transport (Goudie, 2009); in summary, these are (1) a source area of sufficient size containing deflatable particles, such as fine sediment or soil, that are available at the landscape surface; (2) low threshold friction velocities at the surface of the source region, which is enhanced by limited vegetation, low soil moisture, and/or an absence of physical or biological soil crusts; and (3) sufficient local and regional wind speeds to loft fine sediment particles to a sufficient atmospheric height, allowing transport at the regional to global scale.

1.2.1 Large source areas

Sources of dust affecting SLC, located on the eastern edge of the Great Basin physiographic province, are thought to include nearby desert surfaces, including ephemeral lakes known as playas. Playas are among the dominant sources of dust in the world; these are flat sediment filled valleys located in deserts, where strong wind gusts entrain the surface particles, dispersing sediments aloft into the air (Giles, 2005; Gill, 1996; Goudie, 1983, 2009; Pelletier and Cook, 2005; Reheis, 2006; Reynolds et al., 2007). The Great Basin region is well known for its playas characteristically present in the Basin and Range landscape. In addition, ancient paleolakes such as Lake Bonneville and its modern remnant, the Great Salt Lake (Grayson, 2011) have deposited fine

deflatable sediments across a vast area spanning three states (Nevada, Utah, Idaho).

1.2.2 Low threshold friction velocities

It has become apparent that deserts are not homogeneous dust sources (Prospero et al., 2002). Dust tends to be emitted from specific source regions, or *hot spots*, within deserts, which may include agricultural lands, dry watercourses, and playas (e.g., Gillette, 1999; Washington et al., 2006; Engelstaedter and Washington, 2007; Lee et al., 2008). The Great Basin is a vegetation limited region with low surface roughness and many playas and dry sediments available as a continuous supply of deflatable soil (Gill, 1996; Grayson, 2011).

1.2.3 High local and regional wind speeds

The third factor in regional dust transport is sufficient regional wind speeds. Jewell and Nicoll (2011) have documented the wind regimes of the Great Basin, and their effective aeolian transport of sand sized particles. In the drylands of southwestern North America, the most persistent episodes of high winds and blowing dust occur with the presence of a strengthening low pressure system over a dust source area (Brandli et al., 1977; Sheppard et al., 2002; Novlan et al., 2007). In this pattern, a strengthening pressure gradient (cyclogenesis) in the prefrontal atmosphere creates strong and persistent south and southwesterly winds (in the northern hemisphere).

The eastern Great Basin region is well known for strong prefrontal south and southwesterly winds. These characteristic winds have even been named “Hatu winds,” “Utah” spelled backwards (Eubank and Brough, 1979). Hatu winds are recognized to

occur many times each year in the western valleys of Utah, and are typically associated with approaching cold fronts and deepening cyclonic systems. Hatu winds have been observed to be as strong as 93 mph (42 m s^{-1}) (Brough and Stevens, 1989). An association of “Hatu winds” with dust storm events was noticed as early as 1910 (Brough et al., 1987). These dust events are reported most frequently during the months of March and April. Therefore, it is clear that the Great Basin region has the third ingredient for dust transport, namely, strong regional scale winds.

1.3. Summary

This research project aims to quantitatively determine the meteorological controls, sources, and composition of dust to the Wasatch Front, UT. Dust storms in this region can be a significant impact to human health, visibility, transportation, chemical inputs to ecosystems, and changing rates of snowmelt in mountainous regions. The Wasatch Front is predicted to continue to increase in population in future years putting increasing stress on current and future water supply. This study aims to determine the causes of significant dust transport to the Wasatch Front region. The project will use unique instrumentation and analytical techniques to create a full picture of the dust transport complex in the eastern Great Basin. The unique methodology and experimental design will help gain new knowledge about dust transport to the Wasatch Front and Wasatch Mountains which will be applicable to interdisciplinary research studies in areas from forest ecology to hydrology to epidemiology.

The following chapter will analyze first, the meteorological controls on dust transport in the region, and its impacts on air quality; second, the characteristics of dust

sources and how they may change in response to disturbance and local hydroclimatic variability; and third, the chemical composition of dust and soil samples from a characteristic source area in the eastern Great Basin region. This project is the first detailed and multidisciplinary analysis of dust transport in this region.



Figure 1.1: Example of dust on snow reducing albedo in the San Juan Mountains of Colorado.



Figure 1.2: Photo looking SE from the House Range of west-central Utah, viewing dust entrainment at the north end of the Sevier Dry Lake on 22 August 2010.

1.4 References

- Alexandrova, O.A., Boyer, D.L., James, R., Anderson, J.R., Fernando, H.J.S., 2003. The influence of thermally driven circulation on PM₁₀ concentration in the Salt Lake Valley Atmospheric Environment, 37, 421–437.
- Belnap, J., Gillette, D.A., 1998. Vulnerability of desert biological soil crusts to wind erosion: the influences of crust development, soil texture, and disturbance. *Journal of Arid Environments*, 39, 133-142. doi: [10.1006/jare.1998.0388](https://doi.org/10.1006/jare.1998.0388)
- Brandli, H.W., Ashman, J.P., Reinke, D.L., 1977. Pictures of the month; Texas dust moves into Florida. *Monthly Weather Review*, 105, 1068-1070.
- Brough, R.C. Stevens, D.J., 1989. Utah's High Winds: Intensities, Frequencies and Distribution. KTVX Weather Department, Salt Lake City, UT.
- Brough, R.C., Jones, D.L., Stevens, D.J., 1987. Utah's Comprehensive Weather Almanac. Publishers Press, Salt Lake City, UT.
- Brunekreef, B., Forsberg, B., 2005. Epidemiological evidence of effects of coarse airborne particles on health. *European Respiratory Journal*, 26, 309-318.
- Carling, G.T., Fernandex, D.P, Johnson, W.P., 2012. Dust-mediated loading of trace and major elements to Wasatch Mountain snowpack. *Science of the Total Environment*, 432, 65-77. doi: [10.1016/j.scitotenv.2012.05.077](https://doi.org/10.1016/j.scitotenv.2012.05.077)
- Cook, B.I., R.L. Miller, Seager, R., 2009. Amplification of the North American “Dust Bowl” drought through human-induced land degradation. *Proceeding of the National Academy of Science USA*, 106, 4997-5001.
- Derbyshire, E., 2007. Natural minerogenic dust and human health. *AMBIO*, 36, 73-77.
- Engelstaedter, S., Washington, R., 2007. Temporal controls on global dust emissions: the role of surface gustiness. *Geophysical Research Letters*, 34, L15805.
- Eubank, M.E., Brough, R.C., 1979. Mark Eubank's Utah Weather. Horizon Publishers & Distributors, Bountiful, UT.
- Giles, J., 2005. Climate science: the dustiest place on earth. *Nature*, 434, 816–819.
- Gill, T. E. 1996. Eolian sediments generated by anthropogenic disturbance of playas: human impacts on the geomorphic system and geomorphic impacts on the human system. *Geomorphology*, 17, 207-228. doi: [10.1016/0169-555X\(95\)00104-D](https://doi.org/10.1016/0169-555X(95)00104-D).
- Gillette, D.A., 1999. A qualitative geophysical explanation for “hot spot” dust emitting source regions. *Contributions to Atmospheric Physics*, 72, 67-77.

Ginoux, P., M. Chin, I. Tegen, J. M. Prospero, B. Holben, O. Dubovik, Lin, S.-J., 2001. Sources and distributions of dust aerosols simulated with the GOCART model *Journal of Geophysical Research*, 106, 20255–20273. doi:[10.1029/2000JD000053](https://doi.org/10.1029/2000JD000053).

Goudie, A.S., 1983. Dust storms in space and time. *Physical Geography*, 7, 502-530.

Goudie, A.S., 2009. Dust storms: recent developments. *Journal of Environmental Management*, 90, 89-94.

Grayson, D.K., 2011. *The Great Basin: A Natural Prehistory*. University of California Press: Berkeley CA, 418p.

Griffin, D.W., 2007. Atmospheric movement of microorganisms in clouds of desert dust and implications for human health. *Clinical Microbiology Reviews*, 20, 459-477. doi:[10.1128/CMR.00039-06](https://doi.org/10.1128/CMR.00039-06)

Hahnenberger, M. and K. Nicoll, 2012. Meteorological characteristics of dust transport events in the Eastern Great Basin of Utah, U.S.A. *Atmospheric Environment*, 60, 601-612. doi: [10.1016/j.atmosenv.2012.06.029](https://doi.org/10.1016/j.atmosenv.2012.06.029)

Hallar, A.G., Chirokova, G., McCubbin, I., Painter, T.H., Wiedinmyer, C., Dodson, C., 2011. Atmospheric bioaerosols transported via dust storms in the western United States. *Geophysical Research Letters*, 38, L17801. doi:[10.1029/2011GL048166](https://doi.org/10.1029/2011GL048166)

Hanna, S.R., Britter, R., Franzese, P., 2003. A baseline urban dispersion model evaluated with Salt Lake City and Los Angeles tracer data. *Atmospheric Environment*, 37, 5069–5082.

Hashizume, M., Ueda, K., Nishiwaki, Y., Michikawa, T., Onozuka, D., 2010. Health effects of Asian dust events: a review of the literature. *Japan Journal Hygiene*, 65, 413-421.

Jewell, P.W., Nicoll, K., 2011. Wind regimes and aeolian transport in the Great Basin, U.S.A. *Geomorphology*, 129, 1-13. doi:[10.1016/j.geomorph.2011.01.005](https://doi.org/10.1016/j.geomorph.2011.01.005)

Johnston, F., Hanigan, I., Henderson, S., Morgan, G., Bowman, D., 2011. Extreme air pollution events from brushfires and dust storms and their association with mortality in Sydney, Australia 1994-2007. *Environmental Research*, 111, 811-816. doi:[10.1016/j.envres.2011.05.007](https://doi.org/10.1016/j.envres.2011.05.007)

Lee, J.A., Gill, T.E., Mulligan, K.R., Dominguez Acosta, M., Perez, A.E., 2008. Land use/land cover and point sources of the 15 December 2003 dust storm in southwestern North America. *Geomorphology*, 105, 18-27.

Long, R.W., N. L., Mangelson, N.F., Thompson, W. Fiet, K., Smith, S., Smith, R., Eatough, D.J., Pope, C.A., Wilson, W.E., 2003. The measurement of PM_{2.5}, including

semi-volatile components, in the EMPACT program: results from the Salt Lake City Study. *Atmospheric Environment*, 37, 4407–4417.

Malek, E., Davis, T., Martin, R.S., Silva, P.J., 2006. Meteorological and environmental aspects of one of the worst national air pollution episodes (January, 2004) in Logan, Cache Valley, Utah, USA. *Atmospheric Research*, 79, 108-122.

Meng, Z., Lu, B., 2007. Dust events as a risk factor for daily hospitalization for respiratory and cardiovascular diseases in Minqin, China. *Atmospheric Environment*, 41, 7048-7058.

Naftz, D., C. Angereth, T. Kenney, B. Waddell, N. Darnall, S. Silva, C. Perschon, Whitehead, J., 2008. Anthropogenic influences on the input and biogeochemical cycling of nutrients and mercury in Great Salt Lake, Utah, USA. *Applied Geochemistry*, 23, 1731-1744. doi:10.1016/j.apgeochem.2008.03.002

Neff, J.C., A.P. Ballantyne, G.L. Farmer, N.M. Mahowald, J.L. Conroy, C.C. Landry, J.T. Overpeck, T.H. Painter, C.R. Lawrence, Reynolds, R.L., 2008. Increasing eolian dust deposition in the western United States linked to human activity. *Nature Geosciences*, 1, 189-195.

Novlan, D.J., Hardiman, M., Gill, T.E., 2007. A synoptic climatology of blowing dust events in El Paso, Texas from 1932-2005. Preprints, 16th Conference on Applied Climatology, American Meteorological Society, no. J3.12.

Ozer, P., M.B.O.M Laghdaf, S.O.M. Lemine, Gassani, J., 2006. Estimation of air quality degradation due to Saharan dust at Nouakchott, Mauritania, from horizontal visibility data. *Water, Air, and Soil Pollution*, 178, 79-87.

Painter, T.H., A.P. Barrett, C.C. Landry, J.C. Neff, M.P. Cassidy, C.R. Lawrence, K.E. McBride, Farmer, G.L., 2007. Impact of disturbed desert soils on duration of mountain snow cover. *Geophysical Research Letters*, 34, L12502. doi:10.1029/2007GL030284

Painter, T.H., J.S. Deems, J. Belnap, A.F. Hamlet, C.C. Landry, Udall, B., 2010. Response of Colorado River runoff to dust radiative forcing in snow. *Proceedings of the National Academy of Sciences*, 107, 17125-17130. doi:10.1073/pnas.0913139107

Pauley, P.M., N.L. Baker, Barker, E.H., 1996. An observational study of the Interstate 5 dust storm case. *Bulletin of the American Meteorological Society*, 77, 693-720.

Pelletier, J.D. Cook, J.P., 2005. Deposition of playa windblown dust over geologic time scales. *Geology*, 33: 909–912.

Pope III, C.A., 1991. Respiratory hospital admissions associated with PM10 pollution in Utah, Salt Lake, and Cache Valleys. *Archives of Environmental Health*, 46, 90–97.

Princevac, M., Venkatram, A. 2007. Estimating micrometeorological inputs for modeling dispersion in urban areas during stable conditions. *Atmospheric Environment*, 41, 5345–5356.

Prospero, J.M., P. Ginoux, O. Torres, S.E. Nicholson, Gill, T.E., 2002. Environmental characterization of global sources of atmospheric soil dust identified with the Nimbus 7 Total Ozone Mapping Spectrometer (TOMS) absorbing aerosol product. *Reviews of Geophysics*, 40, 1002. doi:10.1029/2000RG000095

Reheis, M.C., 2006. A 16-year record of eolian dust in Southern Nevada and California, USA: Controls on dust generation and accumulation. *Journal of Arid Environments*, 67, 487-520.

Reheis, M.C., Budahn, J.R., Lamothe, P.J., 2002. Geochemical evidence for a diversity of dust sources in the southwestern United States. *Geochim. Cosmochim. Acta*, 66, 1569-1587.

Reynolds, R.L., Yount, J.C., Reheis, M., Goldstein, H., Chaves Jr., P., Fulton, R., Whitney, J., Fuller, C., Forester, R.M., 2007. Dust emission from wet and dry playas in the Mojave Desert, USA. *Earth Surface Processes and Landforms*, 32, 1811-1827.

Roberts, S., Martin, M.A., 2006. Investigating the mixture of air pollutants associated with adverse health outcomes. *Atmospheric Environment*, 40, 984–991.

Sandstrom, T., Forsber, B., 2008. Desert dust, an unrecognized source of dangerous air pollution? *Epidemiology*, 19, 808-809.

Shaw, P., 2008. Application of aerosol speciation data as an in situ dust proxy for validation of the Dust Regional Atmospheric Model (DREAM). *Atmospheric Environment*, 42, 7304–7309. [doi:10.1016/j.atmosenv.2008.06.018](https://doi.org/10.1016/j.atmosenv.2008.06.018)

Sheppard, P.R., Comrie, A.C., Packin, G.D., Angersbach, K., Hughes, M.K., 2002. The climate of the US Southwest. *Climate Research*, 21, 219-238.

Tanaka, T.Y., Chiba, M., 2006. A numerical study of the contributions of dust source regions to the global dust budget. *Global Planetary Change*, 52, 88-104.

U.S. Census Bureau, 2010. State and County QuickFacts.
<http://quickfacts.census.gov/qfd/states/49/49035.html>

Washington, R., Todd, M.C., Lizcano, G., Tegen, I., Flamant, C., Koren, I., Ginoux, P., Engelstaedter, S., Bristow, C.S., Zender, C.S., Goudie, A.S., Warren, A., Prospero, J.M., 2006. Links between topography, wind, deflation, lakes and dust: the case of the Bodele Depression, Chad. *Geophysical Research Letters*, 3, L09401.
[doi:10.1029/2006GL025827](https://doi.org/10.1029/2006GL025827)

Woodward, S., 2001. Modeling the atmospheric life cycle and radiative impact of mineral dust in the Hadley Centre climate model. *Journal of Geophysical Research Atmospheres*, 106, 18,155-18,166.

Zender, C.S., Bian, H., Newman, D., 2003. Mineral dust entrainment and deposition (DEAD) model: description and 1990s dust climatology. *Journal of Geophysical Research*, 108, 4416. doi:[10.1029/2002JD002775](https://doi.org/10.1029/2002JD002775)

CHAPTER 2

METEOROLOGICAL CHARACTERISTICS OF DUST STORM
EVENTS IN THE EASTERN GREAT BASIN OF
UTAH, U.S.A.¹

2.1 Abstract

This study assessed the mesoscale climatology of dust storm events affecting Salt Lake City, Utah (SLC) since the 1930s, and document the ascendant controls on atmospheric dust generation and transport in the semiarid Great Basin. Records indicate a seasonal and diurnal pattern, with dust storms typically occurring in spring months during the afternoon. Since 1930, SLC had 379 dust event days (DEDs), averaging 4.7 per year. Air quality station data from populated regions in Utah indicate that dust events produced elevated PM₁₀ exceeding NAAQS on 16 days since 1993, or 0.9 per year. Analysis of DEDs over the period 1948-2010 (n=331) indicates that approaching midlevel troughs caused 68% of these dust outbreaks and storms. We analyzed two significant DEDs occurring on 19 April 2008 and 4 March 2009, both of which produced elevated particulate matter (PM) levels in the populated region surrounding SLC.

¹ Reprinted from Atmospheric Environment, 60, Hahnenberger, M., Nicoll, K., Meteorological characteristics of dust transport events in the eastern Great Basin of Utah, U.S.A., 601-612, Copyright (2012), with permission from Elsevier.

Strengthening cyclonic systems are the primary producer of dust outbreaks and storms; the Great Basin Confluence Zone (GBCZ) in the lee of the Sierra Nevada is a known region of cyclogenesis. These cyclonic systems produce strong southwesterly winds in the eastern Great Basin of Utah, termed “Hatu winds,” that exceed threshold friction velocities, entrain sediments and loft them into the atmosphere. Plumes identified in MODIS satellite imagery on case study DEDs indicate specific dust source areas, not widespread sediment mobilization. These “hotspots” include playa surfaces at Sevier Dry Lake, Tule Dry Lake, and the Great Salt Lake Desert, as well as Milford Flat, an area burned by Utah’s largest wildfire in 2007. The characteristic mountain-valley topography in the Basin and Range physiographic province creates terrain channeling that enhances deflation and funnels dust bearing winds toward SLC, a growing urban center.

2.2. Introduction

Modeling and satellite observations suggest that the western U.S.A. is a significant dust contributor to the global budget (e.g., Ginoux et al., 2001; Woodward, 2001; Zender et al., 2003; Tanaka and Chiba, 2006). Although numerous studies state that North American deserts export mineral dusts (e.g., Reynolds et al., 2007; Engelstaedter and Washington, 2007; Goudie, 1983, 2009; Prospero et al., 2002; Reheis, 2003, 2006), dust dynamics in the Great Basin region are not well characterized. Recent publications about dust address snowpack and subsequent water supplies (Painter et al., 2007, 2010), air quality and human health (Derbyshire, 2007; Malek et al., 2006; Roberts and Martin, 2006; Hashizume et al., 2010), microbial transport (Griffin, 2007; Hallar et al., 2011), and increases in haze and impaired visibility (e.g., Brough et al., 1987). However, there is

only limited research about dust sources and aeolian transport within the eastern Great Basin (Jewell and Nicoll, 2011).

Air quality and health effects related to elevated airborne particulate matter levels (e.g., Pope, 1991; Sandstrom and Forsberg, 2008; Johnston et al., 2011) are growing concerns in the Salt Lake City, UT metropolitan area (hereafter abbreviated SLC), which is located in the eastern Great Basin (Figure 2.1). SLC is a densely populated area (U.S. Census Bureau, 2010) that is affected by dust storms (Figure 2.2), which mobilize particulate matter (hereafter, PM) derived from natural processes (e.g., deflation erosion; Gill and Cahill, 1992; Gill, 1996) and human activities (e.g., cultivation and disturbance events such as fires; Neff et al., 2008). Local scale controls on aerosols have been assessed in SLC (Alexandrova et al., 2003; Shaw, 2008), with emphasis on transportation and industrial PM at the urban scale (e.g., Hanna et al., 2003; Long et al., 2003; Princevac and Venkatram, 2007). The degree to which dust storms influence SLC aerosol concentrations has not been documented.

We characterize related regional meteorological conditions and identify controls on dust entrainment from primary source regions and transport pathways of dust events affecting SLC. We analyze two dust event days (hereafter, DEDs) to describe the magnitude of PM pollution in SLC, and relate storm development and dust mobilization from source areas. Our analysis is the first to describe the synoptic and mesoscale meteorology leading to regional dust transport in the eastern Great Basin. These analyses assist forecasting and monitoring of dust events that impact a large population in Utah.

2.3. Methods and materials

We assessed meteorological datasets from 1930-2011 for Delta, UT (1973-2011) and SLC International Airport, UT (hereafter, SLC-IA) from the National Climatic Data Center (NCDC) Global Integrated Surface Hourly (ISH) database (NCDC, 2011) (Table 2.1). The ISH database includes worldwide surface weather observations from ~20,000 stations, collected and stored by sources including the Automated Weather Network (AWN), Global Telecommunications System (GTS), and Automated Surface Observing System (ASOS). Meteorological data and surface observations were obtained from MesoWest, a collection of independently operated mesonets across the western U.S.A. MesoWest is managed jointly by the NOAA Cooperative Institute for Regional Prediction at the University of Utah and the SLC National Weather Service Forecast Office (Horel et al., 2002).

We designated a DED when at least one recorded observation at Delta or SLC-IA stations contained a weather code for airborne dust (06, 07, 08, 09, 30, 31, 32, 33, 34, and 35; WMO code 4677, WMO 2010). Records may not be complete because dust events are not automatically recorded and require a human observer to enter codes. Delta station is sporadically staffed, and it is impossible to recognize nonevents (i.e., a dust free day) from days/times when staff was simply not present onsite. Furthermore, airborne dust may be misidentified as haze. Since dust events may not be recognized or reported accurately, and depend on personnel, weather station records underestimate dust frequency, especially for less severe events. Despite these limitations, however, recorded weather codes remain the best datasets available.

We analyzed air quality data monitored by the Division of Air Quality (DAQ) of

Utah's Department of Environmental Quality (DEQ) network (DAQ, 2011) (Table 2.2). Instruments measuring criteria pollutants are U.S. Environmental Protection Agency (EPA) reference or equivalent instruments in compliance with 40 CFR Part 58, Appendix C. We compiled daily average values for PM_{10} and $PM_{2.5}$ (PM with aerodynamic diameters <10 and $2.5 \mu m$, respectively) collected by manual gravimetric samplers at stations in some of Utah's most populated areas.

We assessed air quality parameters PM_{10} and $PM_{2.5}$, which are “criteria” pollutants regulated by the EPA according to the National Ambient Air Quality Standards (NAAQS) in the Clean Air Act as amended in 1990 (EPA, 2011). Primary NAAQS standards set air pollution limits to protect public health, while secondary standards set limits for public welfare. For PM_{10} and $PM_{2.5}$, primary and secondary standards are the same. The NAAQS for PM_{10} is $150 \mu g m^{-3}$ and for $PM_{2.5}$ is $35 \mu g m^{-3}$ averaged over a 24-hour period. $PM_{2.5}$ must meet an annual average standard of $15.0 \mu g m^{-3}$. We evaluated air quality data during DEDs to develop comparisons with these 24-hour standards, considering that dust storms typically occur over short time scales (i.e., less than a day), and additional factors might contribute to annual pollutant averages.

Next, we obtained weather maps for DEDs to characterize the largescale synoptic meteorology using the NCEP/NCAR (National Center for Environmental Prediction/National Center for Atmospheric Research) reanalysis (Kalnay et al., 1996). This dataset has global coverage and a long period of record (1948-present). Daily 700 mb geopotential height maps were constructed for each of the 331 DEDs from 1948-2010. Each day was classified into five synoptic settings and by season to evaluate the dominant conditions: approaching trough, ridge over the region, trough over the region,

exiting trough, and zonal flow. Daily data composites of multiple meteorological variables were created using all DEDs identified. To relate dust mobilization and transport with the progression of synoptic systems, composites were created for days prior to, and after DEDs.

For defined DEDs, we analyzed MODIS (Moderate Resolution Imaging Spectroradiometer) imagery from the NASA Terra satellite. MODIS passes over Utah in the afternoon, which coincides with the maximum boundary layer depth and dust production. We assessed cloud free MODIS images to identify dust source areas or “hotspots,” and to assess dust plume characteristics including cardinal direction, extent and spread (e.g., Baddock et al., 2009; Ginoux et al., 2010). We selected two recent DEDs as case studies to correlate synoptic, mesoscale, and local factors of dust transport. Dates were chosen based on four criteria. First, a dust observation was recorded at either Delta or SLC-IA, and that day was designated a DED. Second, the dust event occurred after the year 2000, when MODIS began collecting data. Third, available MODIS RGB imagery was mainly cloud free and we could recognize ground features and identify dust plumes. Finally, elevated $PM_{2.5}$ or PM_{10} values were recorded at one or more of the Utah DAQ air quality measurement sites. The days 19 April 2008 and 4 March 2009 met all these criteria.

For these DED case studies, we applied the NOAA (National Oceanic and Atmospheric Administration) HYSPLIT (Hybrid Single-Particle Lagrangian Integrated Trajectory) Model version 4.9 to calculate back trajectories and dynamic patterns governing air mass transport (Draxler and Hess, 2004). Calculated air parcel trajectories for these DEDs identified dust transport pathways (e.g., Katragkou et al., 2009; Rivera

Rivera et al., 2009; McGowan and Clark, 2008). HYSPLIT version 4.9 was run using NAM (North American Mesoscale) 12 km model meteorological data (Rogers et al., 2009). Backward trajectories were run for the two DEDs on READY (Real-time Environmental Applications and Display sYstem) provided by the NOAA ARL (Air Resources Laboratory) (NOAA, 2011). Trajectories started in SLC, UT at 1200 MST (1900 UTC) on 19 April 2008 and 4 March 2009, at heights of 100, 500, and 1000 meters above ground level (AGL). Backward trajectories were run for 12 hours, with vertical motion calculated using NAM12 model vertical velocity.

2.4. Results

2.4.1 Temporal and seasonal distribution of all DEDs

Delta station reported 80 DEDs during the period from 1973-2011, ~2 events per year. SLC-IA reported 379 DEDs from 1930-2011, or 4.7 events per year. The greater number of DEDs at SLC-IA may reflect more daily observations due to rigorous recordkeeping at this staffed station.

Over an annual basis, DEDs are not equally distributed (Figure 2.3). At Delta, there is a bimodal distribution within a year; a strong primary peak occurs during the spring months of March-April, and a secondary peak occurs during August-September. The climatology of strong fronts and cyclones occurring in the Great Basin region also shows this bimodal pattern, related to the seasonality of strong baroclinicity (Jeglum et al., 2010; Shafer and Steenburgh, 2008). The SLC-IA records from 1930-2011 shows a similar bimodal distribution of DEDs. Dust observations show a diurnal distribution, with a peak in the afternoon and early evening (Figure 2.4); this coincides with maximum

daily wind speeds due to the expansion of the boundary layer and turbulent mixing. Evening dust observations at SLC-IA reflect a temporal lag, as dust is transported northward from source regions in central Utah.

2.4.2 Pollution measurements during all DEDs

Air quality station data from highly populated regions of Utah indicate that dust events have produced elevated PM_{10} , exceeding NAAQS of $150 \mu\text{g m}^{-3}$, on 16 days over the past 18 years, or 0.9 per year since 1993. Over the period of record, dust events exceeded the NAAQS of $35 \mu\text{g m}^{-3}$ on 7 days over the past 18 years. Mean values for DED PM_{10} and $\text{PM}_{2.5}$ were 73.9 and $12.5 \mu\text{g m}^{-3}$ and mean values for all days of record were 33 and $12.5 \mu\text{g m}^{-3}$, respectively (Table 2.3). The doubling of PM_{10} mean values on DEDs is a function of dust load, whereas $\text{PM}_{2.5}$ mean values respond to multiple factors (e.g., local anthropogenic activities, inversions).

The largest PM_{10} value during a DED was $424 \mu\text{g m}^{-3}$ at Lindon – LN station on 30 March 2010; Lindon – LN also recorded the largest $\text{PM}_{2.5}$ value of $55.7 \mu\text{g m}^{-3}$ on the same day. The 30 March 2010 DED recorded the highest PM values at numerous air quality stations. The Utah Division of Air Quality (2011) called this an “exceptional event” due to regional dust transport.

2.4.3 Wind regimes of all DEDs

Dust observations at Delta coincided with strong ($10\text{-}30 \text{ m s}^{-1}$) winds from the southwest (Figure 2.5). Some occasional winds from the northwest could be associated with local dust transport during frontal passages, or with thunderstorm outflow. Wind

speeds at SLC-IA are slower ($10\text{-}20\text{ m s}^{-1}$), which is consistent with higher surface roughness in the urban corridor. SLC experienced winds mainly from the south due to terrain channeling and the north-south orientation of the SLC valley.

2.4.4 Synoptic and mesoscale meteorology of all DEDs

Composites created from NCEP/NCAR reanalysis dataset helped characterize the synoptic and mesoscale meteorology for all DEDs (Kalnay et al., 1996) (Figure 2.6). We created daily maps and composites of the mean of variables from the NCEP/NCAR reanalysis for all DEDs recorded during 1948-2010. Analysis of individual DEDs ($n=331$) indicates that 67.7% occurred when a trough was approaching the region, and most typically in the spring months (Figure 2.7). Composites of 700 mb geopotential height on the day before DEDs show a longwave trough upstream of Utah approaching the west coast of the U.S.A. On the DEDs, the trough progressed eastward to be centered over the California coast, with a strong pressure gradient over Utah aligned to produce southwesterly winds. By the day after DEDs, the trough has moved over Utah and the pressure gradient decreased.

At the surface sea level pressure, a weak cyclone is centered over the Oregon-Idaho-Nevada border on the day before DEDs (Figure 2.8). On the DEDs, this cyclone strengthens and progresses east and is centered over the Utah-Idaho-Nevada border. A day after the DEDs, the surface cyclone has moved out of Utah. This strengthening of cyclones over central Nevada has been observed previously and is caused in part by the Great Basin Confluence Zone (GBCZ) (Jeglum et al., 2010; West and Steenburgh, 2010). The GBCZ is an airstream boundary that is aligned from the “high” mountains of the

Sierra Nevada downstream toward northwestern Utah. Flow splitting around the Sierra Nevada creates an area of contraction over the Great Basin. Preexisting baroclinic zones associated with intermountain cyclones occur in this area, which concentrates the baroclinicity and creates frontogenesis. Strengthening of surface baroclinic zone enhances frontal strength and increases surface wind speeds.

2.4.5 Case study: 19 April 2008 DED

The day before the 19 April 2008 DED, there was a low pressure trough at midlevels (700mb) to the west of Utah, centered over California (Figure 2.9). On the DED, this trough deepened, moved southward, and progressed toward Utah. However, on the DED, the trough remained located in the west and a strong pressure gradient was present over Utah, producing southwesterly winds at midlevels. The day after the event, the trough broadened and moved over Utah.

Moving toward the surface, a surface cyclone was located over the Oregon-Idaho-Nevada border on the day before the DED (Figure 2.10). On the DED, this cyclone deepened (from 1014 to 1004 mb) and moved over the Utah-Idaho-Nevada border. The day after the DED, the surface cyclone moved through Utah and merged with another low pressure center to the northeast.

HYSPLIT backward trajectories from SLC indicate air parcels moved from the region of west-central and southwestern Utah over dust source areas including the Sevier Dry Lake and the area burned in the 2007 Milford Flat fire (Figure 2.11). At a local scale, strong surface winds demonstrated variable speed and direction (Figure 2.12). Stations near Delta reported wind speeds of $18\text{--}19\text{ m s}^{-1}$ at 1800 UTC, which represent

regional maximum wind speeds. Other stations in western Utah reported concomitant wind speeds of $10\text{--}15\text{ m s}^{-1}$, while eastern Utah stations generally had lower wind speeds.

The DED on 19 April 2008 dramatically affected air quality in the SLC area, with three out of four stations recording 24-hour PM_{10} values above the NAAQS of $150\text{ }\mu\text{g m}^{-3}$. The highest value of PM_{10} from the four stations was $191\text{ }\mu\text{g m}^{-3}$ at Hawthorne – HW. $\text{PM}_{2.5}$ values were high, but did not breach the NAAQS of $35\text{ }\mu\text{g m}^{-3}$, peaking at $31.4\text{ }\mu\text{g m}^{-3}$ at Lindon – LN. For both PM parameters, Ogden – O2 station recorded low values, due to greater distance from source areas. The Utah DEQ issued a “red” air quality alert for SLC and surrounding counties on the afternoon of 19 April 2008 (Maffly, 2008).

On the MODIS image, several dust plumes originate from the northern edge of the area burned in 2007 Milford Flat Fire, the Sevier Dry Lake, Tule Dry Lake, and Great Salt Lake Desert (Dugway Proving Ground), as well as other playas (Figure 2.13). Dust plumes move in a northeasterly direction due to winds from the southwest, and display distinctive color differences reflecting dust compositions.

2.4.6 Case study: 4 March 2009 DED

The day before the 4 March 2009 dust event, there was a long wave midlevel (700mb) trough off the coast of the western U.S. and long wave ridge centered just east of the Rocky Mountains (Figure 2.9). On the DED, the midlevel trough has moved eastward, but is still offshore of the western U.S. The day after the dust event, the long wave trough has widened and moved onshore and is centered over the Rocky Mountains. There is also an embedded shortwave trough centered on the coast of California.

Nearer to the surface on the day before the DED, there is a surface trough

centered over the Oregon-Idaho-Nevada border, and extending southward into Nevada (Figure 2.10). On the DED, the trough deepened and formed a surface cyclone centered over the Utah-Idaho-Nevada border. The day after the DED, the surface trough has moved through Utah over the Utah-Colorado border.

HYSPLIT backward trajectories from SLC indicate air parcels came from the south, across the Sevier Dry Lake and the Milford Flat area burned in 2007 (Figure 2.11). At a local scale, strong surface winds through the region show variations by terrain channeling (i.e., modification and enhancement of near surface winds by topography) and surface roughness differences (Figure 2.14). Delta station reported a wind speed of 20 m s^{-1} at 1800 UTC, a regional maximum. Other stations in the western part of Utah reported winds speeds of $10\text{-}19 \text{ m s}^{-1}$ at this time. Similar to 19 April 2008, the 4 March 2009 DED had weaker winds in eastern Utah, in the area to the east of the Wasatch Plateau. Strong winds near Delta caused dust production from local hotspot sources.

This 2009 dust event had a larger range of PM as compared with the 19 April 2008 DED. On the 4 March 2009 DED, only one station out of four had a value above the NAAQS of $150 \mu\text{g m}^{-3}$. However, the Hawthorne – HW site did not report a value on this day. The highest value of PM_{10} from the three stations was $200 \mu\text{g m}^{-3}$ at Lindon – LN, while the lowest value was $103 \mu\text{g m}^{-3}$ at Ogden – O2. $\text{PM}_{2.5}$ values were lower on this day when compared to 19 April 2008, with the highest value of $22.9 \mu\text{g m}^{-3}$ at Lindon – LN. The Lindon – LN recorded the highest values for both parameters on this DED, and the PM_{10} value was higher than the highest value on 19 April 2008. The comparative difference in the particle size distribution is a function of station distance from source areas; smaller sized particles are held aloft further downwind.

MODIS imagery shows dust plumes originating from the area of Milford Flat burned by wildfire in 2007, the Sevier Dry Lake, Tule Dry Lake, and Great Salt Lake Desert (Dugway Proving Grounds) (Figure 2.15). Images do not indicate net transport from large areas. Instead, dust appears to be entrained from specific ground locations, with distinctive plumes emerging from “hot spots.” Media reported a multiday dust storm, with residents “struggling with the dust fogging the air” for two days before a snowstorm arrived on 4 March 2009 (Fahys, 2009). The National Weather Service in SLC issued wind advisories before the storm, and winter weather advisories for the mountains after the dust event. Wind gusts reached 42.5 m s^{-1} at Windy Peak in the Uinta Mountains and 39.3 m s^{-1} at Ogden Peak in the Wasatch Mountains.

2.5. Discussion

Regional sediment transport in the Great Basin is facilitated by sufficient wind speeds to entrain and move particles (Jewell and Nicoll, 2011). Other factors that predispose the region as a dust source include (1) lack of aggregation or surface crusting of sediments, (2) minimal vegetation cover, and (3) availability of surface areas with silt sized particles (see Gillette, 1999). Collectively, these factors reduce threshold friction velocities (e.g., Kohfeld et al., 2005; Shao, 2008; Park et al., 2009), especially at flat lowland areas like ephemeral streams, dry lakes, silt pans or playas (Gill, 1996; Washington et al., 2006). Great Basin playas are characteristic intermountain features occurring across wide expanses (Grayson, 2011), and are a source of deflatable sediments due to their low threshold friction velocities.

Previous work beyond the Great Basin region has shown that synoptic scale desert

dust outbreaks are initiated by specific weather conditions (Zhang et al., 1997; Tegen et al., 2004; Lee et al., 2009; Rivera Rivera et al., 2009; Strong et al., 2010), which depend on the nature and strength of large scale wind systems affecting a dust source region (Wigner and Peterson, 1987; Yang et al., 2008). Persistent episodes of high winds and blowing dust occur during the passage of a strengthening low pressure system over a dust source area (Brandli et al., 1977; Sheppard et al., 2002; Novlan et al., 2007).

Similar ascendant meteorological conditions causing dust transport occur in Africa, Asia, Australia, and the Middle East (Goudie, 1978). A strengthening pressure gradient (cyclogenesis) in the prefrontal atmosphere creates strong and persistent south and southwesterly winds in the northern hemisphere. These winds are often strongest in the afternoon due to growth of the boundary layer and turbulent mixing of strong winds down to the surface (Pauley et al., 1996; Dayan et al., 2011). These regional dust transport events are different from “haboob” dust events, which are localized in spatial and temporal scales, and are often produced by strong mesoscale downdrafts associated with thunderstorms (Miller et al., 2008).

The Great Basin region typically experiences strong prefrontal south and southwesterly winds. These characteristic winds are called “Hatu winds,” “Utah” spelled backwards (Eubank and Brough, 1979), and their association with dust storms was noticed in 1910 (Brough et al., 1987). Hatu winds occur several times a year, and are typically associated with approaching cold fronts and deepening cyclonic systems. Observed Hatu winds may be as strong as 93 mph (42 m s^{-1}) (Brough and Stevens, 1989).

Dust events are reported most frequently during the months of March and April. Frequency climatology of intermountain cyclones that produce strong winds shows a

bimodal distribution, with a primary peak in spring and a smaller secondary peak in the fall (Jeglum et al., 2010). This seasonal pattern also occurs during strong cold frontal passages (Shafer and Steenburgh 2008). An area of confluent winds in the lee of the Sierra Nevada, termed the Great Basin Confluence Zone (GBCZ), causes both cyclogenesis and frontogenesis as storms move across Nevada (West and Steenburgh, 2010). Analyses of strong storms demonstrate that cyclonic systems strengthen in this region, which is a “breeding ground for cold fronts” (Shafer and Steenburgh, 2008; Steenburgh et al., 2009). Salt Lake City, UT is positioned downwind and in the direction of these strong frontal passages.

Maximum wind speeds near Delta occur due to a large fetch upstream; fetch is the distance winds travel without interacting with high or complex terrain. Western Utah is characterized by north-south trending valleys located between mountain ranges, a topography described as “an army of caterpillars crawling northward” (Dutton, 1885). Therefore, when wind direction is north-south, it is aligned with the regional trend of the intermountain topography of the Basin and Range physiographic province, and dust bearing wind can travel long distances with little disruption (Gillette et al., 1996). This coincidence of flow aligned with playa-filled topographic corridors, or terrain channeling, enhances dust production and transport toward SLC, especially when wind speed is high.

2.6. Conclusions

We identified primary dust source regions and transport pathways affecting the SLC metropolitan area, and characterized synoptic meteorological conditions leading to dust entrainment and transport during two specific DEDs. Both case studies illustrate the

importance of an approaching midlevel trough in mobilizing dust toward SLC; 68% of the DEDs occurring between 1948-2010 are associated with this synoptic setting. In summary, controls on regional dust transport in the eastern Great Basin include: (1) aerially extensive source areas containing deflatable dust sized particles (e.g., fine sediment or soil); (2) low threshold friction velocities at the landscape surface, enhanced by limited vegetation, low soil moisture, and/or an absence of cementation, pavements or biological soil crusts; and (3) wind at sufficient speeds to loft fine sediment particles into the atmosphere, allowing dust deflation and transport.

Records since 1930 suggest the Eastern Great Basin produces 4-5 dust events per year that impact a large region in northern Utah. These events usually occur in spring, coincident with strong southerly pre frontal Hatu winds that develop in advance of strengthening intermountain cyclones and frontal passages. Dust activity peaks during the afternoon with the maximum boundary layer depth and wind speeds.

MODIS images demonstrate that the Eastern Great Basin region does not uniformly produce dust; rather, plumes from specific hotspot areas contribute to the dust load. Important dust sources include playa surfaces located in the intermountain corridors in the Basin and Range province, and remnants of Pleistocene Lake Bonneville in the Great Salt Lake Desert. Important dust sources we identified in the Eastern Great Basin region include the Sevier Dry Lake, Tule Dry Lake, and the Great Salt Lake Desert. In addition, geographically extensive dust sources can result after disturbance events such as fire and reclamation. MODIS images show that the region burned in the 2007 Milford Flat Fire is an active dust source during 2008 and 2009 case study DEDs.

With an abundance of dust sources and its ideal meteorological and physiographic

conditions, the eastern Great Basin region is a major source, identified using Total Ozone Mapping Spectrometry (TOMS) data (Prospero et al., 2002), of dust in North America. The regional physiographic orientation of its mountain-valley topography exacerbates terrain channeling, and funnels dust bearing winds toward SLC. Observed dust storms significantly impact air quality in the populated regions of Utah; records over the past 18 years indicate 16 days exceeding NAAQS for PM₁₀ on DEDs. Elevated PM levels result after most dust events, and pose some health risks. Further understanding the meteorological characteristics of dust storm events aids the forecasting, prediction, and monitoring of dust outbreaks affecting the SLC metropolitan area, and beyond.

2.7. Acknowledgements

We acknowledge use of data from various governmental agencies, commercial firms, and educational institutions participating in MesoWest; air quality data from the United States Environmental Protection Agency (EPA); longterm meteorological data from National Climatic Data Center (NCDC); meteorological maps from National Center for Environmental Prediction (NCEP) National Center for Atmospheric Research (NCAR) Reanalysis I; and MODIS imagery from NASA's Land and Atmosphere Near real-time Capability for Earth Observing Systems (EOL) (LANCE) Rapid Response. We thank NOAA Air Resources Laboratory (ARL) for provision of the HYSPLIT transport and dispersion model and READY website (<http://www.arl.noaa.gov/ready.php>). TimeScience LLC provided webcam images.

Table 2.1: Meteorological data station information (data from NCDC).

Station Name	Lat./Lon.	Elevation (m)	Call Sign/ICS	COOP ID	WMO ID	Period of record used
Delta, UT	39.33/ -112.58	1408	U24/ KU24	422090	72479	1973-2010
Salt Lake City International Airport	40.78/ -111.97	1288	SLC/ KSLC	427598	72572	1930-2010

Table 2.2: Utah Air Monitoring Network station information (data from EPA).

Station Name	Lat./Lon.	Elevation (m)	EPA AIRS Code	Period of record used	Station Address
Hawthorne – HW	40.74/ -111.87	1306	490353006	PM ₁₀ : 1997-2010 PM _{2.5} : 1999-2010	1675 S. 600 E. Salt Lake City
Lindon - LN	40.34/ -111.71	1442	490484001	PM ₁₀ : 1993-2010 PM _{2.5} : 1999-2010	50 North Main Street, Lindon
North Salt Lake – N2	40.81/ -111.92	1286	490350012	PM ₁₀ : 1993-2010 PM _{2.5} : 1999-2007	1795 N 1000 W, Salt Lake City
Ogden #2 – O2	41.21/ -111.97	1316	490570002	PM ₁₀ : 2001-2010 PM _{2.5} : 2001-2010	228 East 32nd Street , Ogden City

Table 2.3: Summary of PM₁₀ and PM_{2.5} data during DEDs (data from EPA).

Station Name	Mean PM₁₀ for all days	Mean PM₁₀ for DEDs	Median PM₁₀ for DEDs	Min PM₁₀ for DEDs	Max PM₁₀ for DEDs	Date of Max PM₁₀ for DEDs	DEDs exceeding NAAQS
Hawthorne – HW	26.9	67.2	46.5	11	360	April 1, 2003	7
Lindon – LN	30.7	69.3	46	10	424	March 30, 2010	9
North Salt Lake – N2	43.4	90.9	68	19	385	March 30, 2010	11
Ogden #2 – O2	27.4	65.3	50	10	229	April 1, 2003	4
All Stations	33.1	73.9	53	10	424	March 30, 2010	16
Station Name	Mean PM_{2.5} for all days	Mean PM_{2.5} for DEDs	Median PM_{2.5} for DEDs	Min PM_{2.5} for DEDs	Max PM_{2.5} for DEDs	Date of Max PM_{2.5} for DEDs	DEDs exceeding NAAQS
Hawthorne – HW	11.1	12.5	8.9	3.6	49.9	March 30, 2010	4
Lindon – LN	10.3	12.8	9	2.7	55.7	March 30, 2010	3
North Salt Lake – N2	14.1	13.9	13	9	22.1	July 18, 2006	0
Ogden #2 – O2	10.7	11.4	9.2	3.3	32.2	August 6, 2009	0
All Stations	11.7	12.5	9.4	2.7	55.7	March 30, 2010	7



Figure 2.1: Study area location of Lake Bonneville Basin (white) within the Great Basin Physiographic Province (grey), and places mentioned within text. Abbreviations on figure: D = Delta Station, SLC = Salt Lake City, GSLD = Great Salt Lake Desert, TDL = Tule Dry Lake subbasin, SDL = Sevier Dry Lake, MF = Milford Flat, area disturbed by wildfire in 2007.

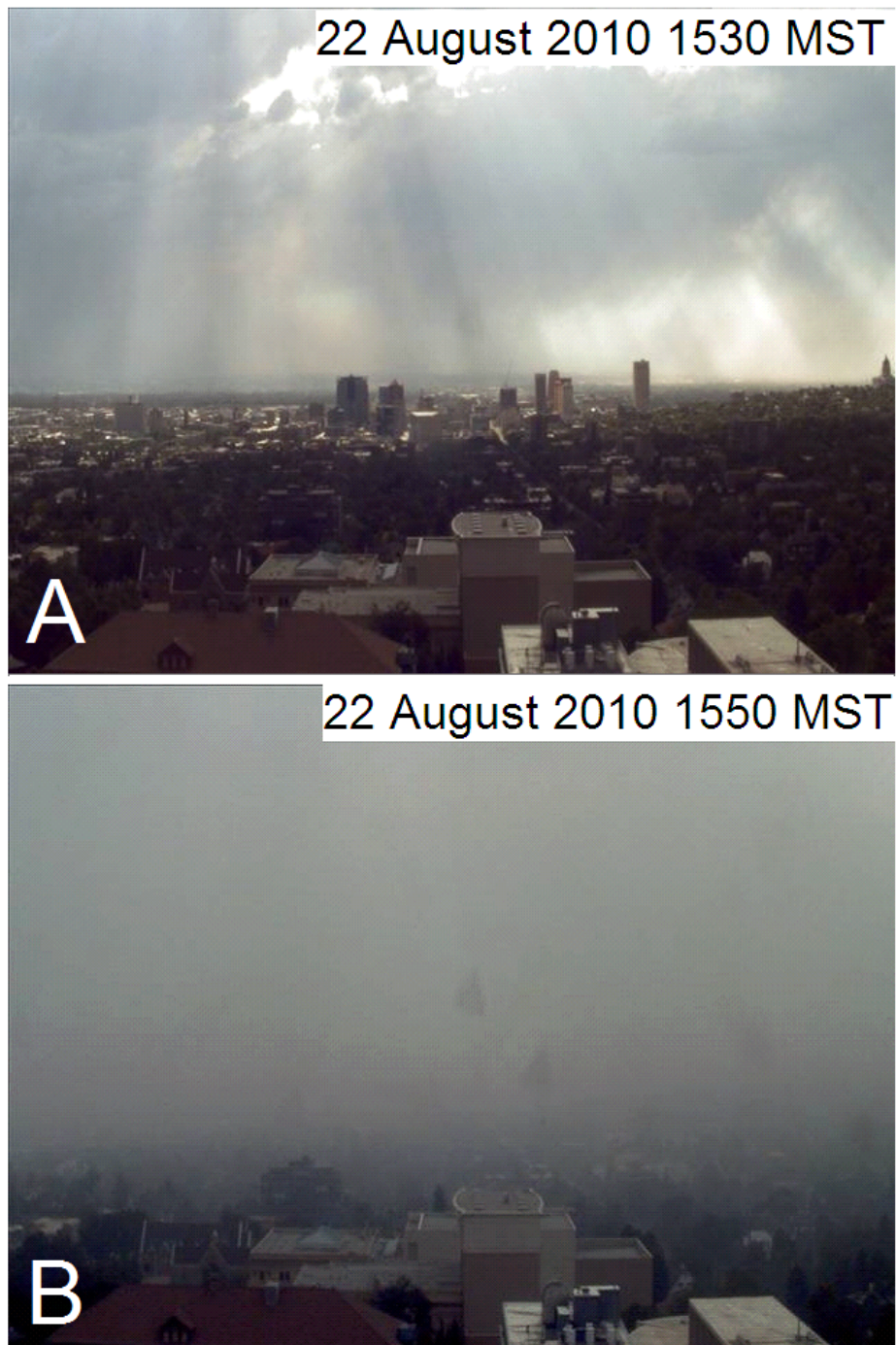


Figure 2.2: Webcam photos from the roof of the William Browning Building at the University of Utah (40.76623 N -111.84755 W), looking west toward downtown Salt Lake City, UT. A. Before (1530 MST) and B. after (1550 MST) the arrival of a dust storm on 22 August 2010 (Images copyright Tim Brown / TimeScience).

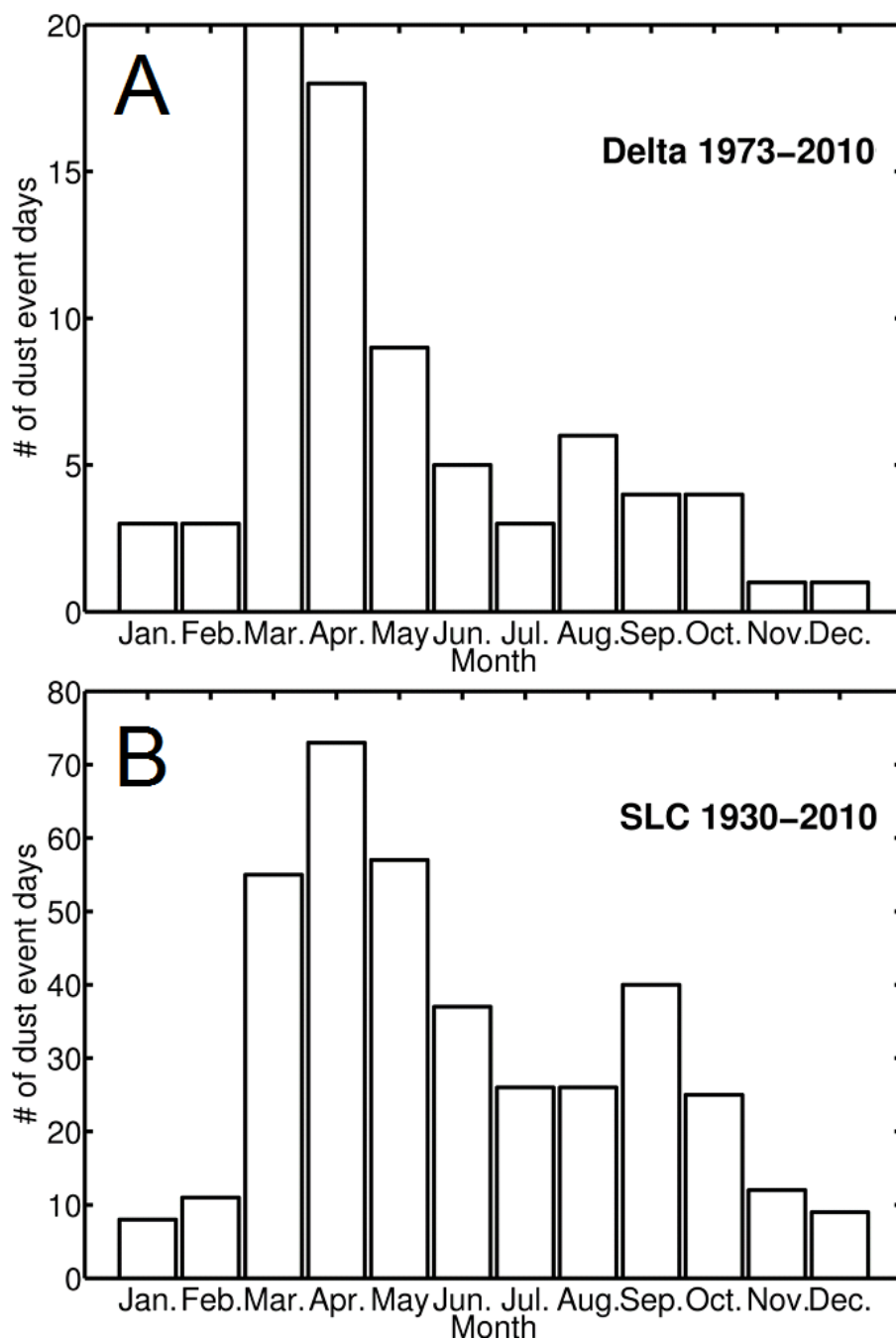


Figure 2.3: Frequency of DEDs by month for A. Delta (1973-2011) and B. SLC-IA (1930-2011) (data from NCDC).

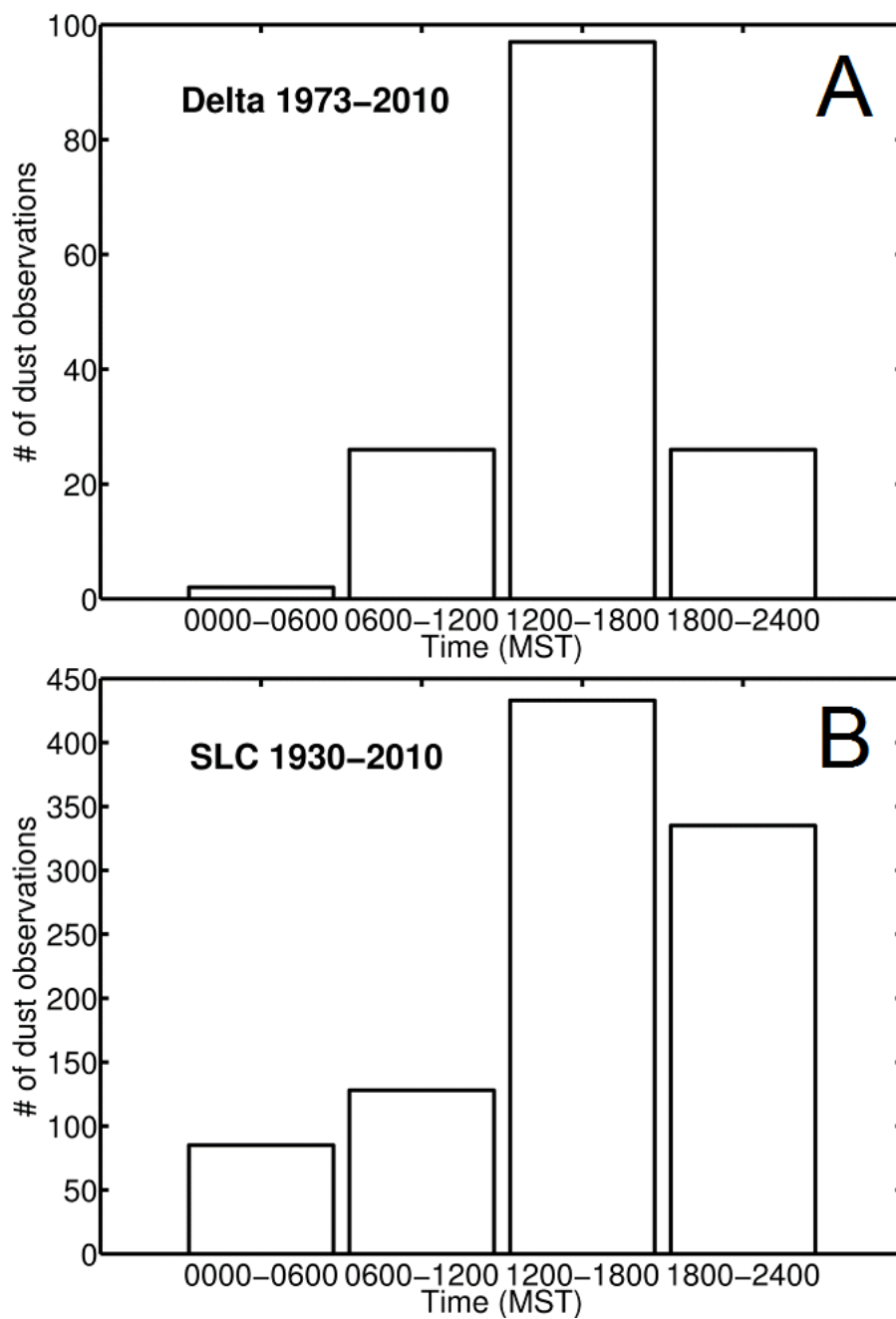


Figure 2.4: Frequency of dust observations by hour of the day for stations at A. Delta (1973-2011) and B. SLC-IA (1930-2011) (data from NCDC).

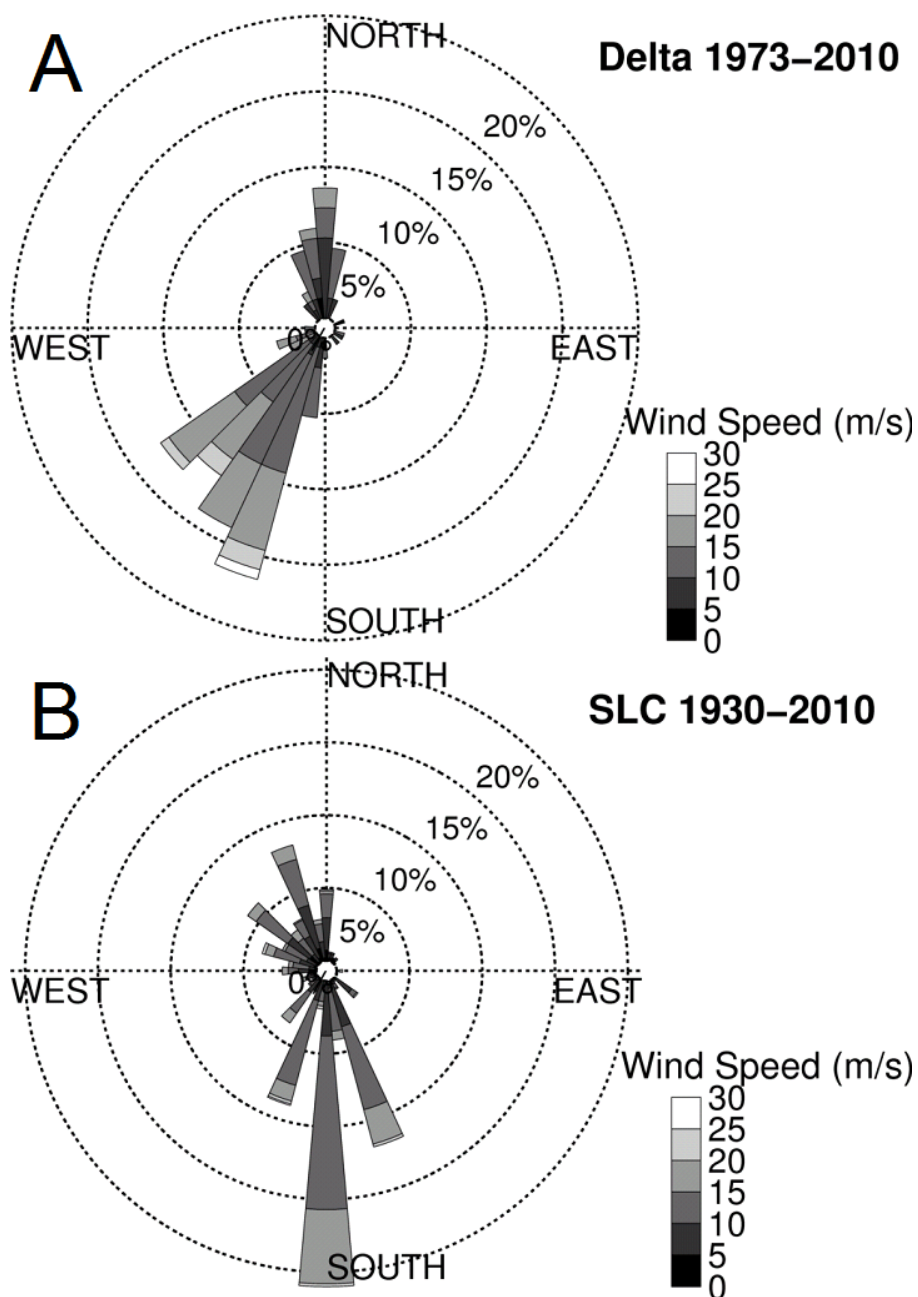


Figure 2.5: Wind roses for all observations indicating dust is present at A. Delta (1973–2011) and B. SLC-IA (1930–2011) (data from NCDC).

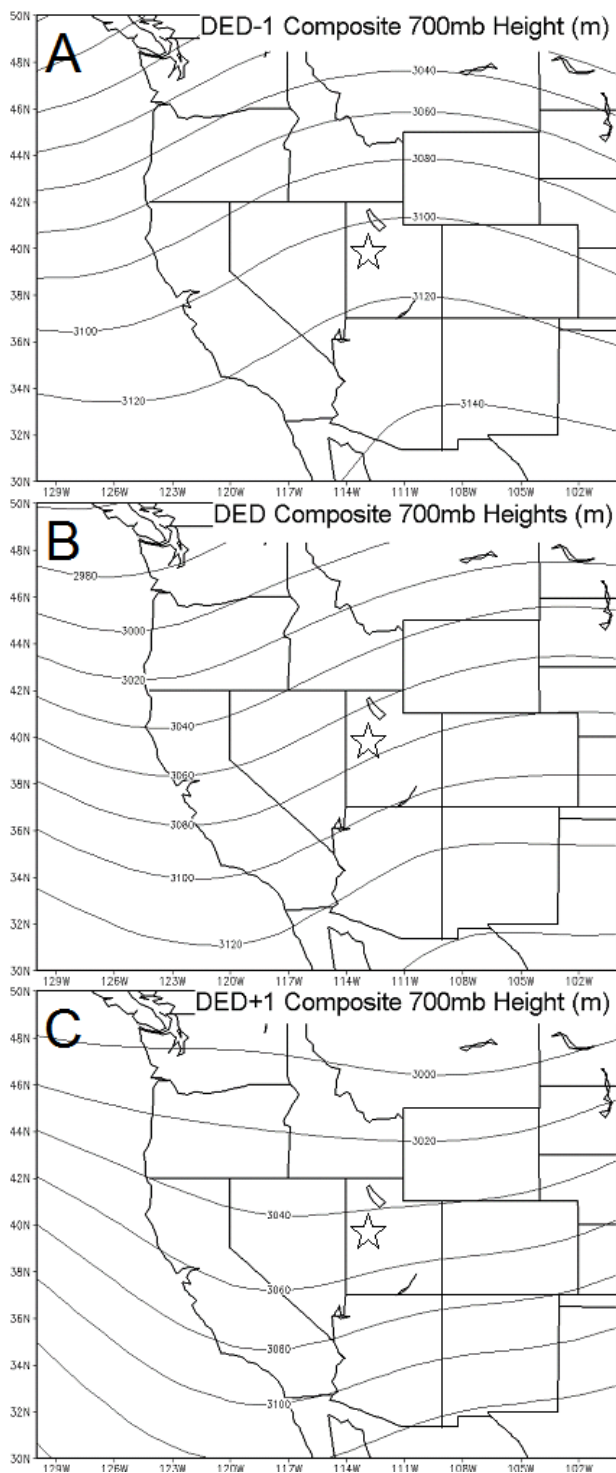


Figure 2.6: Composite of 700mb geopotential height (m) on all DEDs. A. One day prior to DED. B. Day of the DEDs. C. One day after. Great Salt Lake is depicted. Star indicates the center of the study region (data from NCEP/NCAR Reanalysis I).

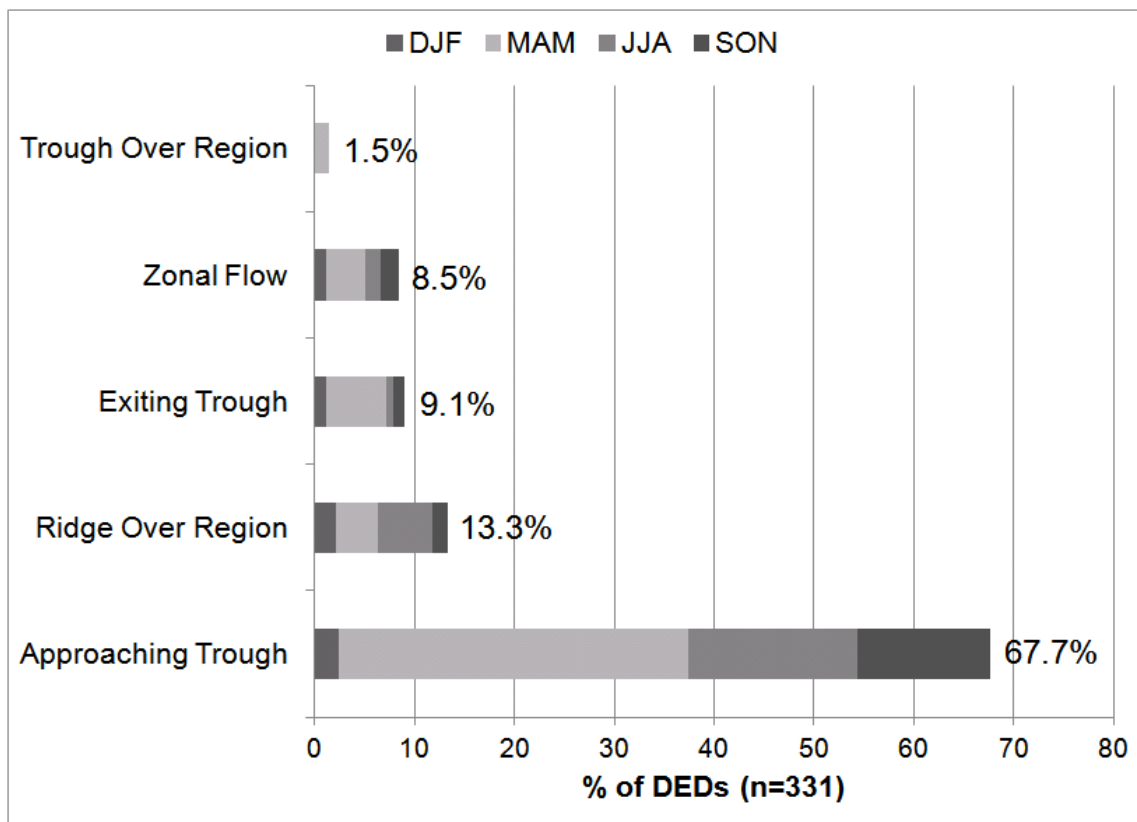


Figure 2.7: Synoptic classification of 331 DEDs for 1948-2010 using 700 mb geopotential height maps from the NCEP/NCAR reanalysis. DED are subdivided by month of occurrence: DJF (December-January-February), MAM (March-April-May), JJA (June-July-August), SON (September-October-November) for each synoptic classification, with the number indicating the percentage of the total (data from NCEP/NCAR Reanalysis I).

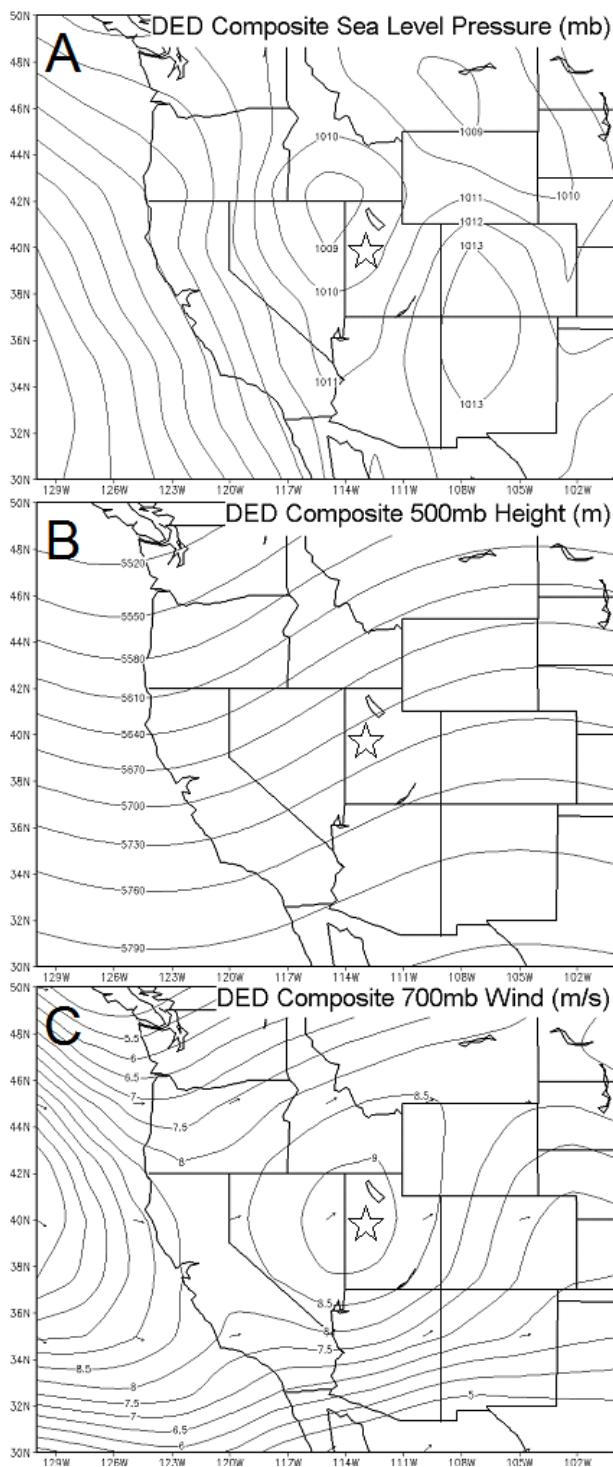


Figure 2.8: Composite synoptic maps from NCEP/NCAR Reanalysis I. A. Composite of sea level pressure (mb) on all DEDs. B. Composite of geopotential height (m) at 500 mb on all DEDs. C. Composite of 700 mb wind (m s^{-1}) on all DEDs. Great Salt Lake is depicted. Star indicates the center of the study region (data from NCEP/NCAR Reanalysis I).

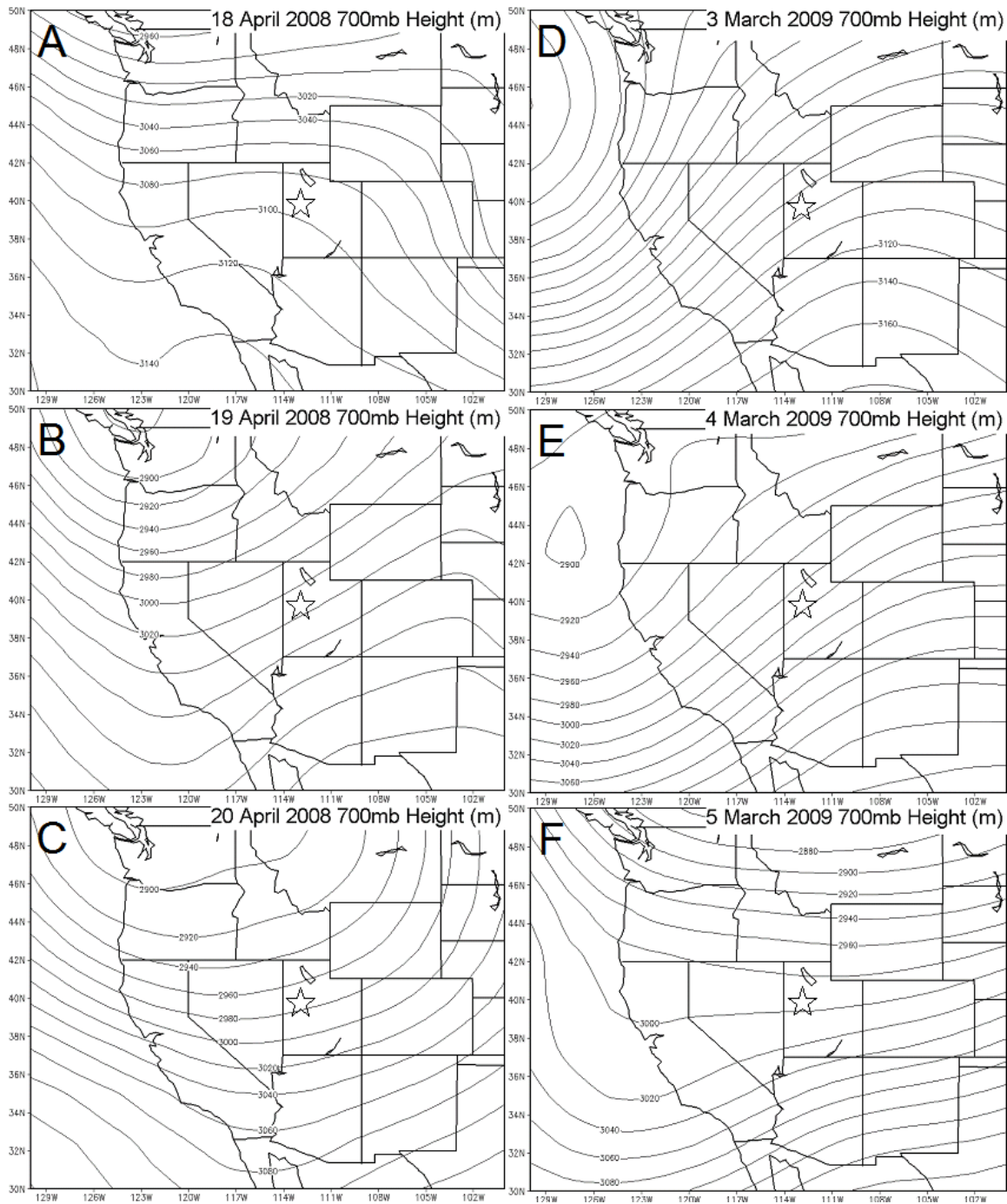


Figure 2.9: Synoptic 700 mb geopotential height (m) maps from NCEP/NCAR Reanalysis I. A. 18 April 2008, B. 19 April 2008, C. 20 April 2008, D. 3 March 2009, E. 4 March 2009, F. 5 March 2009. Great Salt Lake is depicted. Star indicates the center of the study region (data from NCEP/NCAR Reanalysis I).

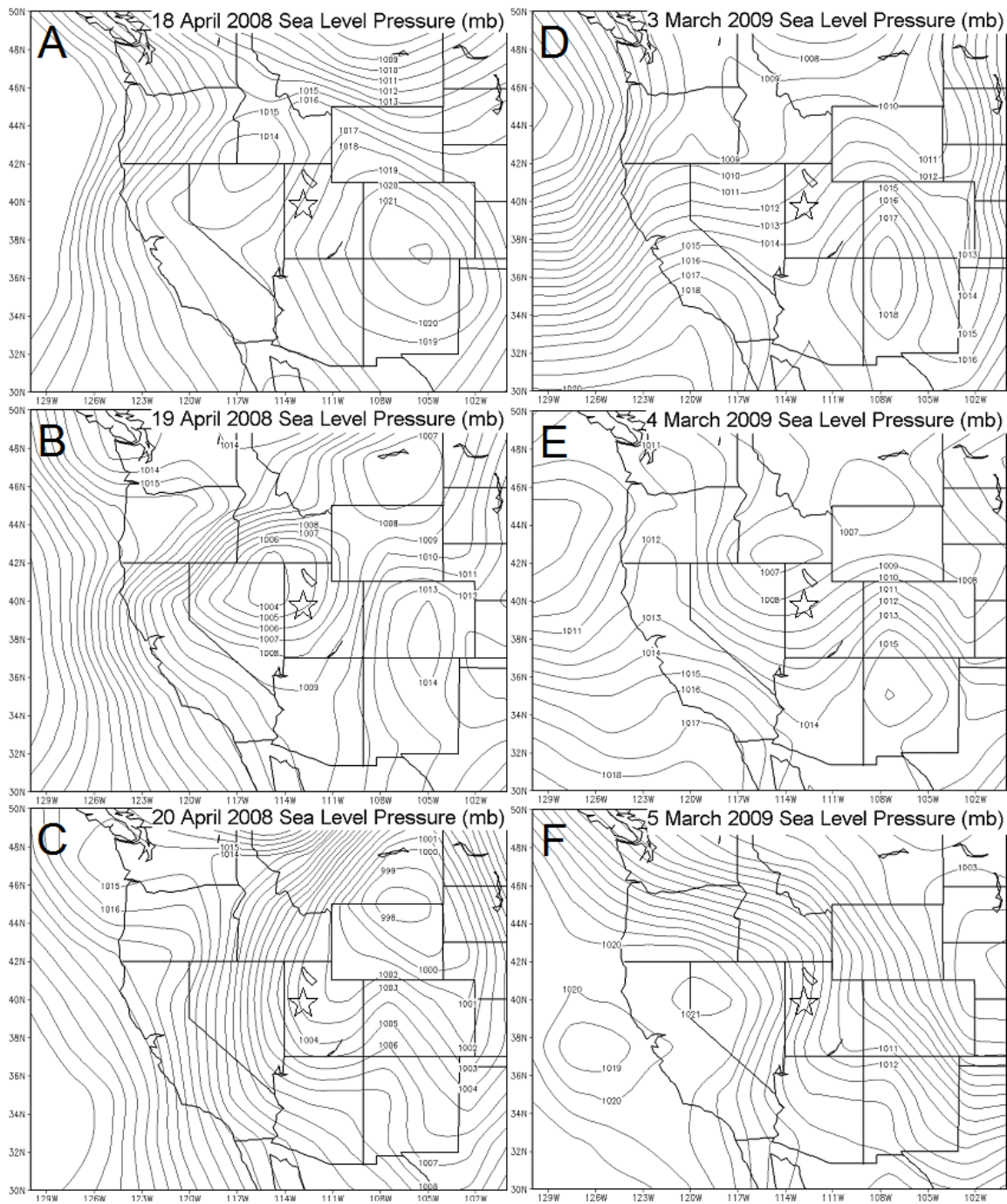


Figure 2.10: Surface sea level pressure (mb) maps from NCEP/NCAR reanalysis. A. 18 April 2008, B. 19 April 2008, C. 20 April 2008, D. 3 March 2009, E. 4 March 2009, F. 5 March 2009. Great Salt Lake is depicted. Star indicates the center of the study region (data from NCEP/NCAR Reanalysis I).

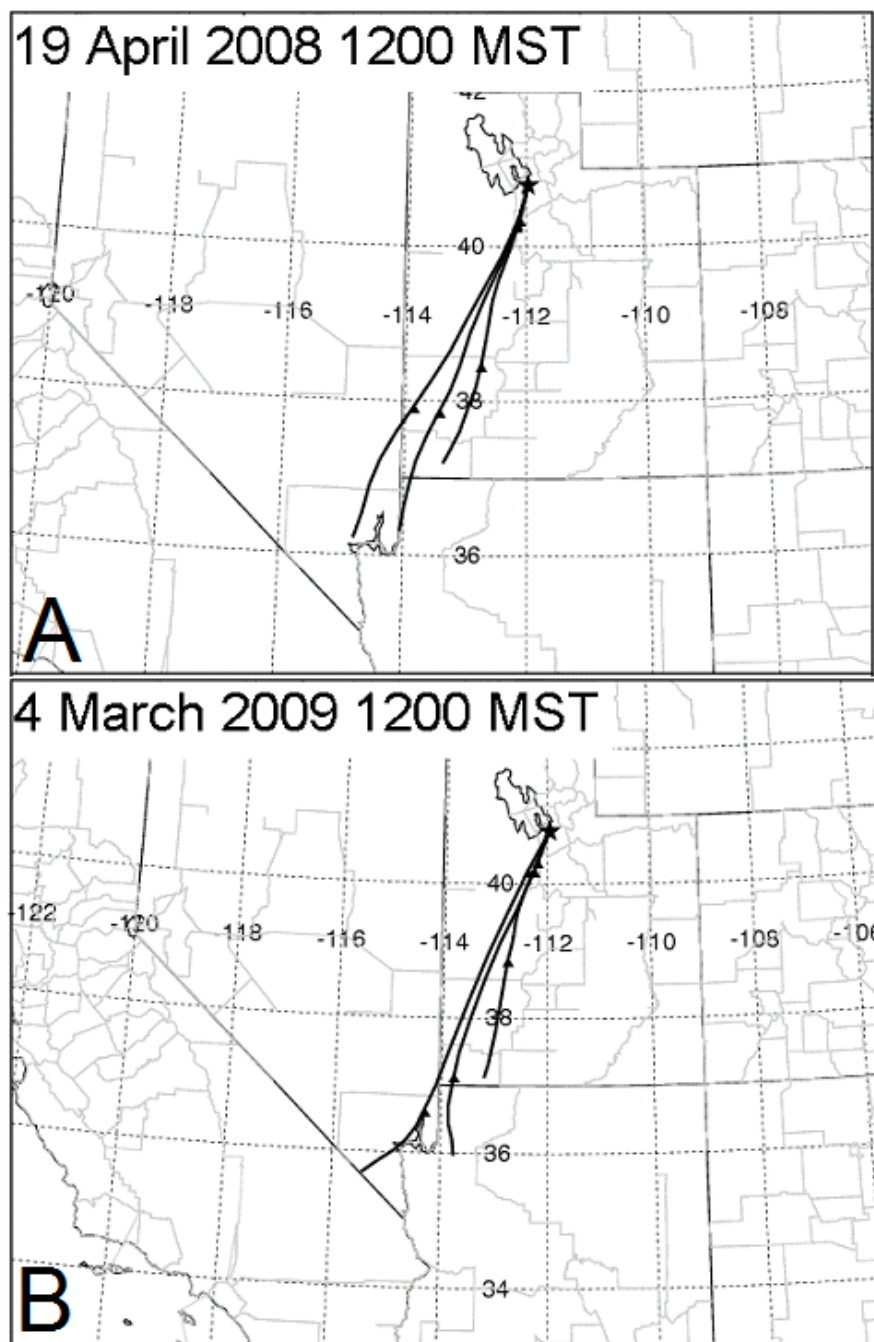


Figure 2.11: NOAA HYSPLIT 4.9 12-hour backward trajectories using NAM12 meteorological data for A. 19 April 2008 and B. 4 March 2009. Great Salt Lake is depicted (data from ARL).

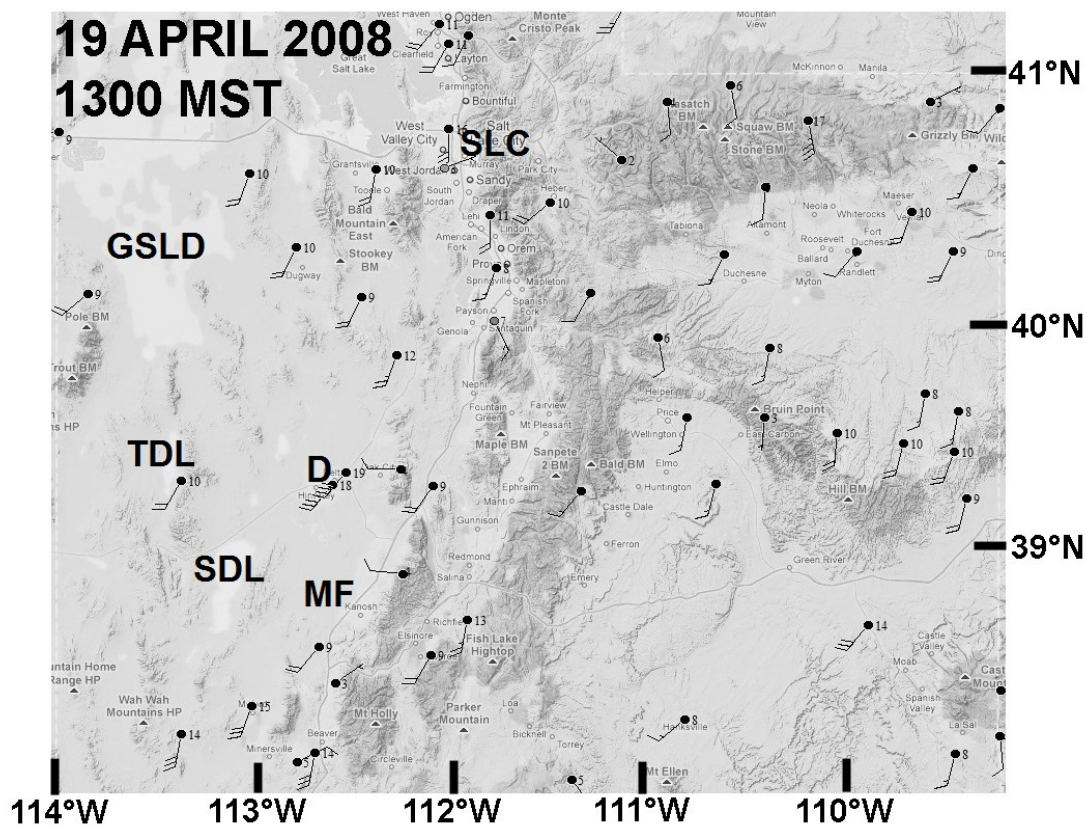


Figure 2.12: MesoWest surface weather maps at 2000 UTC (1300 MST) for 19 April 2008. Numbers are wind speeds in m/s; barbs indicate wind speeds in knots (data from MesoWest).

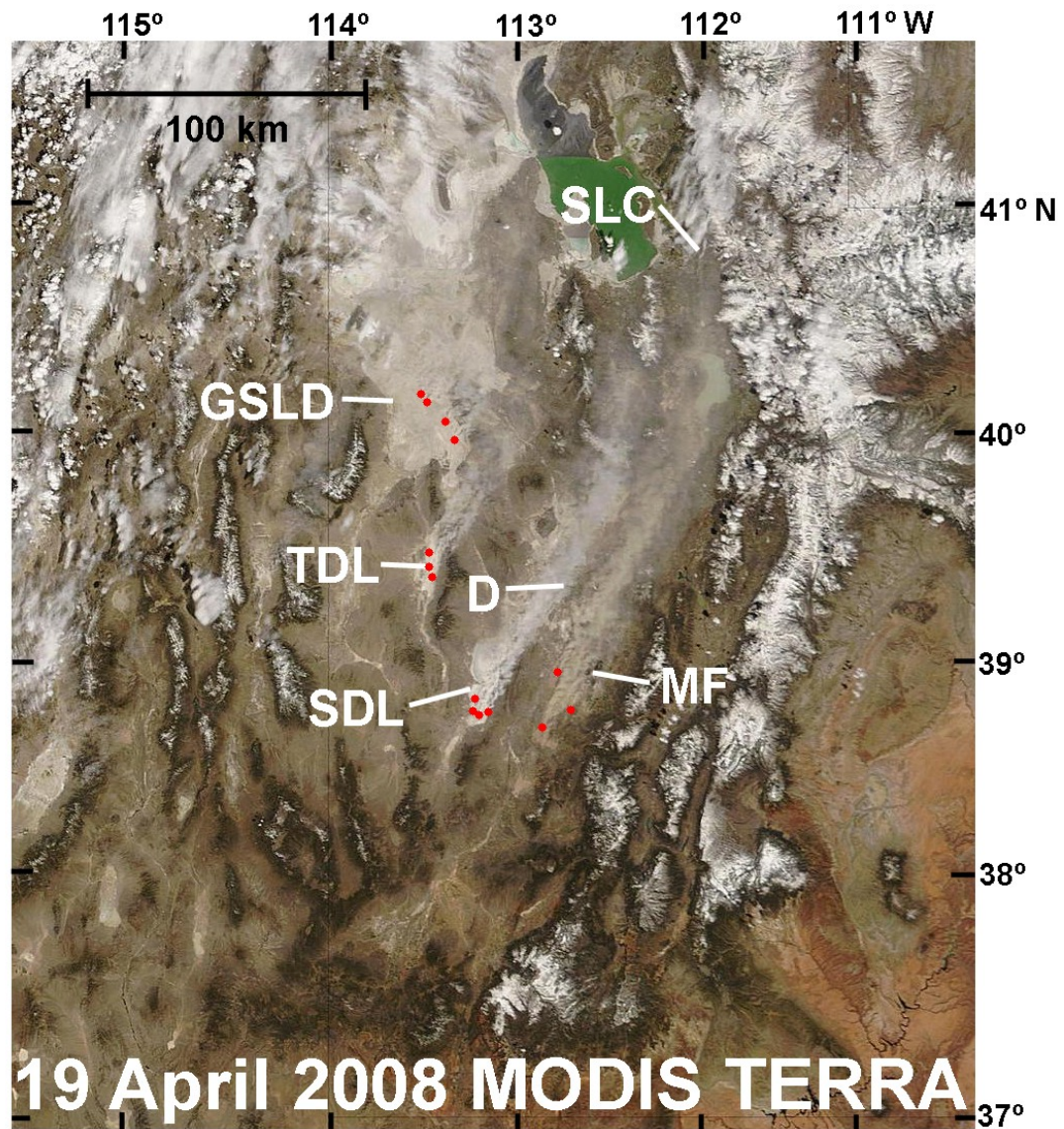


Figure 2.13: MODIS TERRA RGB imagery for 19 April 2008. Dust plume origins are indicated by the red dots (data from NASA LANCE).

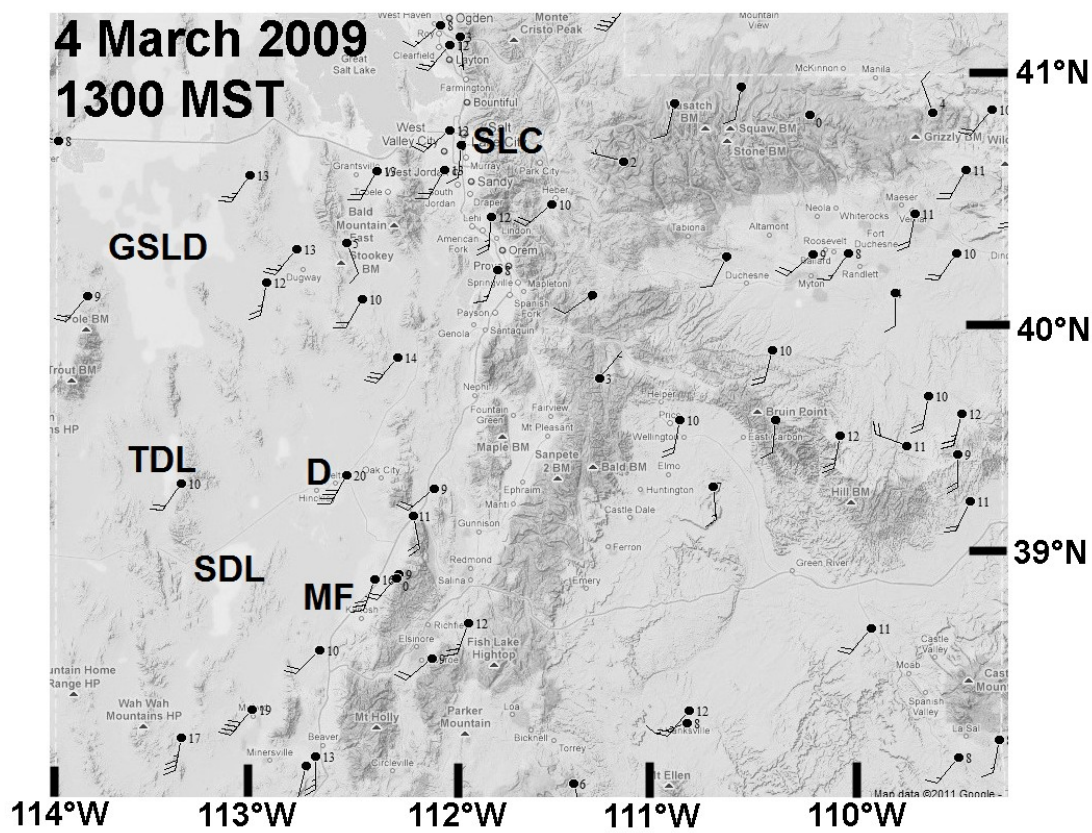


Figure 2.14: MesoWest surface weather maps at 2000 UTC (1300 MST) for 4 March 2009. Numbers are wind speeds in m s^{-1} ; barbs indicate wind speeds in knots (data from MesoWest).

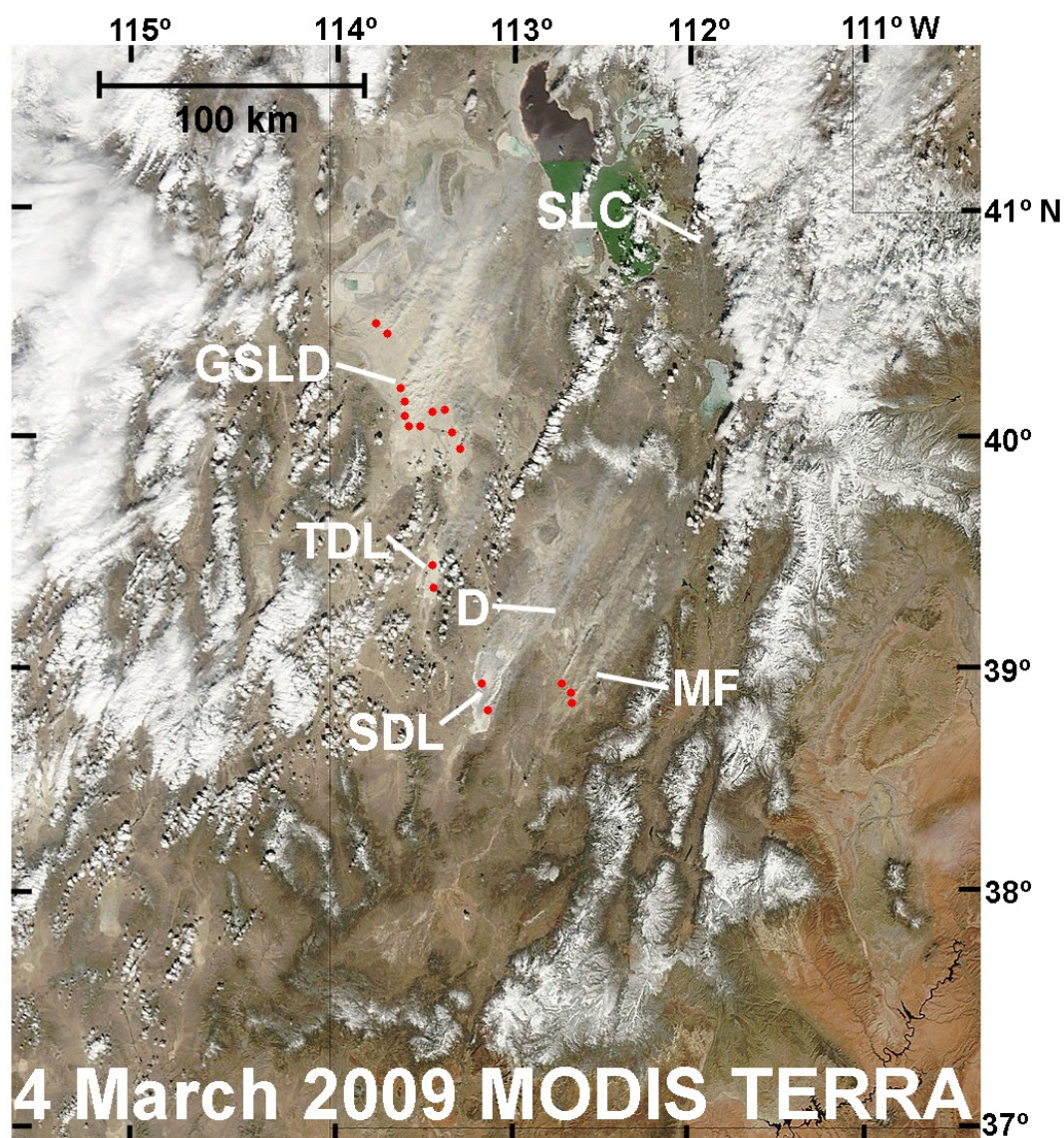


Figure 2.15: MODIS TERRA RGB imagery for 4 March 2009. Dust plume origins are indicated by the red dots (data from NASA LANCE).

2.8 References

- Alexandrova, O.A., Boyer, D.L., James R. Anderson, J.R., Fernando, H.J.S., 2003. The influence of thermally driven circulation on PM₁₀ concentration in the Salt Lake Valley. *Atmospheric Environment*, 37, 421–437. [doi:10.1016/S1352-2310\(02\)00803-8](https://doi.org/10.1016/S1352-2310(02)00803-8)
- Baddock, M.C., Bullard, J.E., Bryant, R.G., 2009. Dust source identification using MODIS: a comparison of techniques applied to the Lake Eyre Basin, Australia. *Remote Sensing of Environment*, 113, 1511–1528. [doi:10.1016/j.rse.2009.03.002](https://doi.org/10.1016/j.rse.2009.03.002)
- Brandli, H.W., Ashman, J.P., Reinke, D.L., 1977. Pictures of the month; Texas dust moves into Florida. *Monthly Weather Review*, 105, 1068–1070. doi: 10.1175/1520-0493(1977)105<1068:TDMIF>2.0.CO;2
- Brough, R.C., Jones, D.L., Stevens, D.J., 1987. *Utah's Comprehensive Weather Almanac*. Publishers Press, Salt Lake City, UT.
- Brough, R.C., Stevens, D.J., 1989. *Utah's High Winds: Intensities, Frequencies and Distribution*. KTVX Weather Department, Salt Lake City, UT.
- Dayan, U., Erel, Y., Shpund, J., Kordova, L., Wanger, A., Schauer, J.J., 2011. The impact of local sources and meteorological factors on nitrogen oxide and particulate matter concentrations: a case study of the Day of Atonement in Israel. *Atmospheric Environment*, 45, 3325–3332. [doi:10.1016/j.atmosenv.2011.02.017](https://doi.org/10.1016/j.atmosenv.2011.02.017)
- Derbyshire, E., 2007. Natural minerogenic dust and human health. *AMBIO*, 36, 73–77.
- Division of Air Quality (DAQ), Utah State Department of Environmental Quality (DEQ), 2011. *Utah 2011 Air Monitoring Network Plan*. <http://www.airmonitoring.utah.gov/network/2011AirMonitoringNetworkPlan.PDF>
- Draxler, R.R., Hess, G.D., 2004, Description of the HYSPLIT_4 Modeling System (NOAA Technical Memorandum ERL ARL-224), <http://www.arl.noaa.gov/data/web/models/hysplit4/win95/arl-224.pdf>. NOAA Air Resources Laboratory, Silver Spring, MD, Dec., 1997, revised Jan., 2004.
- Dutton, C.E., 1885. Mount Taylor and the Zuni plateau. *Annual Report 6* [p. 113–198]. In Powell, J.W., *Sixth Annual report of the United States Geological Survey to the Secretary of the Interior, 1884–1885*. U.S. Geological Survey.
- Engelstaedter, S., Washington, R., 2007. Temporal controls on global dust emissions: the role of surface gustiness. *Geophysical Research Letters*, 34, L15805. [doi:10.1029/2007GL029971](https://doi.org/10.1029/2007GL029971)
- Eubank, M.E., Brough, R.C., 1979. *Mark Eubank's Utah Weather*. Horizon Publishers & Distributors, Bountiful, UT.

Fahys, J., 2009. Winter Bounces Back. The Salt Lake Tribune, March 4, 2009.

Gill, T.E., 1996. Eolian sediments generated by anthropogenic disturbance of playas: human impacts on the geomorphic system and geomorphic impacts on the human system. *Geomorphology*, 17, 207-228. [doi:10.1016/0169-555X\(95\)00104-D](https://doi.org/10.1016/0169-555X(95)00104-D).

Gill, T.E., Cahill, T.A., 1992. Playa-generated Dust Storms from Owens Lake in The History of Water: Eastern Sierra Nevada, Owens Valley, White-Inyo Mountains. Hall, C.A., Doyle-Jones, V., and B. Widaski, eds. University of California Press, Los Angeles, pp. 63-73.

Gillette, D.A., 1999. A qualitative geophysical explanation for “hot spot” dust emitting source regions. *Contributions to Atmospheric Physics*, 72, 67-77.

Gillette, D.A., Herbert, G., Stockton, P.H., Owen, P.R., 1996. Causes of the fetch effect in wind erosion. *Earth Surface Processes & Landforms*, 21, 641-659. [DOI: 10.1002/\(SICI\)1096-9837\(199607\)21:7<641::AID-ESP662>3.0.CO;2-9](https://doi.org/10.1002/(SICI)1096-9837(199607)21:7<641::AID-ESP662>3.0.CO;2-9)

Ginoux, P., Chin, M., Tegen, I., Prospero, J.M., Holben, B., Dubovik, O., Lin, S.-J., 2001. Sources and distributions of dust aerosols simulated with the GOCART model. *Journal of Geophysical Research*, 106, 20,255-20273. [doi:10.1029/2000JD000053](https://doi.org/10.1029/2000JD000053)

Ginoux, P., Garbuzov, D., Hsu, N.C., 2010. Identification of anthropogenic and natural dust sources using Moderate Resolution Imaging Spectroradiometer (MODIS) Deep Blue level 2 data. *Journal of Geophysical Research*, 115, D05204. [doi:10.1029/2009JD012398](https://doi.org/10.1029/2009JD012398)

Goudie, A.S., 1978. Dust storms and their geomorphological implications. *Journal of Arid Environments*, 1, 291-310.

Goudie, A.S., 1983. Dust storms in space and time. *Progress in Physical Geography*, 7, 502-530. [doi: 10.1177/030913338300700402](https://doi.org/10.1177/030913338300700402)

Goudie, A.S., 2009. Dust storms: recent developments. *Journal of Environmental Management*, 90, 89-94. [doi:10.1016/j.jenvman.2008.07.007](https://doi.org/10.1016/j.jenvman.2008.07.007)

Grayson, D.K., 2011. *The Great Basin: A Natural Prehistory*. University of California Press: Berkeley CA, 418p.

Griffin, D.W., 2007. Atmospheric movement of microorganisms in clouds of desert dust and implications for human health. *Clinical Microbiology Reviews*, 20, 459-477. [doi: 10.1128/CMR.00039-06](https://doi.org/10.1128/CMR.00039-06)

Hallar, A.G., Chirokova, G., McCubbin, I., Painter, T.H., Wiedinmyer, C., and Dodson, C., 2011. Atmospheric bioaerosols transported via dust storms in the western United States. *Geophysical Research Letters*, 38, L17801. [doi:10.1029/2011GL048166](https://doi.org/10.1029/2011GL048166)

Hanna, S.R., Britter, R., Franzese, P., 2003. A baseline urban dispersion model evaluated

with Salt Lake City and Los Angeles tracer data. *Atmospheric Environment*, 37, 5069–5082. [doi:10.1016/j.atmosenv.2003.08.014](https://doi.org/10.1016/j.atmosenv.2003.08.014)

Hashizume, M., Ueda, K., Nishiwaki, Y., Michikawa, T., Onozuka, D., 2010. Health effects of Asian dust events: a review of the literature. *Japan Journal Hygiene*, 65, 413–421.

Horel, J., Splitt, M., Dunn, L., Pechmann, J., White, B., Ciliberti, C., Lazarus, S., Slemmer, J., Zaff, D., Burks, J., 2002. Mesowest: cooperative mesonets in the western United States. *Bulletin of the American Meteorological Society*, 83, 211–225. [doi:10.1175/1520-0477\(2002\)083<0211:MCMITW>2.3.CO;2](https://doi.org/10.1175/1520-0477(2002)083<0211:MCMITW>2.3.CO;2)

Jeglum, M.E., Steenburgh, W.J., Lee, T.P., Bosart, L.F., 2010. Multi-reanalysis climatology of intermountain cyclones. *Monthly Weather Review*, 138, 4035–4053. [doi:10.1175/2010MWR3432.1](https://doi.org/10.1175/2010MWR3432.1)

Jewell, P.W., Nicoll, K., 2011. Wind regimes and aeolian transport in the Great Basin, U.S.A. *Geomorphology*, 129, 1–13. [doi:10.1016/j.geomorph.2011.01.005](https://doi.org/10.1016/j.geomorph.2011.01.005)

Johnston, F., Hanigan, I., Henderson, S., Morgan, G., Bowman, D., 2011. Extreme air pollution events from brushfires and dust storms and their association with mortality in Sydney, Australia 1994–2007. *Environmental Research*, 111, 811–816. [doi:10.1016/j.envres.2011.05.007](https://doi.org/10.1016/j.envres.2011.05.007)

Kalnay, E., Kanamitsu, M., Kistler, R., Collins, W., Deaven, D., Gandin, L., Iredell, M., Saha, S., White, G., Woollen, J., Zhu, Y., Leetmaa, A., Reynolds, R., Chelliah, M., Ebisuzaki, W., Higgins, W., Janowiak, J., Mo, K.C., Ropelewski, C., Wang, J., Jenne, R., Joseph, D., 1996. The NCEP/NCAR Reanalysis 40-year Project. *Bulletin American Meteorological Society*, 77, 437–471. [doi:10.1175/1520-0477\(1996\)077<0437:TNYP>2.0.CO;2](https://doi.org/10.1175/1520-0477(1996)077<0437:TNYP>2.0.CO;2)

Katragkou, E., Kazadzis, S., Amiridis, V., Papaioannou, V., Karathanasis, S., Melas, D., 2009. PM₁₀ regional transport pathways in Thessaloniki, Greece. *Atmospheric Environment*, 43, 1079–1085. [doi:10.1016/j.atmosenv.2008.11.021](https://doi.org/10.1016/j.atmosenv.2008.11.021)

Kohfeld, K.E., Reynolds, R. L., Pelletier, J.D., Nickling, B., 2005. Linking the scales of observation, process, and modeling of dust emissions. *EOS*, 86, 113–114. [doi:10.1029/2005EO110005](https://doi.org/10.1029/2005EO110005)

Lee, J.A., Gill, T.E., Mulligan, K.R., Dominguez Acosta, M., Perez, A.E., 2009. Land use/land cover and point sources of the 15 December 2003 dust storm in southwestern North America. *Geomorphology*, 105, 18–27. [doi:10.1016/j.geomorph.2007.12.016](https://doi.org/10.1016/j.geomorph.2007.12.016)

Long, R.W., N. L., Mangelson, N.F., Thompson, W. Fiet, K., Smith, S., Smith, R., Eatough, D.J., Pope, C.A., Wilson, W.E., 2003. The measurement of PM_{2.5}, including semi-volatile components, in the EMPACT program: results from the Salt Lake City

Study. *Atmospheric Environment*, 37, 4407–4417. [doi:10.1016/S1352-2310\(03\)00585-5](https://doi.org/10.1016/S1352-2310(03)00585-5)

Maffly, B., 2008. Storm Kicks Up Dust, Sets Off Health Advisory. *The Salt Lake Tribune*, April 20, 2008.

Malek, E., Davis, T., Martin, R.S., Silva, P.J., 2006. Meteorological and environmental aspects of one of the worst national air pollution episodes (January, 2004) in Logan, Cache Valley, Utah, USA. *Atmospheric Research*, 79, 108-122.
[doi:10.1016/j.atmosres.2005.05.003](https://doi.org/10.1016/j.atmosres.2005.05.003)

McGowan, H., Clark, A., 2008. Identification of dust transport pathways from Lake Eyre, Australia using Hysplit. *Atmospheric Environment*, 42, 6915–6925.
[doi:10.1016/j.atmosenv.2008.05.053](https://doi.org/10.1016/j.atmosenv.2008.05.053)

Miller, S.D., Kuciauskas, A.P., Liu, M., Ji, Q., Reid, J.S., Breed, D.W., Walker, A.L., Mandoos, A.A., 2008. Haboob dust storms of the southern Arabian Peninsula, *Journal of Geophysical Research*, 113, D01202. [doi:10.1029/2007JD008550](https://doi.org/10.1029/2007JD008550)

National Climatic Data Center (NCDC), 2011. Global Integrated Surface Hourly (ISH) database. <http://www.ncdc.noaa.gov/oa/land.html>

National Oceanic and Atmospheric Administration (NOAA), 2011. Air Resources Laboratory READY - Real-time Environmental Applications and Display sYstem. <http://ready.arl.noaa.gov/>

Neff, J.C., Ballantyne, A.P., Farmer, G.L., Mahowald, N.M., Conroy, J.L., Landry, C.C., Overpeck, J.T., Painter, T.H., Lawrence, C.R., Reynolds, R.L., 2008. Increasing eolian dust deposition in the western United States linked to human activity. *Nature Geoscience*, 1, 189-195. [doi:10.1038/ngeo133](https://doi.org/10.1038/ngeo133).

Novlan, D.J., Hardiman, M., Gill, T.E., 2007. A synoptic climatology of blowing dust events in El Paso, Texas from 1932-2005. Preprints, 16th Conference on Applied Climatology, American Meteorological Society, no. J3.12.

Painter, T.H., Barrett, A.P., Landry, C.C., Neff, J.C., Cassidy, M.P., Lawrence, C.R., McBride, K.E., Farmer, G.L., 2007. Impact of disturbed desert soils on duration of mountain snow cover. *Geophysical Research Letters*, 34, L12502.
[doi:10.1029/2007GL030284](https://doi.org/10.1029/2007GL030284)

Painter, T.H., Deems, J.S., Belnap, J., Hamlet, A.F., Landry, C.C., Udall, B., 2010. Response of Colorado River runoff to dust radiative forcing in snow. *Proceedings of the National Academy of Sciences*, 107, 17125-17130. [doi: 10.1073/pnas.0913139107](https://doi.org/10.1073/pnas.0913139107)

Park, S.H., Gong, S.L., Gong, W., Makar, P.A., Moran, M.D., Stroud, C.A., Zhang, J., 2009. Sensitivity of surface characteristics on the simulation of wind-blown-dust source in North America. *Atmospheric Environment*, 43, 3122–3129.

[doi:10.1016/j.atmosenv.2009.02.064](https://doi.org/10.1016/j.atmosenv.2009.02.064)

Pauley, P.M., Baker, N.L., Barker, E.H., 1996. An observational study of the “Interstate 5” dust storm case. *Bulletin American Meteorological Society*, 77, 693-720. DOI: [10.1175/1520-0477\(1996\)077<0693:AOSOTD>2.0.CO;2](https://doi.org/10.1175/1520-0477(1996)077<0693:AOSOTD>2.0.CO;2)

Pope III, C.A., 1991. Respiratory hospital admissions associated with PM₁₀ pollution in Utah, Salt Lake, and Cache Valleys. *Archives of Environmental Health*, 46, 90–97. [doi:10.1080/00039896.1991.9937434](https://doi.org/10.1080/00039896.1991.9937434)

Princevac, M., Venkatram, A., 2007. Estimating micrometeorological inputs for modeling dispersion in urban areas during stable conditions. *Atmospheric Environment*, 41, 5345–5356. [doi:10.1016/j.atmosenv.2007.02.029](https://doi.org/10.1016/j.atmosenv.2007.02.029)

Prospero, J.M., Ginoux, P., Torres, O., Nicholson, S.E., Gill, T.E., 2002. Environmental characterization of global sources of atmospheric soil dust identified with the NIMBUS-7 TOMS absorbing aerosol product. *Reviews of Geophysics*, 40, 2-1–2-31. [doi:10.1029/2000RG000095](https://doi.org/10.1029/2000RG000095)

Reynolds, R.L., Yount, J.C., Reheis, M.C., Goldstein, H., Chavez Jr., P., Fulton, R., Whitney, J., Fuller, C., Forester, R.M., 2007. Dust emission from wet and dry playas in the Mojave Desert. *Earth Surface Processes and Landforms*, 32, 1811-1827. DOI: [10.1002/esp](https://doi.org/10.1002/esp)

Reheis, M.C., 2003. Dust deposition in Nevada, California and Utah, 1984-2002. U.S. Geological Survey Open-File Report 03-138. http://pubs.usgs.gov/of/2003/ofr-03-138/ofr_03_138_508.pdf

Reheis, M.C., 2006. A 16-year record of eolian dust in Southern Nevada and California, USA: Controls on dust generation and accumulation. *Journal of Arid Environments*, 67, 487-520. [doi:10.1016/j.jaridenv.2006.03.006](https://doi.org/10.1016/j.jaridenv.2006.03.006)

Rivera Rivera, N.I., Gill, T.E., Gebhart, K.A., Hand, J.L., Bleiweiss, M.P., Fitzgerald, R.M., 2009. Wind modeling of Chihuahan Desert dust outbreaks. *Atmospheric Environment*, 43, 347-354. [doi:10.1016/j.atmosenv.2008.09.069](https://doi.org/10.1016/j.atmosenv.2008.09.069)

Roberts, S., Martin, M.A., 2006. Investigating the mixture of air pollutants associated with adverse health outcomes. *Atmospheric Environment*, 40, 984–991. [doi:10.1016/j.atmosenv.2005.10.022](https://doi.org/10.1016/j.atmosenv.2005.10.022)

Rogers, E. and coauthors, 2009. The NCEP North American mesoscale modeling system: recent changes and future plans. 23rd Conf. on Weather Analysis and Forecasting/19th Conf. on Numerical Weather Prediction, Omaha, NE, American Meteorological Society 2A.4.

Sandstrom, T., Forsberg, B., 2008. Desert dust, an unrecognized source of dangerous air

pollution? *Epidemiology*, 19, 808-809.

Shafer, J.C., Steenburgh, W.J., 2008. Climatology of strong intermountain cold fronts. *Monthly Weather Review*, 136, 784-807. DOI: [10.1175/2007MWR2136.1](https://doi.org/10.1175/2007MWR2136.1)

Shao, Y., 2008. *Physics and Modelling of Wind Erosion*, 2nd ed. Springer Science Business Media B.V., Dordrecht.

Shaw, P., 2008. Application of aerosol speciation data as an in situ dust proxy for validation of the Dust Regional Atmospheric Model (DREAM). *Atmospheric Environment*, 42, 7304–7309. doi:[10.1016/j.atmosenv.2008.06.018](https://doi.org/10.1016/j.atmosenv.2008.06.018)

Sheppard, P.R., Comrie, A.C., Packin, G.D., Angersbach, K., Hughes, M.K., 2002. The climate of the US Southwest. *Climate Research*, 21, 219-238. DOI: [10.3354/cr021219](https://doi.org/10.3354/cr021219)

Steenburgh, W.J., Neuman, C.R., West, G.L., Bosart, L.F., 2009. Discrete frontal propagation over the Sierra-Cascade mountains and intermountain west. *Monthly Weather Review*, 137, 2000-2020. doi: [10.1175/2008MWR2811.1](https://doi.org/10.1175/2008MWR2811.1)

Strong, C.L., Parsons, K., McTainsh, G.H., Sheehan, A., 2010. Dust transporting wind systems in the lower Lake Eyre Basin, Australia: a preliminary study. *Aeolian Research*, 2, 205-214. doi:[10.1071/SR9900323](https://doi.org/10.1071/SR9900323)

Utah Division of Air Quality, 2011. PM10 & PM2.5 Exceptional Event – High Wind. Event Date - March 30, 2010.

Tanaka, T.Y., Chiba, M. 2006. A numerical study of the contributions of dust source regions to the global dust budget. *Global and Planetary Change*, 52, 88-104. doi:[10.1016/j.gloplacha.2006.02.002](https://doi.org/10.1016/j.gloplacha.2006.02.002)

Tegen, I., Werner, M., Harrison, S.P., Kohfeld, K.E. 2004. Relative importance of climate and land use in determining present and future global soil dust emission. *Geophysical Research Letters*, 31, L05105. doi:[10.1029/2003GL019216](https://doi.org/10.1029/2003GL019216)

U.S. Census Bureau, 2010. State and County QuickFacts. <http://quickfacts.census.gov/qfd/states/49/49035.html>

U.S. Environmental Protection Agency, 2011. National Ambient Air Quality Standards (NAAQS).

Washington, R., Todd, M.C., Lizcano, G., Tegen, I., Flamant, C., Koren, I., Ginoux, P., Engelstaedter, S., Bristow, C.S., Zender, C.S., Goudie, A.S., Warren, A., Prospero, J.M., 2006. Links between topography, wind, deflation, lakes and dust: the case of the Bodele Depression, Chad. *Geophysical Research Letters*, 3, L09401. doi:[10.1029/2006GL025827](https://doi.org/10.1029/2006GL025827)

West, G.L., Steenburgh, W.J., 2010. Life cycle and mesoscale frontal structure of an intermountain cyclone. *Monthly Weather Review*, 138, 2528-2545. [doi: 10.1175/MWR-D-10-05076.1](https://doi.org/10.1175/MWR-D-10-05076.1)

Wigner, K.A., Peterson, R.E., 1987. Synoptic climatology of blowing dust on the Texas South Plains, 1947-84. *Journal of Arid Environments*, 13, 199-209.

Woodward, S., 2001. Modeling the atmospheric life cycle and radiative impact of mineral dust in the Hadley Centre climate model. *Journal of Geophysical Research*, 106, 155-18,166. [doi:10.1029/2000JD900795](https://doi.org/10.1029/2000JD900795)

World Meteorological Organization (WMO), 2010. Manual on Codes (WMO-No. 306). <http://www.wmo.int/pages/prog/www/WMOCodes.html>

Yang, Y.Q., Hou, Q., Zhou, C.H., Liu, H.L., Wang, Y.Q., Niu, T., 2008. Sand/dust storm processes in Northeast Asia and associated large-scale circulations. *Atmospheric Chemistry and Physics*, 8, 25–33. [DOI: 10.5194/acp-8-25-2008](https://doi.org/10.5194/acp-8-25-2008)

Zender, C.S., Bian, H., Newman, D., 2003. Mineral Dust Entrainment and Deposition (DEAD) model: description and 1990s dust climatology. *Journal of Geophysical Research*, 109, 4416-4435. [doi:10.1029/2002JD002775](https://doi.org/10.1029/2002JD002775)

Zhang, X.Y., Arimoto, R., An, Z.S., 1997. Dust emission from Chinese desert linked to variations in atmospheric circulation. *Journal of Geophysical Research*, 102, 28041-28047. [doi:10.1029/97JD02300](https://doi.org/10.1029/97JD02300)

CHAPTER 3

GEOMORPHIC AND LAND COVER IDENTIFICATION OF DUST SOURCES IN THE EASTERN GREAT BASIN OF UTAH, U.S.A.¹

3.1 Abstract

This study identifies anthropogenically disturbed areas and barren playa surfaces as the two primary dust source types that repeatedly contribute to dust storm events in the eastern Great Basin of western Utah, USA. This semiarid desert region is an important contributor to dust production in North America, with this study being the first to specifically identify and characterize regional dust sources. From 2004-2010, a total of 51 dust event days (DEDs) affected the air quality in Salt Lake City, UT. MODIS satellite imagery during 16 of these DEDs was analyzed to identify dust plumes, and assess the characteristics of dust source areas. A total of 168 plumes were identified, and showed mobilization of dust from Quaternary deposits located within the Bonneville Basin. This analysis identifies four major and five secondary source areas for dust in this region, which produce dust primarily during the spring and fall months and during moderate or

¹ Reprinted from *Geomorphology*, 204, Hahnenberger, M., Nicoll, K., Geomorphic and land cover identification of dust sources in the eastern Great Basin of Utah, U.S.A., 657-672, Copyright (2014), with permission from Elsevier.

greater drought conditions, with a Palmer Drought Index (PDI) of -2 or less. The largest number of observed dust plumes (~60% of all plumes) originated from playas (ephemeral lakes) and are classified as barren land cover with a silty clay soil sediment surface. Playa surfaces in this region undergo numerous recurrent anthropogenic disturbances, including military operations and anthropogenic water withdrawal. Anthropogenic disturbance is necessary to produce dust from the vegetated landscape in the eastern Great Basin, as evidenced by the new dust source active from 2008-2010 in the area burned by the 2007 Milford Flat fire; this fire was the largest in Utah's history due to extensive cover of invasive cheatgrass (*Bromus tectorum*) along with drought conditions. However, dust mobilization from the Milford Flat Burned Area (MFBA) was limited to regions that had been significantly disturbed by postfire land management techniques that consisted of seeding, followed by chaining or tilling of the soil. Dust storms in the eastern Great Basin negatively impact air quality and transportation in the populated regions of Utah; this study details an improved forecasting protocol for dust storm events that will benefit transportation planning and improve public health.

3.2. Introduction

Dust entrainment, transport, and deposition are important geomorphic surface processes that impact multiple disciplines, including public health, hydroclimatology, and ecosystem ecology (e.g., McTainsh and Strong, 2007). Dust transport in dryland regions elevates particulate matter levels above health advisory thresholds (Griffin, 2007; Dayan et al., 2011; Hahnenberger and Nicoll, 2012), and can adversely impact human health (Pope III et al., 1995; Derbyshire, 2007; Brook et al., 2010; Hashizume et al., 2010;

Grineski et al., 2011; Johnston et al., 2011). In some cases, dust transport of bacteria, viruses, and fungi have caused disease (Kellogg and Griffin, 2006), including outbreaks of Valley Fever in the western U.S. (Williams et al., 1979; Sing and Sing, 2010).

Dust deposition on mountain snowpack affects the radiation balance, accelerating seasonal melting and reducing springtime runoff totals in the Colorado River watershed (Painter et al., 2007, 2009). Dust transport removes nutrients in source areas and contributes nutrients in deposition region, which has ecological implications (Reynolds et al., 2001, 2006; Prospero, 2002; McTainsh and Strong, 2007; Hasselquist et al., 2011; Sankey et al., 2012a). Further, aeolian inputs of organic materials such as pollen, seeds, bacteria, and fungi can affect the function of sensitive ecosystems, such as coral reefs and alpine regions (Hallar et al., 2011). Atmospheric processes can be directly influenced by the absorption and scattering of radiation by dust, and dust also acts as microphysically active species in clouds, functioning as condensation nuclei (Twohy et al., 2009; Chen et al., 2010; Wang and Niu, 2013). Changes in dust transport have the potential to affect climate on both regional and global scales (Maher et al., 2010; Martinez-Garcia et al., 2011).

Assessing dust origins and the relative contribution from anthropogenic land use (e.g., agriculture, mining, disturbance events) as compared with “natural” dust sources (e.g., playas, aeolian deposits) and natural disturbance events (e.g., wildfire, flood, landslide) remains an unsettled question; estimates of the human caused component of dust production from a region range from 10 to 50 % (Tegen and Fung, 1995; Tegen et al., 2004; Ginoux et al., 2012). Determining the fraction of dust produced by human activities is complicated by the variable range of scales of the processes involved in dust

dynamics. Entrainment of dust into the atmosphere can occur on the microscale (Sankey et al., 2012b), while transport is most obvious and observable at regional and global scales (Ginoux et al., 2012). To effectively identify dust sources and track dust transport it is necessary to cross from the microscale to the mesoscale and then to the regional scale. Coarse scale satellite remote sensing is not sufficient to identify individual dust sources such as a single fallow field in an agricultural region or the margin of a playa (e.g., Crouvi et al., 2012). Environmental controls on dust production operate at local spatial scales, and include these factors: (1) lack of aggregation or surface crusting of sediments; (2) vegetation cover and spatial arrangement; (3) availability of surface areas with silt sized particles; and (4) wind speeds sufficient to overcome threshold friction velocities (Gillette, 1999). Models estimating dust transport tend to be global in scale and at low spatial resolution, and must parameterize these small scale processes. Furthermore, dust transport models lack high resolution datasets of dust sources at global, regional, and local scales.

Methods for identifying dust sources typically have analyzed datasets with relatively low resolution over broad regions (e.g., Prospero et al., 2002; Ginoux et al., 2012). In order to more accurately predict and model dust transport, high resolution, local scale observations about dust source location are required. Bullard et al. (2011) proposed a methodology for categorizing dust sources based on geomorphic characteristics determined using medium resolution (1-10 km) satellite data. Lee et al. (2012) further developed a classification to include land cover classes of dust sources, which assessed the anthropogenic vs. natural contributions.

In a global assessment of dust loading using satellite data, Prospero et al. (2002)

highlighted the eastern Great Basin as a major source area for dust export in North America. Recent studies of the eastern Great Basin hydrographic region showed a direct linkage between dust storm meteorology and elevated particulate levels in the Salt Lake City metropolitan area (SLC) of Utah, where exceedances of federal air quality standards affect more than 2 million people (Hahnenberger and Nicoll, 2012). The dust storms occur in the afternoon and can decrease visibility and endanger transportation, particularly during the spring months. Popular reports about dust storms and “raining mud” date back to the 1930s in western Utah (Brough et al., 1987). While seasonal dust storms are generally considered “natural events” that originate from uninhabited areas, specific dust sources in the eastern Great Basin are not well described. This landscape is generally uninhabited, but has been significantly affected by cattle and sheep grazing, water withdrawal for agriculture, agricultural fields left fallow, military operations, cheatgrass (*Bromus tectorum*) invasion, wildfire, and related reclamation programs (Hahnenberger and Nicoll, 2012; Miller et al., 2012). The accurate delineation of dust source areas and relation to the dominant hydroclimatic controls and meteorological events affecting this region is critical for the potential forecasting, mitigation and/or prevention of dust storm events and their adverse effects.

This study describes actively eroding landscape elements that act as dust sources in the eastern Great Basin; we identify the specific geomorphic surfaces and land cover types that produce dust within this region during specific days when high particulate levels were measured. MODIS satellite data are used to identify plumes and pinpoint specific locations of dust source areas, which is the most accurate and high resolution technique available (Lee et al., 2012). The methodology first identifies plumes, and then

describes source areas in context of the broader landscape. We characterize the eastern Great Basin landscape in a way that is specific to this region, because it is generally less vegetated, and more topographically complex than other documented dust source regions of similar size, such as the Chihuahuan Desert and the Southern High Plains of Texas (Lee et al., 2009; Rivera Rivera et al., 2010; Baddock et al., 2011; Lee et al., 2012).

Various studies of dust sources in deserts of the U.S. at the regional scale have focused on collected dust (Reheis, 2003, 2006), and others have identified plumes during a single dust event, over one year or over a few years (Lee et al., 2009, 2012; Rivera Rivera et al., 2010). Our study of dust sources in the eastern Great Basin assesses seven years of data, and analyzes 16 dust event days in detail. The study period from 2004-2010 includes a moist interval and a persistent drought period, during which various disturbances, including continuous (e.g., water withdrawals, military operations, recreation) and episodic (e.g., wildfire, land rehabilitation practices) disturbances occurred at specific locations (Miller et al., 2012). In this context, we analyzed the temporal and spatial variability of dust sources in the eastern Great Basin, examined some of the ascendant controls, and characterized these source areas for comparison with other known dust production regions throughout the world (e.g., Wang et al., 2006, 2008; Warren et al., 2007; Bullard et al., 2008, 2011; Lee et al., 2009, 2012; Rivera Rivera et al., 2010). This study aims to (1) identify dust sources using a landform approach and a combination of satellite data and field observation, (2) specifically identify anthropogenic activities that are potentially contributing to increased dust flux from source regions, (3) identify meteorological conditions associated with large dust events in the region and air quality impact on nearby populated regions, (4) put the eastern Great Basin in a regional

and global context relative to other dust producing areas, and (5) provide a solution to the problem of forecasting and warning dust storms in the eastern Great Basin.

3.3. Regional setting of study area

The Great Basin is a hydrographically closed, internally drained portion of the western USA (Frémont, 1845), and the largest desert region in North America. As part of the larger Basin and Range physiographic province, the terrain has a characteristic topography with alternating mountain ranges and valleys (Fig. 3.1). The analysis region for this study was limited to the western part of the state of Utah, with boundaries of latitudes 37 - 42° N, and longitudes 111 - 114° W (Fig. 3.2). The Basin and Range has many north-south trending mountain ranges, many of which are >3,000 m in elevation; the mountains are typically composed of Precambrian – Palaeozoic sedimentary rocks, and some Tertiary igneous rocks (Grayson, 2011). The high relief between the elevated ranges and the basin valleys is delineated by N-S trending normal faults. Along the mountain front, alluvial fans intermittently erode sediments and deposit materials downslope and into the intermontane valleys, which act as local sinks for sediment and water runoff (Oviatt, 2003; Grayson, 2011). As such, terminal lakes or playas comprise local base levels that are not integrated into fluvial systems that drain into the Pacific Ocean.

The largest subbasin in the eastern portion of the hydrographic Great Basin is the Bonneville Basin, which was first described by G.K. Gilbert (1890). During the Late Pleistocene, much of this basin contained standing water. At its maximum extent ~20,000 BP, Lake Bonneville had a surface area in excess of 50,000 km² and with possible

drainage to the Pacific Ocean via the Snake and Columbia drainages when the water volume exceeded $>10,000 \text{ km}^3$. Erosion and deposition associated with the dynamics of Pleistocene Lake Bonneville resurfaced much of the lowland areas in western Utah (Oviatt, 1997; Oviatt et al., 2003). The Great Salt Lake is the modern remnant of ancient Lake Bonneville, which regressed and became hypersaline as its water volume was reduced as a function of hydroclimatic change through the Holocene (Grayson, 2011).

The modern region of western Utah is dominated by a semiarid cold desert environment, which can support a shrub and steppe vegetation (*Artemesia*, or sage, dominant) with occasional woodland elements, particularly at higher elevations (Wise, 2012). Much of the year is characterized by low precipitation and clear skies due to the quasipermanent subtropical high pressure ridge positioned over the region, which is only occasionally displaced by low pressure systems originating over the Pacific Ocean (Sheppard et al., 2002). Precipitation, while limited, reaches a maximum in the winter and spring, with limited summer rainfall contributed by the North American Monsoon (Adams and Comrie, 1997).

Dust events in the eastern Great Basin region peak in the spring, with additional occurrences during the early fall (Hahnenberger and Nicoll, 2012). This is consistent with the ascendant meteorological pattern of strong intermountain cyclones that strengthen in the Great Basin Confluence Zone (GBCZ) over Nevada during the spring and fall months. The GBCZ is formed from low to midlevel winds that are blocked by the Sierra Nevada as they approach from the west and then converge downstream of the Sierra Nevada over central Nevada. The confluence over central Nevada acts to intensify the surface temperature gradient, increasing pressure gradients, and creates stronger winds

preceding the surface front. The cyclonic storms produce strong prefrontal warm and dry winds, termed Hatu winds (Eubank and Brough, 1979). The position of Salt Lake City is situated at a local maximum for these strong frontal passages, due to the intensification that occurs just west of the eastern Great Basin (Shafer and Steenburgh, 2008). Prefrontal dry winds are a known dust producer in other regions of the world (e.g., Liu et al., 2004). Additionally, in the eastern Great Basin, Basin and Range physiography tends to channel and sometimes further intensifies winds flowing in alignment with the north-south trend of the mountain physiography (Hahnenberger and Nicoll, 2012).

These dust storms caused by strong prefrontal winds are distinctly different from the haboob type dust storms that are common in arid regions throughout the world (Brazel and Nickling, 1986; Miller et al., 2008; Seigel and van den Heever, 2012). Haboobs are formed from the cold outflows, or gust fronts, emerging from mesoscale convection, such as the thunderstorms that form in the Arizona summer as part of the North American Monsoon (Adams and Comrie, 1997). Forecasting of mesoscale thunderstorms and the haboob dust storms they produce is challenging because these phenomena occur on the scale of minutes to hours. While haboobs can occur in our region of study, most regional scale dust storms affecting the eastern Great Basin, however, are formed by synoptic scale weather systems that develop over a much longer time scale and, therefore, they can be forecasted days in advance (Hahnenberger and Nicoll, 2012). However, similar to haboob type events, these dust storms do not last multiple days in most cases, and the effects seen in the populated regions are felt only a couple hours after dust transport begins, due to the distance between the dust sources and the population centers in Utah.

While the primary control of dust in this region is winds of sufficient speed to dislodge and loft sediment, there are several other factors that affect erosion and dust production in the eastern Great Basin. First, there is the necessary condition of a supply of sediment that can be entrained. This is often determined by sediment or soil type, and can vary due to runoff supplying sediment and creation of efflorescent evaporite minerals that precipitate from shallow groundwater (Reynolds et al., 2007). Therefore, geomorphic settings that tend to collect sediment, such as terminal dry lakes (playas), alluvial and fluvial landforms, and aeolian deposits, all have potential to generate dust (Gill and Cahill, 1992; Gill, 1996; Bullard et al., 2011). A second factor that reduces threshold friction velocities is the absence of nonerodible roughness elements, such as plants, and/or the absence of physical or biological soil crusts, which bind the soils (Belnap and Gillette, 1998; Urban et al., 2009). Land cover types that are characterized by little vegetation or areas that have undergone either natural or anthropogenic disturbance that removed vegetation or soil crusts will have a higher propensity for dust transport (Goossens and Buck, 2009).

The presence or absence of drought conditions can exacerbate dust in some regions, particularly if it causes a decrease in threshold friction velocities (McTainsh et al., 1998). Further, in the adjacent physiographic region of the Colorado Plateau, increasing mean annual temperatures lead to decreasing perennial grass cover in some location, which causes a higher susceptibility to erosion by high winds that is further exacerbated by soil disturbance (Munson et al., 2011). Paleoclimatic records in the southwestern United States indicate that long periods of elevated temperatures and drought were present over the past 1,200 years, which were more severe than droughts

during the historic record (Woodhouse et al., 2009). It is plausible, therefore, that similar long and severe droughts will occur in future times in this region. However, drought conditions in a region are not solely sufficient to initiate dust transport; other necessary conditions must be met, or a disturbance event that lowers threshold velocities can induce dust entrainment and transport (Miller et al., 2012).

3.4. Methods and datasets

3.4.1 Defining dust event days (DEDs)

Meteorological datasets over the period from 2004-2010 were acquired from the National Climatic Data Center (NCDC) Global Integrated Surface Hourly (ISH) database (NCDC, 2012) for stations at Delta, UT and Salt Lake City International Airport, UT (hereafter, SLCIA) (Table 3.1). We designated a dust event day (DED) when at least one recorded observation at Delta or SLCIA stations contained a weather code for airborne dust (06, 07, 08, 09, 30, 31, 32, 33, 34, and 35; WMO code 4677, WMO 2010). This dataset and the methodology are described in Hahnenberger and Nicoll (2012). Wind data from these stations, at the standard height of 10 m, was used to characterize the regional wind setting during DEDs.

Air quality parameters during DEDs were obtained from the Division of Air Quality (DAQ) of Utah's Department of Environmental Quality (DEQ) network (DAQ, 2011) (Table 3.1). We compiled daily average values for particulate matter pollutants PM_{10} and $PM_{2.5}$ (PM with aerodynamic diameters <10 and $2.5 \mu m$, respectively) collected by manual gravimetric samplers at stations located in Utah's most populated areas. Daily 24-hr values were obtained to be compared to the Environmental Protection

Agency (EPA) National Ambient Air Quality Standards (NAAQS) 24-hr standards for PM_{10} and $\text{PM}_{2.5}$ of 150 and $35 \mu\text{g m}^{-3}$, respectively.

Meteorological drought was characterized for western Utah during the study period, using the monthly Palmer Drought Index (PDI), also known as the Palmer Drought Severity Index (PDSI), from the North American Drought Monitor (NADM) (NOAA NCDC, 2012). The PDI is a long term cumulative meteorological index that takes into account precipitation, temperature, and water content of the soil to describe the water balance in the region. Despite its utility, the PDI does not fully take into account the complex hydrology of lake, reservoir, and snowpack storage and related delayed runoff (Heim, 2002). We used the PDI to ascribe the coincidence of DEDs with broad hydroclimatic trends in the region.

3.4.2 MODIS imagery on DEDs

We collated available imagery from Moderate Resolution Imaging Spectroradiometer (MODIS) on the Terra and Aqua satellites (LANCE, 2012) for all DEDs over the time period 2004-2010. Over this duration, there were 51 DEDs in all, of which 49 DEDs had data from the MODIS sensor aboard either the Terra or Aqua satellite. The related images were then assessed in the eastern Great Basin study region, which were delimited to the area within Utah between the latitudes 37° - 42° N, and longitudes 111° - 114° W. True color imagery was examined at a resolution of 250 m, which assigns RGB to bands 1 (620-670 nm), 4 (545-565 nm), and 3 (459-479 nm). Images from both the Terra and Aqua satellites were examined on each day to detect dust events that may only be active or visible during the overpass of each satellite, and to

detect which plumes were active at different times of day. The eastern Great Basin overpass times for the Terra and Aqua satellites are between 1000-1200 MST (1700-1900 UTC) and 1300-1500 MST (2000-2200 UTC), respectively.

3.4.3 Dust plume recognition

Dust plumes were identified on the MODIS imagery using criteria of Bullard et al. (2008), Lee et al. (2009), and Walker et al. (2009). Recognition of plumes was based on the following attributes: opacity (whether the dust plume blocked view of surface features near source, then became increasingly transparent due to dispersal); color (brown or tan); shape (cone shaped, starting from a point and spreading out in direction of dispersal); and plume direction (cardinal orientation of the dispersion, and correlation with other plumes in the same image) (Fig. 3.3). If it was unclear whether a potential plume was actually airborne dust, or a surface feature, the image for that day was compared to clear sky imagery in Google Earth™. In this way we were able to ensure that other surface features were not mistaken for dust plumes, and vice versa. In cases where it was unclear if a plume was a cloud or a dust plume, MODIS 7-2-1 imagery were analyzed. In this imagery red, green, and blue are assigned channels 7 (2155 nm), 2 (876 nm), and 1 (670 nm), respectively; this assignment places clouds in light blue and water bodies in dark blue to black, and permits the discrimination of surface features, and dust plumes.

Images that contained at least one visible dust plume within the study area were further analyzed to describe plume locations and to identify local point sources; in all, this satellite dataset included 24 images from 16 of the observed DEDs (Fig. 3.3). The

MODIS Terra data recorded 11 days with visible plumes, and MODIS Aqua data recorded 13 days with visible plumes. These 24 images were systematically analyzed, and a total of 168 individual dust plumes were identified (Appendix A). On individual images, the number of identified plumes ranged from 1 to 33. Factors that affected ability to detect visible plumes included: cloud cover, data quality (due to satellite overpass location), whether plumes were active at the time of satellite overpass, and whether plumes were large enough to be detected (Lee et al., 2009).

3.4.4 Description of dust plume and source area attributes

Mapping plume locations for all the DEDs allowed the identification of local point sources for dust, the definition of dust source regions across the larger study area, and assessment of the anthropogenic influences on dust generation. We then were able to describe the related land cover, sediment/soil, and geomorphic characteristics for each point source and to upscale those observations in an assessment of dust source regions in the eastern Great Basin of Utah. High resolution land cover data classifications from the National Land Cover Database 2006 (NLCD2006) were used to characterize the surface type of dust source areas (Fry et al., 2011). NLCD2006 is a 16-class land cover classification created at a spatial resolution of 30 meters from unsupervised classification of Landsat satellite data for the conterminous United States. For each dust plume observed, a source area and land cover class was determined using ArcGIS.

Soil data were accessed from the Soil Survey Geographic (SSURGO) Database provided by the National Resource Conservation Service (NRCS) (Soil Survey Staff, 2012). Due to the remote nature of the dust source locations within the study area, point

scale soil data were not available, so we analyzed the most prominent soil in the map unit at the location of each dust point source. Soil texture class was also determined, and the primary soil texture class for each identified dust source region was assessed as the most common class in that region.

To assess and describe the geomorphic attributes of the observed dust source areas, we examined MODIS satellite data, Google Earth imagery, photographs, reports and published literature, and drew on field observations and personal knowledge. No standard geomorphic dataset or detailed quaternary maps are available for most of western Utah. For each dust source region identified, the standard categorization of Bullard et al. (2011) was applied.

3.5. Results

3.5.1 DED air quality and meteorology

Over the time frame from 2004-2010, there were 51 DEDs recorded, and we identified plumes on MODIS images on 16 days. During most of these 16 days, air quality stations recorded elevated PM_{10} and $\text{PM}_{2.5}$ values in the Salt Lake Metropolitan region (Table 3.2). Seven days out of the 16 DEDs had at least one station that exceeded the 24-hour NAAQS for PM_{10} ($>150 \mu\text{g m}^{-3}$), while three days exceeded the $\text{PM}_{2.5}$ standard ($>35 \mu\text{g m}^{-3}$). Some DEDs, however, do not exhibit elevated particulate levels in the Salt Lake Metropolitan region, which probably results from active dust sources that were not upwind of these sites on that day, or the dust being lofted and dispersed above the valley floor, where the air quality instruments are located. Further, the number of plumes detected does not predict the air quality values observed; the highest PM_{10} value

recorded, $424 \mu\text{g m}^{-3}$, on 30 March 2010 had only 17 plumes, while the day with the maximum number of plumes, 4 March 2009, had a maximum PM_{10} value of $200 \mu\text{g m}^{-3}$.

For each DED, the maximum wind speed during the time range of the MODIS overpasses was recorded for both SLCIA and Delta stations, along with the wind direction at that time. At SLCIA, 13 of 16 DEDs had winds with a mainly southerly direction, and Delta reported southerly winds 15 of the 16 days (Table 3.2). This wind pattern is consistent with previous observations made in this region (Jewell and Nicoll, 2011), and observations that the primary driver of dust transport is prefrontal dry southerly Hatu winds (Hahnenberger and Nicoll, 2012). Maximum wind speeds during these DEDs generally range from 10 to 20 m s^{-1} , which exceeds generally accepted thresholds for dust entrainment and transport (Marticorena, 1997).

3.5.2 Spatial variability of observed dust plumes

Spatial analysis of the 169 plumes observed on MODIS images during DEDs demonstrates that the eastern Great Basin does not produce dust uniformly. Instead, dust plumes originate from specific points in eroding features within the landscape, and certain areas are prone to reactivation. Fig. 3.3 shows the spatial distribution of dust plumes observed on the 3 March 2009 DED, with clusters of plumes in the productive regions. Analysis of the MODIS images indicates that plumes form in nine specific geographic regions; nearby place names were used to refer to these dust source areas (Table 3.3, Appendix A).

While most regions had identifiable plumes during numerous DEDs, two of the dust source regions, Pot Playas and Skull Valley, had identifiable plumes only during

single DEDs (Fig. 3.3). It is likely that these two source areas produce airborne dust during other DEDs, but plumes may not be detectable for a number of reasons, including: the plume is smaller in size than the pixel resolution of the satellite image; the dust concentration is too low to be discerned on the satellite imagery; sources are not actively eroding at the time of the particular satellite overpass; or the dust generated is obscured by (swamped by) the dust contributed from larger sources upwind.

Of the nine dust source regions, the largest numbers of dust plumes produced are located in four regions of the eastern Great Basin (Table 3.3): Great Salt Lake Desert - Dugway Proving Ground; Milford Flat Burned Area; Sevier Dry Lake; and Tule Dry Lake (Fig. 3.3). These four source regions consistently produce dust plumes in the MODIS imagery analyzed. These regions are not equal in size, however, and plumes are not uniformly located throughout each area.

3.5.2.1 Great Salt Lake Desert – Dugway Proving Ground

Great Salt Lake Desert - Dugway Proving Ground (GSLD – DPG) is the largest source area for dust, both in terms of number of plumes observed, and its areal extent. All the plumes in this region are located within the boundaries of the Dugway Proving Ground (DPG), which is a major test and training range for the Chemical, Biological, Radiological, Nuclear and high yield Explosives (CBRNE) Command. The DPG is closed to the public and comprises about 800,000 acres for “defensive developmental and operational testing and training in chemical and biological warfare in the areas of protection, detection and decontamination” (DPG, 2012). The GSLD is generally a nonvegetated playa surface fed by ephemeral streams (Oviatt et al., 2003). While many

locations within the region produce plumes, the two most active “hot spots” are located just south of Granite Peak and west of the town of Dugway in the south central GSLD. No dust plumes were identified in the GSLD north of Interstate 80.

3.5.2.2 Milford Flat Burned Area

The area producing the second highest number of dust plumes is in the Milford Flat Burned Area (MFBA), located west of the towns Fillmore and Kanosh, south of Delta, UT, and east of the Cricket Mountains. This region is a high plateau called Milford Flat, and it was the northern extent of the largest wildfire in Utah history; during July 2007. The Milford Flat fire burned over 145,000 hectares (363,046 acres) of piñon-juniper forest and sagebrush steppe parts of which are subject to cheatgrass invasion (Miller et al., 2012). After the fire, numerous different rehabilitation techniques were applied for soil stabilization and restoration, including drill seeding, single chaining, and imprinter seeding. Due to wind and lack of precipitation, some locations in the burned region had multiple treatments over numerous years (Miller et al., 2012). Prior to 2008, no dust plumes were identified from this region, whereas after the fire and postfire land treatments, we observed 52 plumes over the period from 2008-2010 (Fig. 3.4).

3.5.2.3 Sevier Dry Lake and Tule Dry Lake

The third and fourth largest producing areas of dust plumes are Sevier Dry Lake (SDL) and Tule Dry Lake (TDL). Tule Dry Lake is located in the Tule Valley, just west of the House Range. Sevier Dry Lake is located in the Sevier Desert, west of the Cricket Mountains, and is the terminus of the Sevier River. Both SDL and TDL are generally non

vegetated playa surfaces. Although Tule Dry Lake is a smaller geographic area than the Sevier Dry Lake, it produces nearly the same number of dust plumes, and these emanate at multiple points along a north-south oriented transect. The Sevier Dry Lake area does not have a uniform distribution of plumes, with most originating from the southern part and along the eastern and western margins. The northern part of the Sevier Dry Lake that does not exhibit any plumes is lower in topographic elevation, and is often wet during certain times of the year.

3.5.3 Temporal variability of observed dust plumes

The temporal variations of dust plumes observed are broadly consistent with previous seasonal analyses showing the greatest number of DEDs during the spring months of March and April, with a few events in the early fall (Hahnenberger and Nicoll, 2012) (Figs. 3.3, 3.4; Table 3.2). This seasonality is controlled by the synoptic meteorology, with strong prefrontal winds associated with strengthening cyclonic storms over the Great Basin during the spring, and to a lesser extent in the fall.

On an interannual time scale, there were a few moderate dust events in 2004, followed by a three year period with no visible plumes, and then an increase in dust events during the period from 2008-2010 (Fig. 3.4). While DEDs are recorded from 2005-2007, no plumes were visible on MODIS images during these days, possibly due to cloud cover, or because the dust plumes were not large or opaque enough to be visible at the satellite scale. During the study period, the Palmer Drought Index (PDI) indicates two main wet and dry periods (Fig. 3.4). A wet period lasting from late 2004 to the end of 2006 appears to have provided sufficient moist conditions to stabilize erodible landforms;

no dust plumes were visible during this period, though there were DEDs recorded at both Delta and SLCIA. From 2007-2009, the region generally experienced drought conditions. Drought is a perturbation that can increase dust production, but is not anthropogenic in origin. The combination of drought conditions, the disturbance of the Milford Flat fire, and subsequent postfire treatments affected the upsurge in dust events occurring during the period from 2008-2009 (Miller et al., 2012).

Prior to 2008, there were no plumes detected from the Milford Flat Burned Area, while following the fire and postfire treatments in 2007-2008, a large number of plumes were detected. However, there was a large increase in plumes detected from the Great Salt Lake Desert – Dugway Proving Ground, Sevier Dry Lake, and Tule Dry Lake during the 2008-2009 period, as well (Fig. 3.3). There are no known acute natural or anthropogenic disturbance events during that period for the other regions, though there were likely continuous recurrent disturbances affecting those regions, such as water withdrawal, military operations, and recreation. Therefore, the resulting increase in plumes in the playa regions is associated with the arrival of persistent drought to the eastern Great Basin in 2007 (Fig. 3.4). Dust plumes become more frequent as the PDI values drop below a value of -2, the threshold for moderate drought conditions (Heim, 2002). There is a lag period between the onset of drought in 2007 and the large numbers of dust plumes observed in the spring of 2008. This could be because the terminal lake basins (playas) might be covered with snow or meltwater during the winter months, and/or these geomorphic elements take longer to respond, as compared to the surrounding vegetated alluvial landscape. In vegetated landscapes the lag may be explained by senesced vegetation that establish during the moist to drought transition but still provide

soil stabilization during the early period of drought. Previous studies have shown that in nearby regions perennial grasses decrease following years of increased temperatures (Munson et al., 2012).

3.5.4 Land cover of dust sources

Barren land cover was identified at many active sites of erosion, comprising 101 dust plumes of the total 168 identified from source areas in the eastern Great Basin (Fig. 3.5). This relationship is expected, because vegetation increases threshold friction velocities and decreases the probability of dust transport (Urban et al., 2009). A large number of plumes are sourced in areas with shrub/scrub land cover; however, most of these plumes were located in the Milford Flat Burned Area, which was a shrub/scrub land cover that was disturbed in 2007 (Fig. 3.5). A small number of plumes originate from areas with a grassland/herbaceous land cover, although this type of land cover is not common in the eastern Great Basin. If we partition the vegetated land covers into those that were burned in the Milford Flat fire, and those that were not, we see that about 75% of plumes in these land cover types were burned in the 2007 fire (Fig. 3.5). Therefore, we conclude that vegetated landscapes in the eastern Great Basin are not typically prone to dust emission, unless they are disturbed.

3.5.5 Geomorphic and soil characteristics of dust source areas

Our regional assessment of dust sources described the geomorphic settings of the important dust producing source areas within the eastern Great Basin (Fig. 3.2). Dust plumes sourced to ephemeral lakes or playas are evident in these areas: Great Salt Lake

Desert-Dugway, Skull Valley, Sevier Dry Lake, Tule Dry Lake, and Pot Playas (Table 3.3). The dust source regions dominated by alluvial and fluvial landscape elements include Milford Flat Burned Area, Beaver Bottoms, Wah Wah Valley, and Beryl-Zane.

Silty clay soil is present in the source area for 98 dust plumes, out of 168 in total. This fine grained sediment texture is characteristic of playa features (Fig. 3.6). Other soil types that are being eroded at dust plume locations include variations of loam that occur in alluvial-fluvial settings. The playa surfaces exhibit greater salinity compared to the soil surfaces in the surrounding landscape, due to the terminal nature of the playa lakes (Appendix A).

3.6. Discussion

3.6.1 Comparing primary dust source areas

Ephemeral and dry lakes known as playas are a common dust source in deserts (Gill and Cahill, 1992; Gill, 1996; Mahowald et al., 2003), with 3 to 66% of dust point sources originating from them, depending on the region (Bullard et al., 2008, 2011; Lee et al., 2009, 2012; Rivera Rivera et al., 2010; Baddock et al., 2011). However, ephemeral lakes often cover only a very small percentage of the land surface in desert regions, and therefore have a large number of plumes relative to the amount of area covered by this geomorphic surface type (Lee et al., 2012). The Chihuahuan Desert that spans an area of southern New Mexico, western Texas, and northern Mexico features 48 to 51% of dust plumes from playas (Lee et al., 2009; Baddock et al., 2011; Bullard et al., 2011). The Sahara features a large percentage, ~66%, of plumes from dry and ephemeral lakes (Bullard et al., 2011).

Reynolds et al. (2007) indicated, however, that not all playa surfaces are equal when it comes to the propensity for dust emission, and that both playa hydrology and playa surface sediments control the type and amount of dust emitted. They observed that wet playas, with groundwater close to the surface, have dynamic surfaces with evaporite minerals forming that are often susceptible to wind erosion. Dry playas, whereby groundwater is at depth, have more static surfaces that inhibit dust emission, though could potentially emit dust if disturbed. This study of eastern Great Basin observed that 59.5% of dust plumes originated from playas; playa landscape features are characteristic of the Basin and Range topography within the Great Basin. Data are not available to determine whether the active playas in this region would be considered wet or dry playas from the definitions used by Reynolds et al. (2007). Further, anthropogenic disturbance of playa surfaces can lead to increased propensity for dust transport (Gill, 1996). The large number and size of playas in the eastern Great Basin is due to its many internal drainage networks and the legacy of Lake Bonneville, which covered most of the region during the Pleistocene.

Gillette et al. (1980) identify numerous geomorphological surface types that show a propensity for dust entrainment, namely, disturbed soils > sand dunes > alluvial and aeolian sand deposits > disturbed playa soils > skirts of playas > playa center > desert pavements. While the eastern Great Basin contains all of these geomorphic types, we do not see the same propensity for regional scale dust transport from sand surfaces. In other desert regions, aeolian deposits, such as dunes and sand sheets, produce from 4 to 88.2% of dust plumes (Bullard et al., 2008, 2011; Baddock et al., 2011; Lee et al., 2012). The highest production is from the southern high plains on the Texas-New Mexico border,

which has a large region of aeolian sand sheet that has a land cover type of cultivated crop (Lee et al., 2012). Dust emission studies in the Mojave Desert found dunes to be prone to lofting of sediment, though there was a very high variability in the measurement (Sweeney et al., 2011). In the Bodélé Depression in the Sahara, dust is generated from barchan dune areas (Crouvi et al., 2012). However, the lofted sediment may actually be produced from the interdune corridors where friable diatomite deposits are exposed (Warren et al., 2007). There are some aeolian sand deposits in the eastern Great Basin (Jewell and Nicoll, 2011), but these do not seem to significantly impact dust transport. Some of the source areas have aeolian sand deposits upstream, which may help to loft dust sized particles in source areas due to saltation bombardment from the sand sized grains. No plumes were seen originating directly from aeolian sand deposits.

Alluvial and fluvial source areas were not found to contribute a large amount of dust plumes in the eastern Great Basin. However, these are significant sources in other dust producing region worldwide, including the Lake Eyre Basin of Australia, the Gobi Desert of China, and the Mojave Desert in the United States (Wang et al., 2006, 2008; Bullard et al., 2008; Sweeney et al., 2011, 2013). In the Mojave Desert, most of the sand and silt that comprise the Av soil horizons (topsoil with vesicular pores) below desert pavement surfaces is sourced from alluvial sediments, which cover nearly 60% of the land surface of the region, instead of playas, which cover only about 1% of the surface (Sweeney et al., in press). Alluvial areas have the potential to produce dust if they have a supply of dust sized particles that is replenished by flood events or weathering of larger particles. The Gobi Desert of China is characterized by dust transport from alluvial areas between the high elevation mountains and low elevation playas, possibly originating from

sediment rich wadis in this intermediate region (Wang et al, 2006, 2008). Similarly, the alluvial channels that move downward into the internally drained Lake Eyre Basin, Australia produce more than 25% of the dust plumes in this region (Bullard et al. 2008). Dust emission from alluvial and fluvial geomorphic types can be enhanced by the wide variety of grain sizes present; loose sand can bombard smaller sized sediments that are lofted and then remain suspended in the air stream (Shao et al., 1993; Sweeney et al., 2011). While numerous source areas in the eastern Great Basin have alluvial-fluvial features, these do not contribute a large amount of dust that is evident as plumes, except in disturbed areas such as the Milford Flat Burned Area (Table 3.3).

3.6.2 Natural and anthropogenic factors affecting dust transport

Determining whether the origin of transported dust is natural or anthropogenic is important, both in terms of land management and for global change studies. In most regions, land cover classification is used to assess the degree of anthropogenic activities on dust transport, because land cover types such as cultivated crops and built environments are anthropogenic, and cover types such as barren, shrub/scrub, and grassland are categorized as natural. In considering the dust source areas of the eastern Great Basin, the key land cover types, barren and shrub/scrub, would normally be considered natural sources. However, much of the vegetated landscape in this region has undergone conversion from shrubland and perennial grassland to increasingly dominant annual grasses, primarily resulting from cheatgrass invasion (Knapp, 1996). This conversion alters the fire cycle and can further result in longer periods of the year when portions of the soil surface are bare of vegetation. It is also, notable that most dust

production areas in this study region are influenced by human activities, including military range testing, fire disturbance, postfire rehabilitation efforts, and water diversion.

The largest dust source area, the Great Salt Lake Desert-Dugway Proving Ground, is an active military test and training range. While the details of specific activities are not available to the public, some known operations on site include military training, ATV operations, weather station maintenance, weapons detonations, and testing of chemical and biological agents. Such operations in the Great Salt Lake Desert have the potential to damage or destroy land cover and surfaces (e.g., Gill, 1996; Goossens and Buck, 2009), including any physical and biological soil crusts that are particularly vulnerable to decreased threshold friction velocities (Belnap and Gillette, 1997). A range of activities in this dust source area likely contribute to dust production.

The recent invasion of cheatgrass predisposed the Milford Flat area to fire disturbance; after the 2007 wildfire, numerous postfire land reclamation and seeding techniques exacerbated dust transport from this area (Miller et al., 2012). Across the American West, human caused disturbance has favored invasive cheatgrass, which has dynamically changed the fire regime across the Great Basin (D'Antonio and Vitousek, 1992; Sankey et al., 2009b, 2012d). Cheatgrass replaces local native grasses; because this invasive is a highly flammable fuel, fires in the Great Basin now tends to burn more often, spread faster, and disturb larger geographic areas in the landscape. Such burned areas have a strong propensity for dust emission as compared to similar unburned landscapes that retain native grasses and shrubs (Sankey et al., 2009a, 2010, 2011, 2012b, 2012c).

Following the 2007 Milford Flat fire, dust and sand deflation and deposition was

observed in the burned area (Figs. 3.4; 3.7). Miller et al. (2012) found that sediment flux downwind from burned plots that were subjected to rehabilitation treatments from October 2007-2010 was larger than the flux from burned plots that were not treated similarly. This study concluded that the treatments administered “exacerbated rather than mitigated wind erosion” during the study period of one to three years during the postfire interval (Miller et al., 2012 and references therein). Fig. 3.7 depicts the large amounts of deflation and deposition in the MFBA in July 2010, still occurring three years after the fire. Soils with a high proportion of small particles are more prone to wind erosion following natural or anthropogenic disturbance; many of the soils in this region were lake bottom sediments from Lake Bonneville and therefore have a large fraction of fines (Gilbert, 1890). Miller et al. (2012) also found that vegetation did begin to establish near the end of the study period in July 2010, but it consisted primarily of exotic annual plants, and not manually seeded perennial plants that were part of the reclamation effort. Regional scale analysis throughout the Great Basin and Columbia Plateau has found that postfire seeding did not reduce the time window of bare ground to established vegetation (Sankey et al., 2013). Therefore, the Milford Flat Burned Area has been affected by three distinct anthropogenic influences: exotic cheatgrass invasions, fire effects, and postfire rehabilitation treatments, all of which enhance soil disturbance and dust production (Fig. 3.7).

The Sevier Dry Lake, which is an ephemeral stream and terminal lake system in central Utah, has had significant changes to its hydrology due to intensive agricultural water use of the Sevier River, similar to other terminal water systems in the southwestern US (Gill, 1996). Agricultural use of the Sevier River began around 1850, when Mormon

pioneers settled the region (SRWUA, 2012). Water use of the Sevier River began with direct diversion from the river, and by 1900 construction of dams and canal systems had begun. There are now seven reservoirs along the Sevier River with a combined capacity of over 480,000 acre-feet. During the Holocene, the Sevier Dry Lake was inundated, and in the mid-1800s had a surface altitude of 1379.5 m (Oviatt, 1988). However, from 1880 until 1982, the Sevier Dry Lake was essentially dry. Two inundation events, one in 1982-1985 and another in 2011-2012, were caused by abnormally high runoff from mountain snowpack (Oviatt, 1988; LANCE, 2012). Diversion of water for agriculture has contributed to the drying of the Sevier Dry Lake. However, hydroclimatic changes may be an influential factor as well. The drying of the Sevier Dry Lake has clearly contributed to significant dust production over this study period.

3.6.3 Forecasting eastern Great Basin dust storms

Detailed information on the meteorological conditions (Hahnenberger and Nicoll, 2012) and dust source areas identified in this study have specific implications for an improved forecast and warning system for dust storms in the eastern Great Basin. We define a dust storm as any event with strong winds, which transport dust downstream of regional source areas. We present suggestions for a forecasting system for this region that would involve five main components: synoptic weather forecasts, drought and disturbance monitoring, hourly surface weather observations, satellite data, and air quality monitoring.

First, synoptic weather forecasts would assess the potential for strong prefrontal winds in the eastern Great Basin. These forecasts can be generated four to five days in

advance using standard regional meteorological weather forecast models, and would be potentially the most accurate for dust storm forecasting in the one to three day prior time range. Next, forecasters would identify the status of drought or wetness in the region using the Palmer Drought Index from NOAA, which would inform the likelihood for significant dust transport beyond the threshold PDI value of -2. Additionally, a log of regional disturbance events including fire, documented overgrazing, or large construction projects would be kept as potential new and active dust sources. If the forecaster determined that dust transport was likely, they would indicate this in their forecast, giving the general public advance warning of dust storm development and potential impacts at specific locales.

On the day of the potential prefrontal wind event, forecasters could monitor surface weather stations near the source regions, to determine if wind speeds are exceeding the expected threshold velocities in the eastern Great Basin. Realtime satellite data acquired from the MODIS sensor on both the Aqua and Terra satellites could be analyzed to detect if any dust plumes are present, and for very large events, dust plumes may also be visible on geostationary satellite data as well. Realtime monitoring of PM₁₀ and PM_{2.5} values at air quality monitoring stations in the populated regions of Utah could indicate the arrival of a dust storm and associated reduction in air quality. Additional air quality monitoring stations in the rural regions with active dust sources is recommended as they would aid in early warning of dust events and quantification of the impact of dust on air quality degradation in Utah. Further, webcam networks could be utilized to monitor decreases in visibility in areas that do not have surface weather stations with visibility sensors.

An improvement to the forecasting system we envision would be networked webcams and air quality monitoring stations placed in the dust source regions that would provide high resolution temporal data and actual pictures. This would improve realtime forecasting, and would also provide a much more detailed and comprehensive view of dust production in these regions at local scales, which is more useful than what can be observed from satellite data. Limitations and challenges with this proposal are that, first, most of these regions are very remote and lack established power and communication infrastructure, and, second, some of the dust source regions cover very large spatial areas, requiring several webcams for a sufficient spatial coverage.

An improved dust storm forecasting system could supplement current protocols at the Weather Forecast Offices of the National Weather Service and the Department of Transportation, which would help inform transportation professionals and the general public to better prepare for dust storm events. There are two heavily used federal highways dissecting this dust transport region in the eastern Great Basin, and actions such as road advisory signs warning of dust and visibility degradation could be put in place for real time advisories. Precautions could be taken on roads and at airports, and sensitive populations could remain indoors to limit exposure to elevated levels of particulate matter. While dust storms in the eastern Great Basin are not as large or as severe as the biggest dust producing regions of the world, they impact one of the largest and fastest growing population centers in the intermountain west.

3.7. Conclusions and implications

Recent studies have described the dominant meteorological controls on dust production from the eastern Great Basin region (Hahnenberger and Nicoll, 2012). Large regional scale dust storms occur in the eastern Great Basin four to five times per year and degrade visibility and air quality in the most populated regions of Utah. Using high resolution datasets over a multiyear time period, we identify and characterize specific dust producing source areas in this region, and relate dust production to drought and disturbance.

Analysis of MODIS satellite data of the eastern Great Basin during 16 dust event days from 2004-2010 identified dust plumes emanating from four primary source areas, and five secondary source areas. Barren land cover produced 60% of dust plumes observed. Of the vegetated land cover areas that produce dust, 75% of the plumes originated in areas burned by the 2007 Milford Flat fire. Many of the dust source regions in the eastern Great Basin contain ephemeral lakes or playas that are remnant features from Pleistocene Lake Bonneville. Two of the dust producing areas, the Great Salt Lake Desert-Dugway Proving Ground and Sevier Dry Lake, are particularly influenced by anthropogenic activity, including military operations and agricultural water use.

The area burned by the 2007 Milford Flat fire has been an important dust source area since 2008; this was the largest wildfire recorded in Utah history, with an extensive burn area due to the presence of highly flammable invasive cheatgrass. The portion of the burned area (MFBA) that was subjected to numerous postfire land treatments and seeding did not significantly rehabilitate the environment (Miller et al., 2012), because persistent drought conditions did not permit recruitment of vegetation. Ironically, the rehabilitation

treatments, which included chaining and drill seeding, created more dust production than on the untreated burned landscape, as evident by the high number of plumes we detected in this region of Utah since 2008. It is important that land managers consider the hydroclimatic setting of the region as well as the surface and soil characteristics of the landscape prior to rehabilitation efforts. In locations with surfaces that are susceptible to wind erosion, further disturbance will likely increase the effects of wind erosion, relative to leaving the landscape to recover naturally, or using alternative treatments such as erosion fences (Goossens and Buck, 2009; Miller et al., 2012).

Variations in drought and wet periods control the amount and severity of dust production, especially on the dry lake and playa dust sources in the eastern Great Basin region. A drought period lasting from 2007-2009 produced the majority of dust plumes identified during the entire study period, though we see a lag of approximately one year between the onset of drought and the onset of significant dust production. A PDI value of -2, indicating moderate drought, seems to be the threshold value for significant generation of dust plumes. The distribution of dust plumes in the eastern Great Basin landscape illustrates that the region is not a uniform emitter of dust, but has distinct geomorphic areas of generation and some “hot spots” in which plumes reactivate during droughts. This aids in dust event forecasting, as the majority of dust transport occurs from distinct source areas in the region, and is not dispersed across the larger region.

The relevance of this study for future work includes numerical modeling applications of dust transport and mesoscale forecasting and warning of dust storms. Although many efforts to model dust transport have been undertaken from a global to local scale, one of the prevailing uncertainties is the identification of land surfaces that

act as dust sources at sufficient wind speeds (e.g., Yin et al., 2005; Rivera Rivera et al., 2009; Seigel and van den Heever, 2012; Tegen and Fung, 2012). Modeling schemes often use prescribed threshold velocities for different land cover types, but these are often static and do not take into account disturbance events or other influences on the susceptibility of a land surface to dust production. The significant dust contributions from the 2007 Milford Flat fire scar in Utah highlights the need for a more dynamic and local approach that takes into account disturbance events and the identification of dust sources at high resolution to inform accurate models of dust transport.

Dust storms degrade visibility and air quality, and can detrimentally impact the health and safety of the population downwind (Rivera Rivera et al., 2009; Hahnenberger and Nicoll, 2012). Our observations about dust storms in the eastern Great Basin can inform forecasting of the onset of dust storm events, and can help develop useful warning systems of value for transportation systems and the general public health. Further work is necessary to understand the composition of the dust contributed from each dust source in this region, as well as to accurately measure the flux of dust emitted.

Table 3.1: Meteorological and air quality station data.

Station Name - Abbreviation	Lat./ Lon.	Elevation (m)	Call Sign/ ICS	COOP/WMO ID
Delta, UT - Delta	39.33/ -112.58	1408	U24/ KU24	422090/72479
Salt Lake City International Airport - SLCIA	40.78/ -111.97	1288	SLC/ KSLC	427598/72572
Station Name - Abbreviation	Lat./ Lon.	Elevation (m)	EPA AIRS Code	Station Address
Hawthorne - HW	40.74/ -111.87	1306	490353006	1675 S. 600 E., Salt Lake City
Lindon – LN	40.34/ -111.71	1442	490484001	50 North Main Street, Lindon
Ogden #2 – O2	41.21/ -111.97	1316	490570002	228 East 32nd Street , Ogden City

Table 3.2: Air quality and wind data for all DEDs with analyzed plumes. Twenty four hour particulate matter (PM) values are reported in $\mu\text{g}/\text{m}^3$, for both PM_{10} and $\text{PM}_{2.5}$. Winds are the maximum speed and direction recorded between the times of the Aqua and Terra satellite overpasses (1000-1500 MST), with wind speed reported in m/s. For station abbreviations, see Table 3.1.

Date	Satellite (# plumes)	# Total Plumes	PM_{10} HW	PM_{10} LN	PM_{10} O2	$\text{PM}_{2.5}$ HW	$\text{PM}_{2.5}$ LN	$\text{PM}_{2.5}$ O2	SLCIA Wind Speed	SLCIA Wind Directi on	Delta Wind Speed	Delta Wind Direc tion
10 May 2004	Aqua (3) /Terra (1)	4	N/A	N/A	N/A	N/A	N/A	N/A	19.0	SSE	16.0	SSW
16 Oct. 2004	Terra(1)	1	35.0	37.0	38.0	5.5	5.6	N/A	8.0	S	6.0	SW
15 Apr. 2008	Terra (3)	3	166.0	164.0	118.0	26.9	24.4	20.6	13.0	NNW	12.0	SW
19 Apr. 2008	Aqua (6) /Terra (17)	23	191.0	181.0	129.0	31.3	31.7	23.9	16.0	S	17.0	SSW
20 Apr. 2008	Aqua (1) /Terra (5)	6	138.0	110.0	93.0	23.5	20.6	18.3	15.0	WNW	9.0	NNW
29 Apr. 2008	Aqua (3)	3	71.0	155.0	58.0	17.0	28.2	11.7	12.0	SSW	10.0	SSW
3 Mar. 2009	Aqua (13) /Terra (23)	36	99.0	108.0	58.0	12.7	17.0	8.5	15.0	SSW	14.0	SW
4 Mar. 2009	Aqua (10) /Terra (33)	43	N/A	200.0	103.0	19.9	23.0	12.5	19.0	S	18.0	SW
21 Mar. 2009	Aqua (7)	7	64.0	67.0	92.0	9.6	12.7	11.1	12.0	S	12.0	SSW
22 Mar. 2009	Terra (4)	4	96.0	89.0	100.0	8.3	10.3	9.3	16.0	S	17.0	WSW
6 Aug. 2009	Aqua (6)	6	167.0	162.0	181.0	36.1	29.7	32.2	19.0	SSW	13.0	S
4 Oct. 2009	Aqua (1) /Terra (1)	2	18.0	45.0	13.0	4.4	8.3	3.5	14.0	S	10.0	SW
30 Mar. 2010	Aqua (9) /Terra (8)	17	166.0	424.0	216.0	50.0	55.8	30.8	17.0	S	19.0	SSW
5 Apr. 2010	Aqua (3)	3	25.0	49.0	31.0	5.1	7.9	6.7	12.0	SSE	21.0	SW
27 Apr. 2010	Aqua (2)	2	278.0	83.0	197.0	47.1	14.6	13.2	13.0	S	13.0	S
28 May 2010	Aqua (5) /Terra (3)	8	42.0	46.0	23.0	6.6	7.9	5.0	12.0	N	16.0	SW
	MEAN	10.5	111.1	128.0	96.7	20.3	19.8	14.8	14.5		13.9	
	MAX	43.0	278.0	424.0	216.0	50.0	55.8	32.2	19.0		21.0	
	MIN	1.0	18.0	37.0	13.0	5.1	5.6	3.5	8.0		6.0	

Table 3.3: Observed plume regions. For geographic location of each region see Figure 3.2. Number and percent of plumes based off all plumes identified from 2004-2010 (n=168). Elevation ranges were estimated using Google Earth. Geomorphic features were identified from MODIS satellite data, Google Earth, and personal field experience. Land cover was identified using the National Land Cover Database 2006. Soil texture was identified using the NRCS Soil Survey Geographic (SSURGO) Database.

Region	# of Plumes	% of total Plumes	Estimated elevation range	Primary Geomorphic features	Primary Land Cover	Primary Soil Texture
Great Salt Lake Desert-Dugway	58	34.5	1290 to 1370 m	Playa	Barren Land	Silty clay
Milford Flat Burned Area	52	30.9	1420 to 1680 m	Alluvial/ Disturbed area	Shrub/ Scrub	Very gravelly sandy loam
Sevier Dry Lake	22	13.1	1380 to 1400 m	Playa	Barren Land	Silty clay
Tule Dry Lake	18	10.7	1350 to 1400 m	Playa	Barren Land	Silty clay
Beaver Bottoms	7	4.2	1510 to 1600 m	Alluvial/ Fluvial	Shrub/ Scrub	Very gravelly sandy loam
Wah Wah Valley	4	2.4	1420 to 1510 m	Alluvial/ Fluvial	Shrub/ Scrub	Gravelly sandy loam
Beryl-Zane	3	1.8	1560 to 1570 m	Alluvial	Shrub/ Scrub	Loam
Skull Valley	2	1.2	1310 to 1370 m	Playa/ Alluvial	Barren Land	Silty Clay
Pot Playas	2	1.2	1390 to 1400 m	Playa	Barren Land	Very gravelly sandy loam



Figure 3.1: Regional map of the hydrographic Great Basin with important locations identified; GSL=Great Salt Lake, SDL=Sevier Dry Lake.

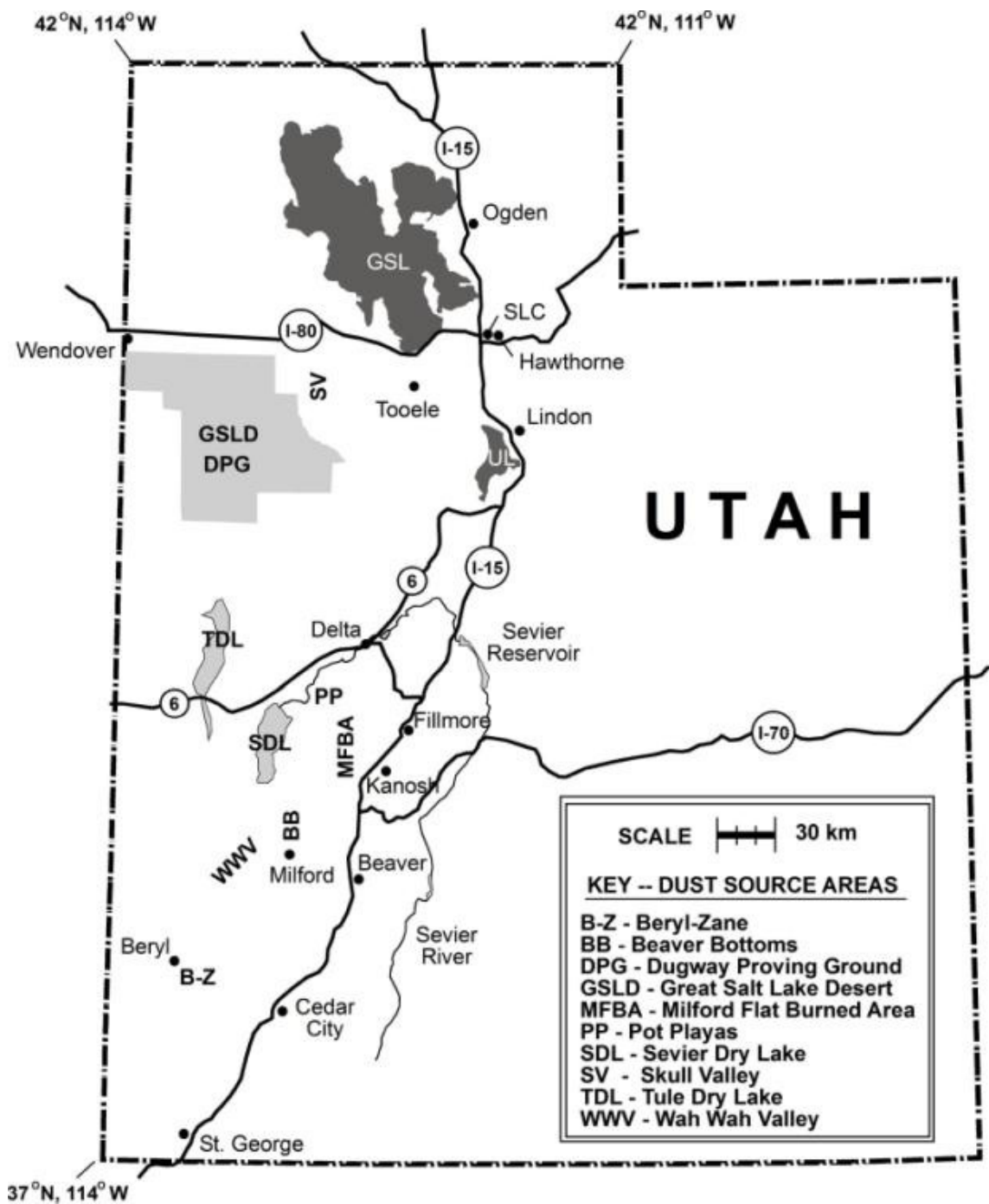


Figure 3.2: Map of Utah with important locations identified.

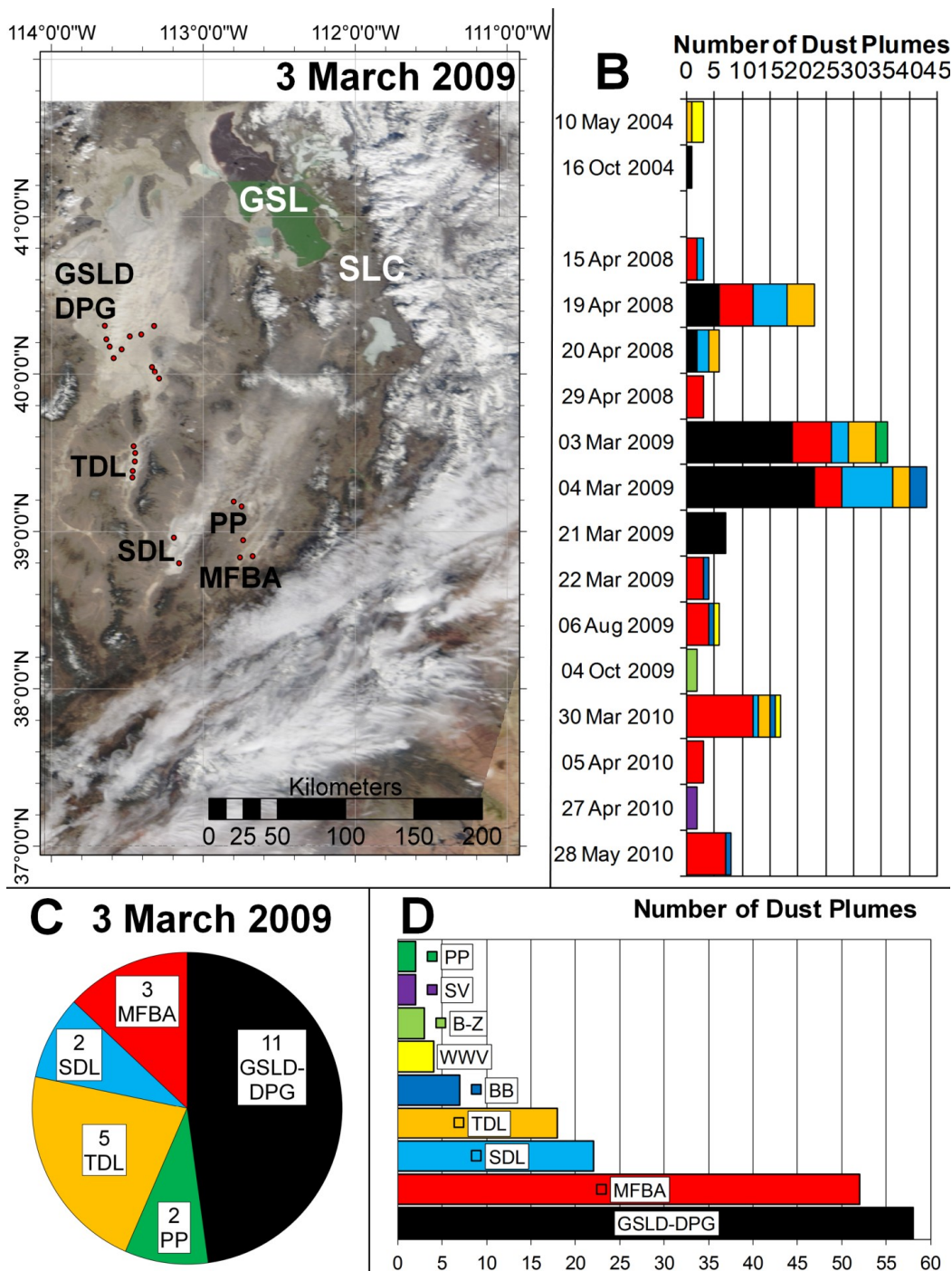


Figure 3.3: Dust plumes described by source location with abbreviations as follows. Pot Playas (PP), Skull Valley (SV), Beryl-Zane (B-Z), Wah Wah Valley (WWV), Beaver Bottoms (BB), Tule Dry Lake (TDL), Sevier Dry Lake (SDL), Milford Flat Burned Area (MFBA), and Great Salt Lake Desert-Dugway Proving Ground (GSLD-DPG). A: MODIS Terra imagery during dust event on 3 March 2009, with plume source locations indicated by red dots. B: number of plumes categorized by source area, for each DED analyzed (n=168). C: number of plumes, categorized by source area for 3 March 2009, MODIS Terra image (n=23). D: number of plumes, categorized by source area (n=168).

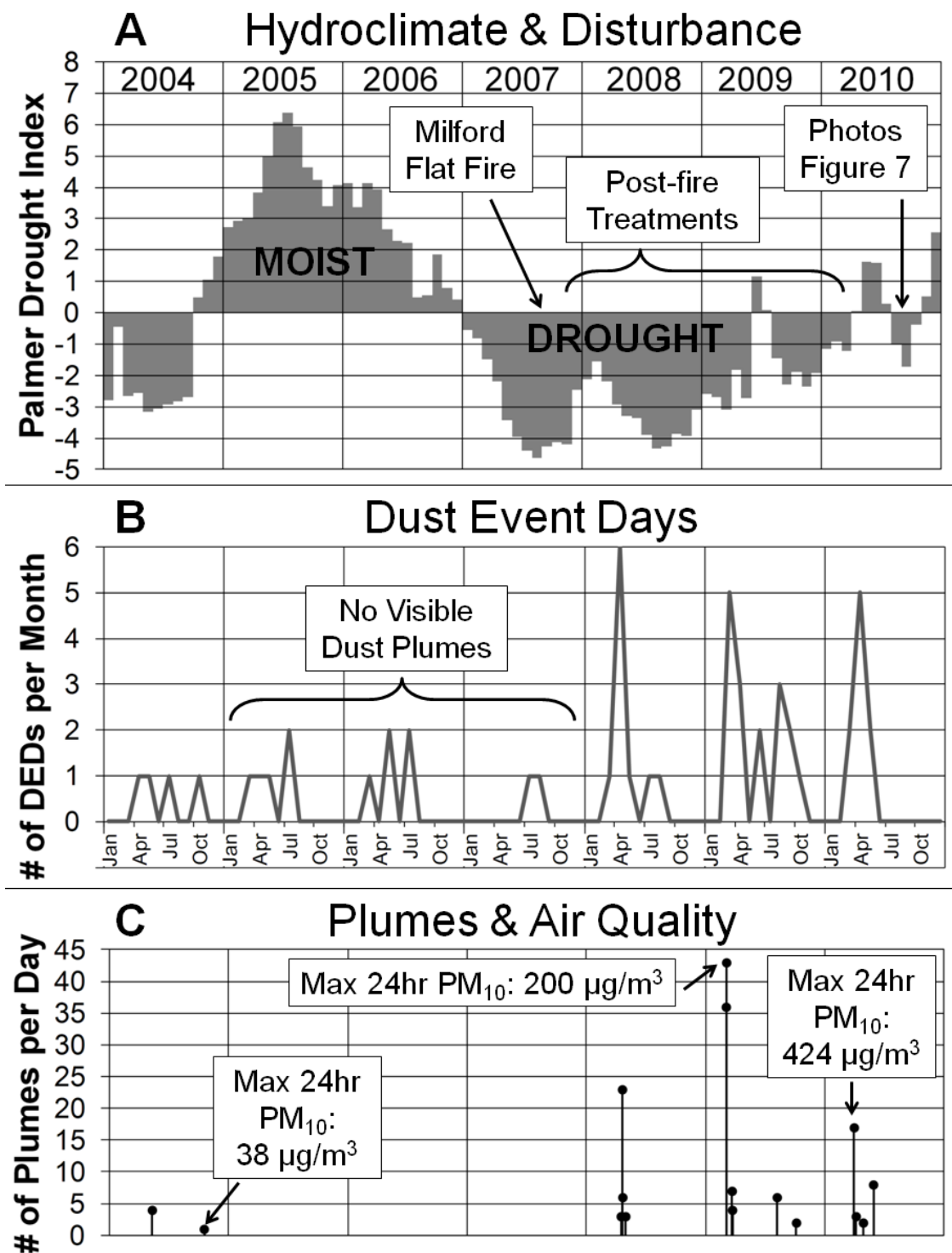


Figure 3.4: Summary of drought, DEDs, and dust plumes during the study period. A: monthly values of the Palmer Drought Index for western Utah from 2004-2010. B: number of DEDs each month from 2004-2010. C: Number of dust plumes identified on 16 DEDs from 2004-2010, with annotations of selected air quality data discussed in the text.

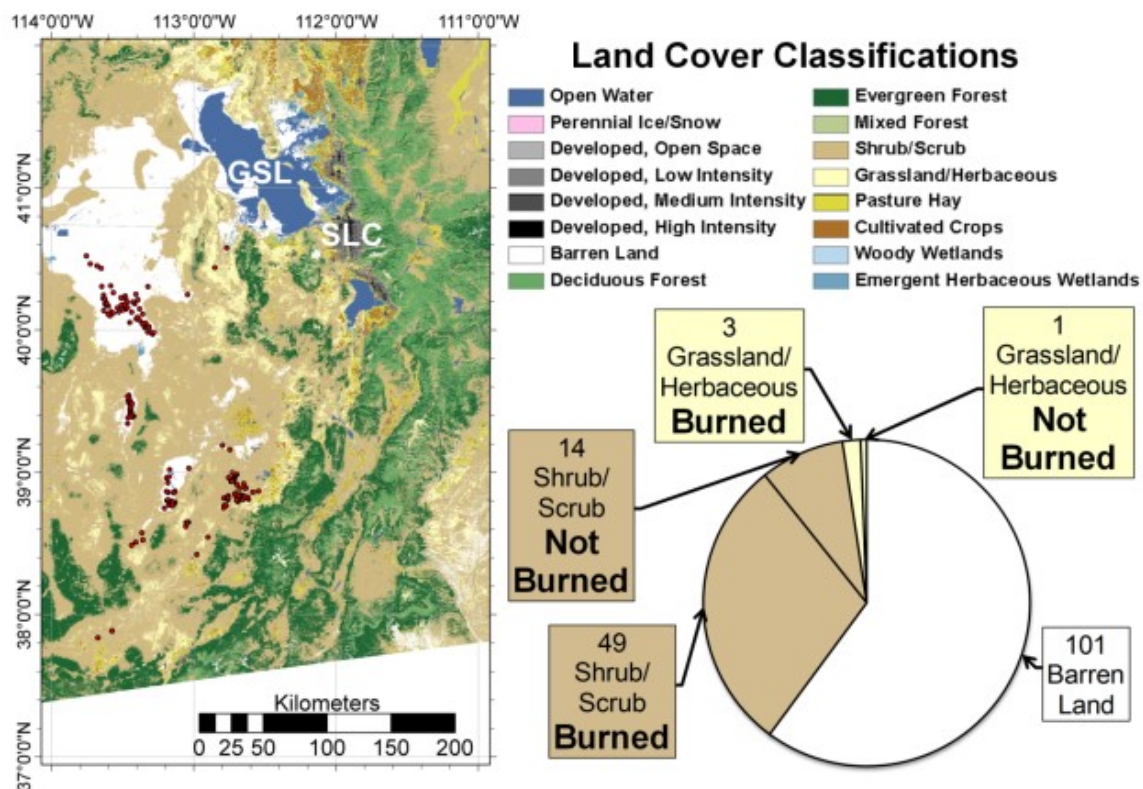


Figure 3.5: National Land Cover Database (Fry et al., 2011) classifications of study region, with plume source locations indicated by red dots (n=168).

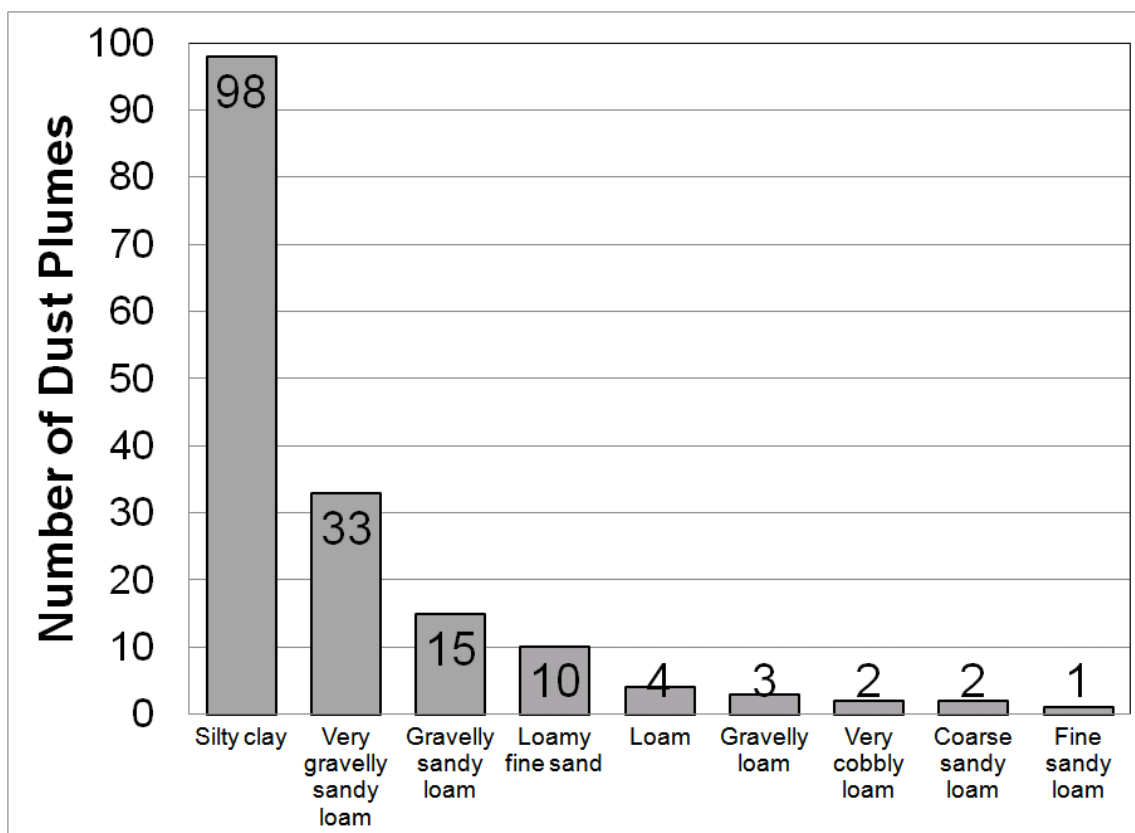


Figure 3.6: Number of dust plumes observed, categorized by soil texture class (n=168) (Data source: Soil Survey Staff, 2012).

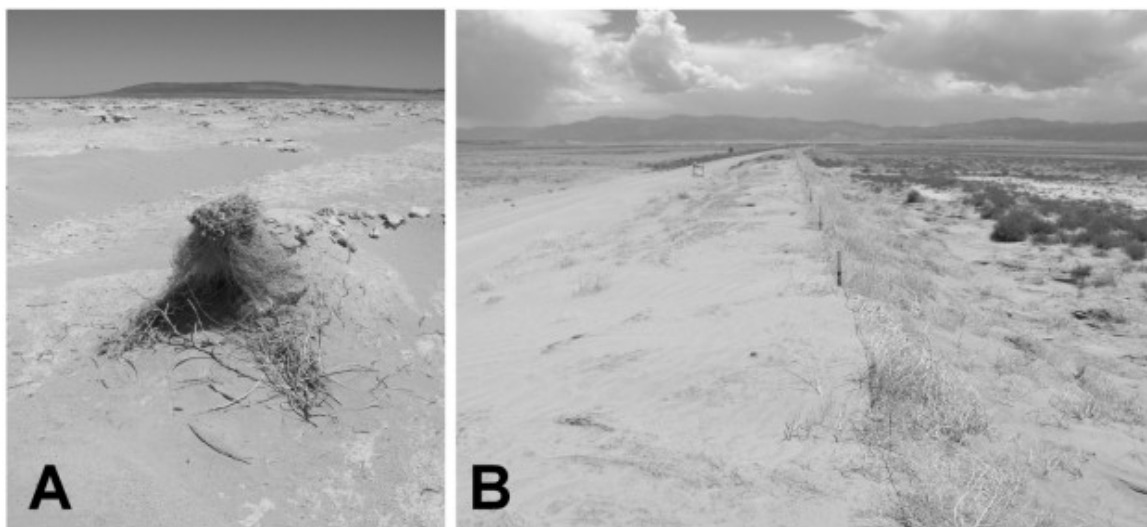


Figure 3.7: Photographs of wind erosion in the Milford Flat Burned Area. A: photo of deflation at Milford Flat Burned Area, July 2010. B: photo of sand dune formation along a fence at Milford Flat Burned Area, July 2010.

3.8 References

- Adams, D.K., Comrie, A.C., 1997. The North American Monsoon. *Bulletin of the American Meteorological Society*, 78, 2197-2213. doi: [10.1175/1520-0477\(1997\)078<2197:TNAM>2.0.CO;2](https://doi.org/10.1175/1520-0477(1997)078<2197:TNAM>2.0.CO;2)
- Baddock, M.C., Gill, T.E., Bullard, J.E, Dominguez Acosta, M., Rivera Rivera, N.I., 2011. Geomorphology of the Chihuahuan Desert based on potential dust emissions. *Journal of Maps*, 7, 249-259. doi: 10.4113/jom.2011.1178
- Belnap, J., Gillette, D.A., 1997. Disturbance of biological soil crusts: impacts on potential wind erodibility of sandy desert soils in southeastern Utah. *Land Degradation and Development*, 8, 355-362. DOI: 10.1002/(SICI)1099-145X(199712)8:4<355::AID-LDR266>3.0.CO;2-H
- Belnap, J., Gillette, D.A., 1998. Vulnerability of desert biological soil crusts to wind erosion: the influences of crust development, soil texture, and disturbance. *Journal of Arid Environments*, 39, 133-142. doi: [10.1006/jare.1998.0388](https://doi.org/10.1006/jare.1998.0388)
- Brazel, A.J., Nickling, W.G., 1986. The relationship of weather types to dust storm generation in Arizona (1965-1980). *Journal of Climatology*, 6, 255-275. DOI: 10.1002/joc.3370060303
- Brook, R.D., Rajagopalan, S., Pope III, C.A., Brook, J.R., Bhatnagar, A., Diez-Rouz, A., Holguin, F., Hong, U., Luepker, R.V., Mittleman, M., Peters, A., Siscovick, D., Smith, S.C., Whitsel, L., Kaufman, J.D., 2010. Particulate matter air pollution and cardiovascular disease: an update to the scientific statement from the American Heart Association. *Circulation*, 121, 2331-2378. doi: 10.1161/CIR.0b013e3181dbece1
- Brough, R.C., Jones, D.L., Stevens, D.J., 1987. *Utah's Comprehensive Weather Almanac*. Publishers Press, Salt Lake City, UT.
- Bullard, J., Baddock, M., McTainsh, G., Leys, J., 2008. Sub-basin scale dust source geomorphology detected using MODIS. *Geophysical Research Letters*, 25, L15404. doi: 10.1029/2008GL033928
- Bullard, J.E., Harrison, S.P., Baddock, M.C., Drake, N., Gill, T.E., McTainsh, G., Sun, Y., 2011. Preferential dust sources: a geomorphological classification designed for use in global dust-cycle models. *Journal of Geophysical Research*, 116, F04034. doi: 10.1029/2011JF002061
- Chen, S.H., Wang, S.H., Waylonis, M., 2010. Modification of Saharan air layer and environmental shear over the eastern Atlantic Ocean by dust-radiation effects. *Journal of Geophysical Research*, 115, D21202. doi:10.1029/2010JD014158
- Crouvi, O., Schepanski, K., Amit, R., Gillespie, A.R., Enzel, Y., 2012. Multiple dust

sources in the Sahara Desert: the importance of sand dunes. *Geophysical Research Letters*, 39, L13401. doi: 10.1029/2012GL052145

D'Antonio, C.M., Vitousek, P.M., 1992. Biological invasions by exotic grasses, the grass/fire cycle, and global change. *Annual Review of Ecology and Systematics*, 23, 63-87.

Dayan, U., Erel, Y., Shpund, J., Kordova, L., Wanger, A., Schauer, J.J., 2011. The impact of local sources and meteorological factors on nitrogen oxide and particulate matter concentrations: a case study of the Day of Atonement in Israel. *Atmospheric Environment*, 45, 3325-3332. doi:10.1016/j.atmosenv.2011.02.017

Derbyshire, E., 2007. Natural minerogenic dust and human health. *AMBIO*, 36, 73-77.

Division of Air Quality (DAQ), Utah State Department of Environmental Quality (DEQ), 2011. Utah 2011 Air Monitoring Network Plan. <http://www.airmonitoring.utah.gov/network/2011AirMonitoringNetworkPlan.PDF>

Dugway Proving Ground (DPG), U.S. Army Test and Evaluation Command (ATEC), 2012. Dugway Proving Ground, www.dugway.army.mil

Eubank, M.E., Brough, R.C., 1979. Mark Eubank's Utah Weather. Horizon Publishers and Distributors, Bountiful, UT.

Frémont, J.C., 1845. Report of the Exploring Expedition to the Rocky Mountains in the Year 1842, and to Oregon and California in the Years 1843-1844. Goles and Seaton, Washington DC.

Fry, J., Xian, G., Jin, S., Dewitz, J., Homer, C., Yang, L., Barnes, C., Herold, N., Wickham, J., 2011, Completion of the 2006 National Land Cover Database for the conterminous United States. *Photogrammetric Engineering and Remote Sensing*, 77, 858-864.

Gilbert, G.K., 1890. Lake Bonneville. Washington Government Printing Office, Washington, D.C.

Gill, T.E., 1996. Eolian sediments generated by anthropogenic disturbance of playas: human impacts on the geomorphic system and geomorphic impacts on the human system. *Geomorphology*, 17, 207-228. doi:10.1016/0169-555X(95)00104-D.

Gill, T.E., Cahill, T.A., 1992. Playa-generated dust storms from Owens Lake in The History of Water: Eastern Sierra Nevada, Owens Valley, White-Inyo Mountains. Hall, C.A., Doyle-Jones, V., and B. Widaski, eds. University of California Press, Los Angeles, pp. 63-73.

Gillette, D.A., Adams, J., Endo, A., Smith, D., Kihl, R., 1980. Threshold velocities for

input of soil particles into the air by desert soils. *Journal of Geophysical Research: Oceans*, 85, 5621-5630. DOI: 10.1029/JC085iC10p05621

Ginoux, P., Prospero, J.M., Gill, T.E., Hsu, N.C., Zhao, M., 2012. Global-scale attribution of anthropogenic and natural dust sources and their emission rates based on MODIS Deep Blue aerosol products. *Reviews of Geophysics*, 50, RG3005. doi:10.1029/2012RG000388

Goossens, D. and Buck, B. 2009. Dust dynamics in off-road vehicle trails: measurements on 16 arid soil types, Nevada, USA. *Journal of Environmental Management*, 90, 3458–3469. doi:10.1016/j.jenvman.2009.05.031

Grayson, D.K., 2011. *The Great Basin: A Natural Prehistory*. University of California Press. 432 pages.

Griffin, D.W., 2007. Atmospheric movement of microorganisms in clouds of desert dust and implications for human health. *Clinical Microbiology Reviews*, 20, 459-477. doi: 10.1128/CMR.00039-06

Grineski, S.E., Staniswalis, J.G., Bulathsinhala, P., Peng, Y., Gill, T.E., 2011. Hospital admissions for asthma and acute bronchitis in El Paso, Texas: do age, sex, and insurance status modify the effects of dust and low wind events? *Environmental Research*, 111, 1148-1155. doi: 10.1016/j.envres.2011.06.007

Hahnenberger, M., Nicoll, K., 2012. Meteorological characteristics of dust transport events in the Eastern Great Basin of Utah, U.S.A. *Atmospheric Environment*, 60, 601-612. <http://dx.doi.org/10.1016/j.atmosenv.2012.06.029>

Hallar, A.G., Chirokova, G., McCubbin, I., Painter, T.H., Wiedinmyer, C., and Dodson, C., 2011. Atmospheric bioaerosols transported via dust storms in the western United States. *Geophysical Research Letters*, 38, L17801. doi:10.1029/2011GL048166

Hashizume, M., Ueda, K., Nishiwaki, Y., Michikawa, T., Onozuka, D., 2010. Health effects of Asian dust events: a review of the literature. *Japan Journal Hygiene*, 65, 413-421.

Hasselquist, N.J., Germino, M.J., Sankey, J.B., Ingram, L.J., Glenn, N.F., 2011. Aeolian nutrient fluxes following wildfire in sagebrush steppe: implications for soil carbon storage. *Biogeosciences*, 8, 3649-3659. doi: 10.5194/bg-8-3649-2011

Heim, R.R., 2002. A review of twentieth-century drought indices used in the United States. *Bulletin of the American Meteorological Society*, 83, 1149-1165.

Jewell, P.W., Nicoll, K., 2011. Wind regimes and aeolian transport in the Great Basin, U.S.A. *Geomorphology*, 129, 1-13. doi:10.1016/j.geomorph.2011.01.005

- Johnston, F., Hanigan, I., Henderson, S., Morgan, G., Bowman, D., 2011. Extreme air pollution events from brushfires and dust storms and their association with mortality in Sydney, Australia 1994-2007. *Environmental Research*, 111, 811-816.
[doi:10.1016/j.envres.2011.05.007](https://doi.org/10.1016/j.envres.2011.05.007)
- Kellog, C.A., Griffin, D.W., 2006. Aerobiology and the global transport of desert dust. *Trends in Ecology and Evolution*, 21, 638–644. doi: [10.1016/j.tree.2006.07.004](https://doi.org/10.1016/j.tree.2006.07.004)
- Knapp, P.A., 1996. Cheatgrass (*Bromus tectorum* L) dominance in the great basin desert. History, persistence, and influences to human activities. *Global Environmental Change*, 6, 37-52. doi: 10.1016/0959-3780(95)00112-3
- Land Atmosphere Near-real time Capability for EOS (LANCE), NASA/GSFC/Earth Science Data and Information System (ESDIS), 2012. Rapid Response, MODIS Subsets.
<http://earthdata.nasa.gov/data/near-real-time-data/rapid-response>
- Lee, J.A., Gill, T.E., Mulligan, K.R., Acosta, M.D., Perez, A.E., 2009. Land use/land cover and point sources of the 15 December 2003 dust storm in southwestern North America. *Geomorphology*, 105, 18-27. doi: 10.1016/j.geomorph.2007.12.016
- Lee, J.A., Baddock, M.C., Mbuh, M.J., Gill, T.E., 2012. Geomorphic and land cover characteristics of aeolian dust sources in West Texas and eastern New Mexico, USA. *Aeolian Research*, 3, 459-466. doi: 10.1016/j.aeolia.2011.08.001
- Liu, J.T., Jiang, X.G., Zheng, X.J., Kang, L., Qi, F.Y., 2004. Intensive Mongolian cyclone genesis induced severe dust storm. *Terrestrial, Atmospheric and Oceanic Sciences*, 15, 1029-1033.
- Maher, B.A., Prospero, J.M., Mackie, D., Gaiero, D., Hesse, P.P., Balkanski, Y., 2010. Global connections between aeolian dust, climate and ocean biogeochemistry at the present day and at the last glacial maximum. *Earth-Science Review*, 99, 61-97.
<http://dx.doi.org/10.1016/j.earscirev.2009.12.001>
- Mahowald, N.M., Bryant, R.G., del Corral, J., Steinberger, L., 2003. Ephemeral lakes and desert dust sources. *Geophysical Research Letters*, 30, 1074. doi: 10.1029/2002GL016041
- Marticorena, B., Bergametti, G., Gillette, D., Belnap, J., 1997. Factors controlling threshold friction velocity in semiarid and arid areas of the United States. *Journal of Geophysical Research*, 102, 23,277-23,287. doi: 10.1029/97JD01303
- Martinez-Garcia, A., Rosell-Mele, A., Jaccard, S.L., Geibert, W., Sigman, D.M., Haug, G.H., 2011. Southern Ocean dust–climate coupling over the past four million years. *Nature*, 476, 312–315. doi:10.1038/nature10310
- McTainsh, G. and Strong, C., 2007. The role of aeolian dust in ecosystems.

Geomorphology, 89, 39–54. doi:10.1016/j.geomorph.2006.07.028

McTainsh, G.H., Lynch, A.W., Tews, E.K., 1998. Climatic controls upon dust storm occurrence in eastern Australia. *Journal of Arid Environments*, 39, 457–466. doi: [10.1006/jare.1997.0373](https://doi.org/10.1006/jare.1997.0373)

Miller, M.E., Bowker, M.A., Reynolds, R.L., Goldstein, H.L., 2012. Post-fire land treatments and wind erosion – Lessons from the Milford Flat Fire, UT, USA. *Aeolian Research*, 7, 29–44. doi: [10.1016/j.aeolia.2012.04.001](https://doi.org/10.1016/j.aeolia.2012.04.001)

Miller, S.D., Kuciauskas, A.P., Liu, M., Ji, Q., Reid, J.S., Breed, D.W., Walker, A.L., Mandoos, A.A., 2008. Haboob dust storms of the southern Arabian Peninsula, *Journal of Geophysical Research*, 113, D01202. doi:10.1029/2007JD008550

Munson, S.M., Belnap, J., Okin, G.S., 2011. Responses of wind erosion to climate-induced vegetation changes on the Colorado Plateau. *Proceedings of the National Academy of Sciences*, 108, 3854–3859. doi: 10.1073/pnas.1014947108

National Climatic Data Center (NCDC) National Oceanic and Atmospheric Administration (NOAA), 2012. Global Integrated Surface Hourly (ISH) database. <http://www.ncdc.noaa.gov/oa/land.html>

National Climatic Data Center (NCDC) National Oceanic and Atmospheric Administration (NOAA), 2012. North American Drought Monitor (NADM), <http://www.ncdc.noaa.gov/temp-and-precip/drought/nadm/index.html>

Oviatt, C.G., 1988. Late Pleistocene and Holocene lake fluctuations in the Sevier Lake basin, Utah, USA. *Journal of Paleolimnology*, 1, 9–21. doi: 10.1007/BF00202190

Oviatt, C.G., 1997. Lake Bonneville fluctuations and global climate change. *Geology*, 25, 155–158. doi: 10.1130/0091-7613(1997)025<0155:LBFAGC>2.3.CO;2

Oviatt, C.G., Madsen, D.B., Schmitt, D.N., 2003. Late Pleistocene and early Holocene rivers and wetlands in the Bonneville basin of western North America. *Quaternary Research*, 60, 200–210. doi:10.1016/S0033-5894(03)00084-X

Painter, T.H., Barrett, A.P., Landry, C.C., Neff, J.C., Cassidy, M.P., Lawrence, C.R., McBride, K.E., Farmer, G.L., 2007. Impact of disturbed desert soils on duration of mountain snow cover. *Geophysical Research Letters*, 34, L12502. doi:10.1029/2007GL030284

Painter, T.H., Deems, J.S., Belnap, J., Hamlet, A.F., Landry, C.C., Udall, B., 2010. Response of Colorado River runoff to dust radiative forcing in snow. *Proceedings of the National Academy of Sciences*, 107, 17125–17130. doi: 10.1073/pnas.0913139107

Pope III, C.A., Thun, M.J., Namboodiri, M.M., Dockery, D.W., Evans, J.S., Speizer,

F.E., Heath Jr., C.W., 1995. Particulate air pollution as a predictor of mortality in a prospective study of U.S. adults. *American Journal of Respiratory and Critical Care Medicine*, 151, 669-674. doi: 10.1164/ajrccm/151.3_Pt_1.669

Prospero, J.M., Ginoux, P., Torres, O., Nicholson, S.E., Gill, T.E., 2002. Environmental characterization of global sources of atmospheric soil dust identified with the NIMBUS-7 TOMS absorbing aerosol product. *Reviews of Geophysics*, 40, 2-1–2-31. doi:[10.1029/2000RG000095](https://doi.org/10.1029/2000RG000095)

Reheis, M.C., 2003. Dust deposition in Nevada, California and Utah, 1984-2002. U.S. Geological Survey Open-File Report 03-138. http://pubs.usgs.gov/of/2003/ofr-03-138/ofr_03_138_508.pdf

Reheis, M.C., 2006. A 16-year record of eolian dust in Southern Nevada and California, USA: controls on dust generation and accumulation. *Journal of Arid Environments*, 67, 487-520. doi:[10.1016/j.jaridenv.2006.03.006](https://doi.org/10.1016/j.jaridenv.2006.03.006)

Reynolds, R., Belnap, J., Reheis, M., Lamothe, P., Luiszer, F., 2001. Aeolian dust in Colorado Plateau soils: nutrient inputs and recent change in source. *Proceedings of the National Academy of Sciences*, 98, 7123-7127. doi: 10.1073/pnas.121094298

Reynolds, R.L., Reheis, M., Yount, J., Lamothe, P., 2006. Composition of aeolian dust in natural traps on isolated surfaces of the central Mojave Desert—insights to mixing, sources, and nutrient inputs. *Journal of Arid Environments*, 66, 42-61. doi: [10.1016/j.jaridenv.2005.06.031](https://doi.org/10.1016/j.jaridenv.2005.06.031)

Reynolds, R.L., Yount, J.C., Reheis, M., Goldstein, H., Chavez, P., Jr., Fulton, R., Whitney, J., Fuller, C., Forester, R.M., 2007. Dust emission from wet and dry playas in the Mojave Desert, USA. *Earth Surface Processes and Landforms*, 32, 1811-1827. doi: 10.1002/esp.1515

Rivera Rivera, N.I., Gill, T.E., Gebhart, K.A., Hand, J.L., Bleiweiss, M.P., Fitzgerald, R.M., 2009. Wind modeling of Chihuahuan Desert dust outbreaks. *Atmospheric Environment*, 43, 347-354. doi:[10.1016/j.atmosenv.2008.09.069](https://doi.org/10.1016/j.atmosenv.2008.09.069)

Rivera Rivera, N.I., Gill, T.E., Bleiweiss, M.P., Hand, J.L., 2010. Source characteristics of hazardous Chihuahuan Desert dust outbreaks. *Atmospheric Environment*, 44, 2457-2468. doi: 10.1016/j.atmosenv.2010.03.019

Sankey, J.B., Germino, M.J., Glenn, N.F., 2009a. Aeolian sediment transport following wildfire in sagebrush steppe. *Journal of Arid Environments*, 73, 912-919. doi: [10.1016/j.jaridenv.2009.03.016](https://doi.org/10.1016/j.jaridenv.2009.03.016)

Sankey, T.T., Sankey, J.B., Weber, K.T., Montagne, C., 2009b. Geospatial assessment of grazing regime shifts and socio-political changes in a Mongolian rangeland. *Rangeland Ecology and Management*, 52, 522-530. doi: [10.2111/1.REM-D-09-00014.1](https://doi.org/10.2111/1.REM-D-09-00014.1)

- Sankey, J.B., Glenn, N.F., Germino, M.J., Gironella, A.I.N., Thackray, G.D., 2010. Relationships of aeolian erosion and deposition with LiDAR-derived landscape surface roughness following wildfire. *Geomorphology*, 119, 135-145. doi: [10.1016/j.geomorph.2010.03.013](https://doi.org/10.1016/j.geomorph.2010.03.013)
- Sankey, J.B., Eitel, J.U.H., Glenn, N.F., Germino, M.J., Vierling, L.A., 2011. Quantifying relationships of burning, roughness, and potential dust emission with laser altimetry of soil surfaces at submeter scales. *Geomorphology*, 135, 181-190. doi: [10.1016/j.geomorph.2011.08.016](https://doi.org/10.1016/j.geomorph.2011.08.016)
- Sankey, J.B., Germino, M.J., Benner, S.G., Glenn, N.F., Hoover, A.N., 2012a. Transport of biologically important nutrients by wind in an eroding cold desert. *Aeolian Research*, 7, 17-27. doi: [10.1016/j.aeolia.2012.01.003](https://doi.org/10.1016/j.aeolia.2012.01.003)
- Sankey, J.B., Germino, M.J., Glenn, N.F., 2012b. Dust supply varies with sagebrush microsites and time since burning in experimental erosion events. *Journal of Geophysical Research*, 117, G01013. doi: [10.1029/2011JG001724](https://doi.org/10.1029/2011JG001724)
- Sankey, J.B., Germino, M.J., Sankey, T.T., Hoover, A.N., 2012c. Fire effects on the spatial patterning of soil properties in sagebrush steppe, USA: a meta-analysis. *International Journal of Wildland Fire*, 21, 545-556. doi: [10.1071/WF11092](https://doi.org/10.1071/WF11092)
- Sankey, J.B., Ravi, S., Wallace, C.S.A., Webb, R.H., Huxman, T.E., 2012d. Quantifying soil surface change in degraded drylands: shrub encroachment and effects of fire and vegetation removal in a desert grassland. *Journal of Geophysical Research*, 117, G02025. doi: [10.1029/2012JG002002](https://doi.org/10.1029/2012JG002002)
- Sankey, J.B., Wallace, C.S.A., Ravi, S., 2013. Phenology-based, remote sensing of post-burn disturbance windows in rangelands. *Ecological Indicators*, 30, 35-44. doi: [10.1016/j.ecolind.2013.02.004](https://doi.org/10.1016/j.ecolind.2013.02.004)
- Seigel, R.B., van den Heever, S.C., 2012. Dust lofting and ingestion by supercell storms. *Journal of the Atmospheric Sciences*, 69, 1453-1473. doi: [10.1175/JAS-D-11-0222.1](https://doi.org/10.1175/JAS-D-11-0222.1)
- Sevier River Water Users Association (SRWUA), 2012. System Description. <http://www.sevierriver.org/about/system-description/>
- Shafer, J.C., Steenburgh, W.J., 2008. Climatology of strong intermountain cold fronts. *Monthly Weather Review*, 136, 784-807. doi: [10.1175/2007MWR2136.1](https://doi.org/10.1175/2007MWR2136.1)
- Shao, Y., Raupach, M.R., Findlater, P.A., 1993. Effect of saltation bombardment on the entrainment of dust by wind. *Journal of Geophysical Research*, 98, 12,719-12,726. doi: [10.1029/93JD00396](https://doi.org/10.1029/93JD00396)
- Sheppard, P.R., Comrie, A.C., Packin, G.D., Angersbach, K., Hughes, M.K., 2002. The climate of the US Southwest. *Climate Research*, 21, 219-238.

Sing, D., Sing, C.F., 2010. Impact of direct soil exposures from airborne dust and geophagy on human health. *Int. J. Environ. Res. Public Health*, 7, 1205-1223. doi:10.3390/ijerph7031205

Soil Survey Staff, Natural Resources Conservation Service, United States Department of Agriculture. 2012. Soil Survey Geographic (SSURGO) Database for Utah. Available online at <http://soildatamart.nrcs.usda.gov>. Accessed January 2012.

Sweeney, M.R., McDonald, E.V., Etyemezian, V., 2011. Quantifying dust emissions from desert landforms, eastern Mojave Desert, USA. *Geomorphology*, 135, 21-34. doi: 10.1015/j.geomorph.2011.07.022

Sweeney, M.R., McDonald, E.V., Markley, C.E., 2013. Alluvial sediment or playas: what is the dominant source of sand and silt in desert soil Av horizons, southwest USA. *Journal of Geophysical Research*, 118, 257-275. doi: 10.1002/jgrf.20030

Tegen, I., Fung, I., 1995. Contribution to the atmospheric mineral aerosol load from land surface modification. *Journal of Geophysical Research*, 100, 18,707-18,726. doi:10.1029/95JD02051

Tegen, I., Werner, M., Harrison, S.P., Kohfeld, K.E., 2004. Relative importance of climate and land use in determining present and future global soil dust emission. *Geophysical Research Letters*, 31, L05105. doi:10.1029/2003GL019216

Tegen, I., Fung, I., 2012. Modeling of mineral dust in the atmosphere: sources, transport, and optical thickness. *Journal of Geophysical Research: Atmospheres*, 117, 22,897-22,914. doi: 10.1029/94JD01928

Twohy, C.H., Kreidenweis, S.M., Eidhammer, T., Browell, E.V., Heymsfield, A.J., Bansemer, A.R., Anderson, B.E., Chen, G., Ismail, S., DeMott, P.J., Van Den Heever, S.C., 2009. Saharan dust particles nucleate droplets in eastern Atlantic clouds. *Geophysical Research Letters*, 36, L01807. doi:10.1029/2008GL035846

Urban, F.E., Reynolds, R.L., Fulton, R., 2009. *The Dynamic Interaction of Climate, Vegetation, and Dust Emission, Mojave Desert, USA*. Arid Environments and Wind Erosion. Nova Science Publishers. Inc.

Walker, A.L., Liu, M., Miller, S.D., Richardson, K.A., Westphal, D.L., 2009. Development of a dust source database for mesoscale forecasting in southwest Asia. *Journal of Geophysical Research*, 114, D18207. doi:10.1029/2008JD011541

Wang, X., Zhou, Z., Dong, Z., 2006. Control of dust emissions by geomorphic conditions, wind environments and land use in northern China: An examination based on dust storm frequency from 1960 to 2003. *Geomorphology*, 81, 292-308. doi: [10.1016/j.geomorph.2006.04.015](https://doi.org/10.1016/j.geomorph.2006.04.015)

- Wang, X., Xia, D., Wang, T., Xue, X., Li, J., 2008. Dust sources in arid and semiarid China and southern Mongolia: impacts of geomorphological setting and surface materials. *Geomorphology*, 97, 583-600. doi: [10.1016/j.geomorph.2007.09.006](https://doi.org/10.1016/j.geomorph.2007.09.006)
- Wang, H., Niu, T., 2013. Sensitivity studies of aerosol data assimilation and direct radiative feedbacks in modeling dust aerosols. *Atmospheric Environment*, 64, 208-218. doi: [10.1016/j.atmosenv.2012.09.066](https://doi.org/10.1016/j.atmosenv.2012.09.066)
- Warren, A., Chappell, A., Todd, M.C., Bristow, C., Drake, N., Engelstaedter, S., Martins, V., M'baye, S., Washington, R., 2007. Dust-raising in the dustiest place on earth. *Geomorphology*, 92, 25-37. doi: [10.1016/j.geomorph.2007.02.007](https://doi.org/10.1016/j.geomorph.2007.02.007)
- Williams, P.L., Sable, D.L., Mendez, P., Smyth, L.T., 1979. Symptomatic coccidioidomycosis following a severe natural dust storm. an outbreak at the Naval Air Station, Lemoore, Calif. *CHEST*, 76, 566-570. doi:10.1378/chest.76.5.566
- Wise, E.K., 2012. Hydroclimatology of the US Intermountain West. *Progress in Physical Geography*, 36, 458-479. doi: 10.1177/0309133312446538
- Woodhouse, C.A., Meko, D.M., MacDonald, G.M., Stahle, D.W., Cook, E.R., 2010. A 1,200-year perspective of 21st century drought in southwestern North America. *Proceedings of the National Academy of Sciences*, 107, 21,283-21,288. doi: 10.1073/pnas.0911197107
- Yin, D., Nickovic, S., Barbadis, B., Chandy, B., Sprigg, W.A., 2005. Modeling wind-blown desert dust in the southwestern United States for public health warning: a case study. *Atmospheric Environment*, 39, 6243-6254. doi: [10.1016/j.atmosenv.2005.07.009](https://doi.org/10.1016/j.atmosenv.2005.07.009)

CHAPTER 4

CHEMICAL COMPARISON OF DUST AND SOIL FROM THE SEVIER DRY LAKE, UT, USA

4.1 Abstract

This study aimed to characterize differences between dust and soil samples at a dust source in the eastern Great Basin of Utah, U.S.A. Dust and soil samples were collected from the Sevier Dry Lake, a known dust producing playa in this region. Samples were resuspended in the laboratory and collected using an 8-stage Davis Rotating-drum Universal-size-cut Monitoring (DRUM) impactor. Collected samples were analyzed for elemental concentration using Synchrotron X-Ray Fluorescence (SXRF). Element concentration was normalized and analyzed for enrichment relative to major soil element Al. Dust and soil samples contain similar enrichments of major soil elements including Si, Fe, Ca, K, Mg, and Ti. However, dust samples were significantly more enriched in Na derived from the surface salts of the Sevier Dry Lake. Trace elements were generally more enriched in dust samples and had larger enrichment values (up to 10^5) than seen in previous studies. Further, for dust and soil samples, the fine fraction ($<2.5 \mu\text{m}$) was more enriched in trace elements than the coarse fraction (2.5 to $10 \mu\text{m}$). Composition of dust transported locally, regionally, and globally has influences on

human health, ecosystem functioning, and biogeochemical cycling.

4.2. Introduction

Dust composition has distinct implications for nutrient loss in source areas, nutrient inputs in deposition areas, human health, and microphysical activity in clouds (e.g., Reynolds et al., 2007; Malek et al., 2006; Reheis, 2003, 2006). The reservoirs and fluxes of major and trace elements in numerous biogeochemical cycles can have significant alteration with inputs of foreign dust (e.g., Ballantyne et al. 2011). These chemical inputs to sensitive ecosystems can have cascading effects throughout the trophic structure, influencing primary productivity and ecosystem health (e.g., Okin et al., 2004; Jickells et al., 2005). Further, variations in the composition of dust, particularly between hygroscopic and hydrophobic particles can change their microphysical activity in clouds, which has implications for both regional and global climate (e.g., Rosenfeld et al., 2001). Finally, elevated particulate matter levels from dust storms can have acute and chronic health impacts, and these can be exacerbated by the presence of toxic or carcinogenic elements or minerals in the dust stream (e.g., Griffin and Kellogg, 2004). While composition of dust has important implications in many consequences of dust transport, there has been little research into the composition of dust in the eastern Great Basin of Utah, U.S.A.

The eastern Great Basin of Utah has numerous well defined dust sources which emit dust that is subsequently transported downwind to the populated regions of Utah (Fig. 3.1) (Hahnenberger and Nicoll, 2014). One of the major dust sources directly upstream of the Salt Lake City Metropolitan area is the Sevier Dry Lake, located

southwest of Delta, UT, between the Cricket Mountains to the east, and the Black Hills to the west (Fig. 4.1).

Previous dust sampling in the region has included 25 Big Spring Number Eight (BSNE) Wind Aspirated Dust Samplers (Custom Products and Consulting 2010) (Fig. 4.2) in the low elevation region of the Milford Flat fire scar west of Fillmore, UT at an elevation of 4800 feet in the summer of 2008 (Miller et al., 2012). They found a large spatial variation in dust flux; certain “hot spots” have very high dust fluxes, while other nearby sites exhibit elevated, but more modest fluxes. The “hot spots” are locations with both preferable wind patterns (located downstream of mountain gaps, allowing higher winds speeds) as well as ineffective revegetation techniques implemented by the Fillmore Bureau of Land Management (BLM). Some of these revegetation techniques such as drilling, chaining, and use of herbicides, have actually had limited success in vegetation growth and produce more dust than areas that were not treated.

Previous studies have identified the Sevier Dry Lake as one of the main “hot spots” of dust production in the eastern Great Basin (Hahnenberger and Nicoll, 2012; Hahnenberger and Nicoll, 2014). The eastern Great Basin is not a uniform producer of dust; deflation of surface material occurs preferentially from barren playa surfaces and disturbed regions such as the Milford Flat fire scar, described above. While there has been some limited previous work on the composition of brines, salt crust, and sediments, in relation to potential mineral resource extraction, there has been no detailed analysis of dust produced from this region (Gwynn, 2006).

In this study we quantify the geochemistry of dust and soil at the source location of the Sevier Dry Lake. Dust and soil samples were obtained in the field, dried, and

resuspended in the lab. Suspended dust was separated by size in an 8-stage Davis Rotating-drum Universal-size-cut Monitoring (DRUM) impactor and collected on Mylar strips, which were subsequently analyzed with Synchrotron X-Ray Fluorescence (SXRF), to resolve elemental composition. This detailed study of size resolved elemental composition has implications for air quality in the populated regions of Utah, ecosystem ecology in the mountain watersheds of the Wasatch Range, and potential microphysical activity of suspended dust in clouds.

4.3. Methods and materials

4.3.1 Dust and soil sample collection

Dust samples were collected using 8 Big Spring Number Eight (BSNE) Wind Aspirated Dust Samplers (Custom Products and Consulting, 2010) (Fig. 4.2), which are designed to collect airborne particulate material. The BSNE has a vertical opening 2 cm wide and 5 cm high. The top of the sampler has a 60 mesh screen that allows air to exit, while collected material remains in the sampler tray below. The sampler has a tail with a metal fin that acts to direct the sampler into the wind. Samplers are mounted onto round poles (half inch steel EMT pipe), and are allowed to freely rotate into the wind. BSNE are passive samplers and will collect airborne material that is lofted and transported with the wind during periods of sufficient wind speeds. The BSNE has an absolute efficiency of 85 to 95%. However, efficiency is reduced for higher wind speeds and smaller particle sizes (Mendez et al., 2011).

A total of 8 BSNE dust samplers were installed in the vicinity of the Sevier Dry Lake during March 2011 (Table 4.1 and Fig. 4.1) to characterize the dust flux and

composition from that region. Dust samplers were sited on the north, east, and west sides of the Sevier Dry Lake (Fig. 4.1). Attempts were made to site the samplers as close to the edge of the lake as possible. However, due to limited existing roads and restrictions on off road travel, some sites are several miles from the lake surface. One additional site is located to the south of the Sevier Dry Lake to assess possible dust flux from the Wah Wah Valley hardpan. Each site had a collector at 1 and 0.5 m with some sites having an additional collector at 0.15 m. Dust samples, from the BSNE dust samplers, were collected in July 2011 and March 2012 and stored in sterile whirl pak sampling bags.

Additionally, surface soil samples from the Sevier Dry Lake were collected in March 2012 to compare particle composition with dust from the BSNE dust samplers. Soil samples of approximately 0.5 L were collected from the top 1 cm of the soil column using a gardening trowel and stored in sterile whirl pak sampling bags. Comparison of dust and soil samples will provide insight into the type and size of particles that are preferentially lofted from the Sevier Dry Lake. Surface soil samples were collected from the same site locations as the BSNE samplers (Fig. 4.1), and were collected in March 2012.

4.3.2 Laboratory resuspension and chemical analysis

Dust and soil samples were resuspended in the lab using a closed chamber and air puff method, also known as fluidization (Gill et al., 2006). Dust and soil samples were dried using a hot plate and beaker. A mass of each soil or dust sample of 0.2 g (unless only a smaller amount was available from collection) was measured into a glass fixture. The fixture had a top input for blown air and a side output into the resuspension chamber.

A uniform puff of air was allowed to flow into the fixture for 120 s, allowing the suspended sediment to flow into the resuspension chamber. At that time the puff of air was ended, the air intake of the 8-stage rotating Davis Rotating-drum Universal-size-cut Monitoring (DRUM) sampler was turned on for 900 s. The suspended sediment was allowed to move into the PM10 inlet to a DRUM sampler, described below.

Resuspended dust and soil was collected with an 8-stage rotating Davis Rotating-drum Universal-size-cut Monitoring (DRUM) impactor and analyzed with Synchrotron X-Ray Fluorescence (SXRF) (Perry et al., 2004). Particles enter the instrument and are separated into 8 unique size bins (1: 10-5 μm ; 2: 5-2.5 μm ; 3: 2.5-1.1 μm ; 4: 1.1-.75 μm ; 5: .75-.54 μm ; 6: .54-.36 μm ; 7: .36-.24 μm ; 8: .24-<.09 μm), based on their aerodynamic diameter using vertical slots of varying widths. The particles are deposited onto a greased (1% Apiezon Type-L dissolved in toluene) Mylar substrate, which is rotated beneath the slots. This instrument provides size resolved measures of particulate matter, which is later analyzed by removing the substrate and analyzing for elemental composition, in a range from sodium to lead, using SXRF. Element concentrations on the substrate are analyzed and reported in ng cm^{-2} .

Synchrotron X-Ray Fluorescence (SXRF) is an active analysis technique using synchrotron radiation to obtain an x-ray emission spectrum from the substance being analyzed (Jones et al. 1988). The SXRF analysis provides a continuous elemental analysis along the collection strip. To extract element concentrations associated with resuspended dust, peaks in Fe were used. The greased Mylar substrate contains Ca, so this element has a large background concentration that can lead to uncertainty in its analysis. Further, for some trace elements, concentrations are near the detection limit of

the analytical technique and can have large uncertainty to concentration ratios. Finally, for some elements that have strong peaks in the x-ray emission spectrum, such as Fe, may overtake the peaks of nearby elements and lead to incorrectly analyzed concentration values.

4.3.3 Analytical techniques

Initial analyses of the chemical composition of the dust and soil samples indicated that within each group only small differences were seen by sample height for the dust samples and by sample location for the dust and soil samples. Further, when positive matrix factorization analysis was done on the samples it indicated only two sources, namely dust and soil. Therefore, for all following analyses all dust samples were grouped and all soil samples were grouped.

Three size groups were used for analysis and were chosen to be comparable to data from previous studies. First, the “PM₁₀” grouping contains all eight stages from the DRUM impactor and includes all sizes less than 10 µm. This size range is analogous to air quality measurements of PM₁₀. The second group, termed “coarse” material, consists of only the largest two stages from the DRUM impactor and includes sizes greater than 2.5 µm and less than 10 µm. The third group, termed “fine” material, includes the smallest six stages from the DRUM impactor and includes all sizes less than 2.5 µm.

Samples were additionally grouped by “major” and “trace” elements. “Major” elements are those which constitute the majority of the sample and include Si, Al, Fe, Ca, Na, K, Mg, and Ti. These are all elements that typically have large concentrations in soils. The remaining elements which constitute the minority of the sample are termed

“trace” elements for analysis.

Elemental concentrations were normalized relative to elemental concentrations in upper continental crust (UCC) to provide consistency of analysis for comparison with previous research (Wedepohl, 1995; Lawrence and Neff, 2009). The resulting normalized values are termed enrichment factors (EF) as they indicate if the sample being analyzed has relatively high or low concentrations of certain elements relative to an average upper continental crust. Values for element concentrations in upper continental crust are averages taken from many sources, and are reported in relative concentrations (usually reported in ppm). This normalization is usually done relative to one of the major soil elements, such as Al, Si, K, Ti, and Fe. Sensitivity analyses were completed by calculating enrichment factors using each of these five elements. No large differences were seen using each element, so Al was chosen for consistency with previous research. The following equation was used to calculate enrichment factors (EF) for all elements in all samples

$$EF_X = [C_X(\text{sample})/C_{Al}(\text{sample})]/[C_X(\text{UCC})/C_{Al}(\text{UCC})]$$

where EF_X is the enrichment factor for element X, C_X is the concentration of element X in the sample or upper continental crust, and C_{Al} is the concentration of Al in the sample or upper continental crust.

Enrichment factors can help determine if samples are enriched in certain elements, and are useful in comparing samples from different regions or sampling techniques. The technique is limited, however, in that small changes in the concentration of some trace elements can lead to very large changes in the enrichment factor, since the concentrations of these elements in UCC is very small (Wedepohl, 1995).

Statistical comparison of samples was completed using the nonparametric Wilcoxon-Mann-Whitney rank-sum test (Wilks, 2006). This nonparametric statistical test was used because it does not use the assumption that the data conforms to a certain distribution. Tests for sample independence were considered statistically significant if p values were less than 0.05 (5% confidence level).

4.4. Results

For most elements we see greater enrichment factors for dust samples compared to soil (Fig. 4.3). The only exceptions to this are for major elements Si, K, Ca, Mn, and Fe, however, the differences are not statistically significant (Table 4.2). Enrichment factors for dust and soil samples are generally above 1, indicating that the samples contain relatively more of most elements compared to UCC. The highest enrichment factors are for the trace elements in the dust samples.

When comparing the coarse and fine fraction for the dust samples we find that for all elements that showed significant differences, the fine fraction had greater mean enrichment factors than the coarse (Fig. 4.4). Most major elements did not have significant differences in the coarse and fine fraction (Table 4.2). For soil samples, none of the major elements showed significant differences between the coarse and fine fractions. For the trace elements that were significantly different the mean enrichment factor for the fine fraction was greater than the coarse, similar to the dust samples.

For the coarse fraction, Na is the only element that had significant differences in enrichment factor between dust and soil samples (Fig. 4.5a and Table 4.2). The mean enrichment factor of Na in the dust samples was an order of magnitude greater than in

soil samples. Most major elements had enrichment factors near a value of 1 for both dust and soil samples, except for Ca, Mg, and Na (dust only). The fine fraction results are very similar, though the enrichment factors for Si and Ti were also found to be significantly different for dust and soil samples (Fig. 4.5b and Table 4.2). However, the mean values for dust and soil for Si and Ti are very close, compared to Na which had a great difference in mean enrichment factors for dust and soil in both the coarse and fine fraction.

For the trace elements, dust samples were generally more enriched than soil samples in both the coarse and fine fractions (Fig. 4.6a & 4.6b). Most of these differences were significant for the coarse fraction, with almost all being significant for the fine fraction (Table 4.2). Mean values of the enrichment factor for dust and soil samples were similar between the coarse and fine fractions and generally ranged from 1 to 10^4 (Fig. 4.6). This indicates that the trace elements are very enriched in soil and particularly dust samples compared to UCC.

4.5. Discussion

While some work has been done on the brines of the Sevier Dry Lake, and their potential as a mineral resource, there has been very little analysis of the surface sediments and salt crusts of the playa (Gwynn, 2006). Two analyses of the salt crusts at the center and margin of the Sevier Dry Lake were completed in 1880 by Johnson and Russell (Gilbert, 1890). They found that at the surface salt crusts were primarily composed of sodium sulfate (Na_2SO_4), sodium chloride (NaCl), magnesium sulfate (MgSO_4), and sodium carbonate (Na_2CO_3). The abundance of sodium bearing salt at the surface of the

Sevier Dry Lake is consistent with our results of high Na content in dust samples collected in this region.

Mineralogical studies of Sevier Dry Lake sediments have determined that a variety of mineral types are present, including halite (NaCl), gypsum ($\text{CaSO}_4 \cdot 2\text{H}_2\text{O}$), calcite (CaCO_3), aragonite (CaCO_3), glauberite ($\text{Na}_2\text{Ca}(\text{SO}_4)_2$), thenardite (Na_2SO_4), and dolomite ($\text{CaMg}(\text{CO}_3)_2$) (Güven and Kerr, 1966; Hampton, 1978; Gwynn, 2006). Here, again, we see many mineral forms containing Na but few containing Cl, which coincides with our result of enriched values of Na, but not Cl. We also found large increases in S from soil to dust, which is supported by the large number of sulfur containing compounds found in previous mineralogical work.

Only one previous study has completed elemental analysis of surface material from the Sevier Dry Lake (Glanzman, 1977). Concentrations of major soil elements are quite similar to our analysis of soil samples. Concentrations of trace elements are generally lower than in our soil samples, which may be a result of actual differences in concentration, soil sample site selection, or differences in analytical technique as we analyzed only particles of 10 μm and less. However, the analysis by Glanzman (1977) was only semiquantitative and relied on only six samples.

Elemental analysis of dust samples has been completed in many locations throughout the world, however, with widely varying sampling methods and analytical techniques. This makes it challenging to directly compare datasets (Lawrence and Neff, 2009). However, despite these differences, previous elemental analysis of dust samples showed relatively constrained ranges for enrichment factors. In general, our dust samples tend to fall outside many of these ranges. In our analysis of trace elements we found large

enrichment values, one to four orders of magnitude greater than UCC. However, Lawrence and Neff (2009) report the largest enrichment value of 14 for Cr in their review of previous analyses. Therefore, our dust and soil tend to be more highly enriched in trace elements than previous reported dust samples. This can have implications in deposition locations, as dust interacts with a variety of ecosystem types.

Further, in our analysis, fine particles were generally more enriched in trace elements relative to larger sizes. These fine particles have the potential for medium to long range transport as they are less likely to fall out of the air stream (McTainsh et al., 1997; Mori et al., 2003). Therefore, it is these smaller particles that are more likely to deposit and impact air quality further downstream. The increased enrichment of trace elements in these fine particles has potential implications for biogeochemical cycling in deposition ecosystems (Reynolds et al., 2006; Carling et al., 2012; Reynolds et al., 2013) as well as on how air quality may be impacted and its resulting effects on human health (Hahnenberger and Nicoll, 2012; Goudie, 2014).

In a deposition region downstream of the Sevier Dry Lake dust samples were collected from snowpack in the Wasatch mountains (Carling et al., 2012). Enrichment factors for major soil elements are similar to results in this study with the exception of Na. While we found elevated levels of Na in our dust samples, Carling et al. (2012) found Na to be depleted in dust layers compared to the total snowpack. This may result from this deposition area receiving most of its dust from the Milford Flat Burned Area and not from the Sevier Dry Lake during the years sampled (Miller et al. 2012; Hahnenberger and Nicoll, 2014). The solubility of Na and the technique of sampling from a snowpack may also explain the differing results seen in our study and in Carling et al. (2012). For trace

elements our results generally similar or larger enrichment values for most elements.

4.6. Conclusions

Composition of dust transported locally, regionally, and globally has influences on human health, ecosystem functioning, and biogeochemical cycling. This study aimed to characterize differences between dust and soil samples at a dust source in the eastern Great Basin of Utah, U.S.A. The Sevier Dry Lake is a remnant playa from ancient Lake Bonneville, which regularly produces dust during strong southerly wind events preceding spring cyclonic storms.

Dust and soil samples contain similar enrichments of major soil elements including Si, Fe, Ca, K, Mg, and Ti. However, dust samples were significantly more enriched in Na, which is associated with halite crystals which form on the surface of the Sevier Dry Lake. Trace elements were generally more enriched in dust samples and had larger enrichment values (up to 10^5) than seen in previous studies. Further, for both dust and soil samples the fine fraction ($<2.5 \mu\text{m}$) was more enriched in trace elements than the coarse fraction (2.5 to $10 \mu\text{m}$).

The enrichment of dust samples in certain elements has particular importance for both ecosystem functioning and human health. First, the depositions of foreign dust into fragile ecosystems, such as wetland, mountain lakes, and high alpine zones, can have distinct impacts on ecosystem functioning and may alter biogeochemical cycling through numerous trophic levels. Further, high concentrations of elementals known to be detrimental to human health, such as Cr, As, Pb, and Ni, can exacerbate the impacts of high particulate matter levels during dust storm events.

Table 4.1: Site information for dust and soil samples.

Site Number	Site Location	Latitude (deg)	Longitude (deg)
1	N of Sevier Dry Lake	39.140	-112.912
2	N of Sevier Dry Lake	39.150	-112.982
3	East Central shore of Sevier Dry Lake	38.918	-113.077
4	E of Sevier Dry Lake	38.905	-113.054
5	South East shore of Sevier Dry Lake	38.831	-113.138
6	NW of Wah Wah Valley Hardpan	38.679	-113.340
7	Needle Point, W shore of Sevier Dry Lake	38.904	-113.160
8	N of Sevier Dry Lake	39.144	-113.058

Table 4.2: Statistical results (p-values) from the Wilcoxon-Mann-Whitney rank-sum test for dust and soil samples. Results in bold indicate statistically significant result to the 5% confidence level ($p < 0.05$). PM10 indicates particle sizes less than 10 μm . Coarse indicates particle sizes from 2.5 to 10 μm . Fine indicates particle sizes less than 2.5 μm .

Elements	DUST PM10 vs. SOIL PM10	DUST Coarse vs. SOIL Coarse	DUST Fine vs. SOIL Fine	DUST Coarse vs. DUST Fine	SOIL Coarse vs. SOIL Fine
Na	1.44E-10	5.39E-10	8.39E-11	5.02E-01	2.65E-01
Mg	5.68E-02	8.39E-02	5.68E-02	7.27E-01	7.34E-01
Al	1.00E+00	1.00E+00	1.00E+00	1.00E+00	1.00E+00
Si	7.53E-02	1.04E-01	4.48E-02	6.55E-01	5.11E-01
P	1.16E-09	3.26E-09	3.26E-09	4.21E-02	5.76E-03
S	6.95E-07	1.44E-05	4.70E-07	3.00E-01	3.95E-02
Cl	1.46E-06	1.93E-05	1.75E-06	5.76E-01	5.41E-01
K	1.60E-01	1.33E-01	1.84E-01	2.81E-01	4.54E-01
Ca	8.75E-01	2.38E-01	9.52E-01	4.35E-04	1.64E-01
Ti	2.00E-03	7.95E-02	2.57E-05	9.92E-05	1.25E-01
V	1.44E-08	1.89E-05	8.03E-10	5.11E-01	3.46E-01
Cr	1.44E-08	5.61E-08	2.47E-08	4.61E-04	1.80E-04
Mn	9.71E-01	1.84E-01	3.13E-01	1.15E-02	7.69E-01
Fe	5.52E-01	1.68E-01	8.94E-01	4.06E-02	4.01E-01
Ni	1.44E-05	2.52E-06	5.80E-05	2.64E-02	3.40E-05
Cu	1.90E-08	2.55E-07	1.09E-08	4.99E-03	4.91E-03
Zn	1.20E-11	1.20E-11	2.40E-11	4.75E-01	6.46E-04
Ga	2.28E-10	8.39E-11	1.16E-09	8.23E-01	4.14E-04
As	7.32E-02	4.22E-01	2.78E-01	9.83E-01	1.00E+00
Se	5.73E-07	2.29E-05	5.73E-07	2.18E-02	1.56E-04
Br	1.44E-05	2.22E-05	2.57E-05	3.66E-02	4.10E-03
Rb	5.26E-03	9.83E-02	1.51E-03	1.41E-02	4.97E-02
Sr	2.09E-06	2.23E-05	3.49E-06	8.53E-03	1.06E-02
Y	1.44E-08	2.55E-07	6.09E-09	2.55E-04	1.41E-02
Zr	2.06E-07	6.61E-05	1.90E-08	8.15E-05	2.96E-03
Pb	5.05E-02	9.27E-01	6.20E-03	7.96E-04	3.95E-02

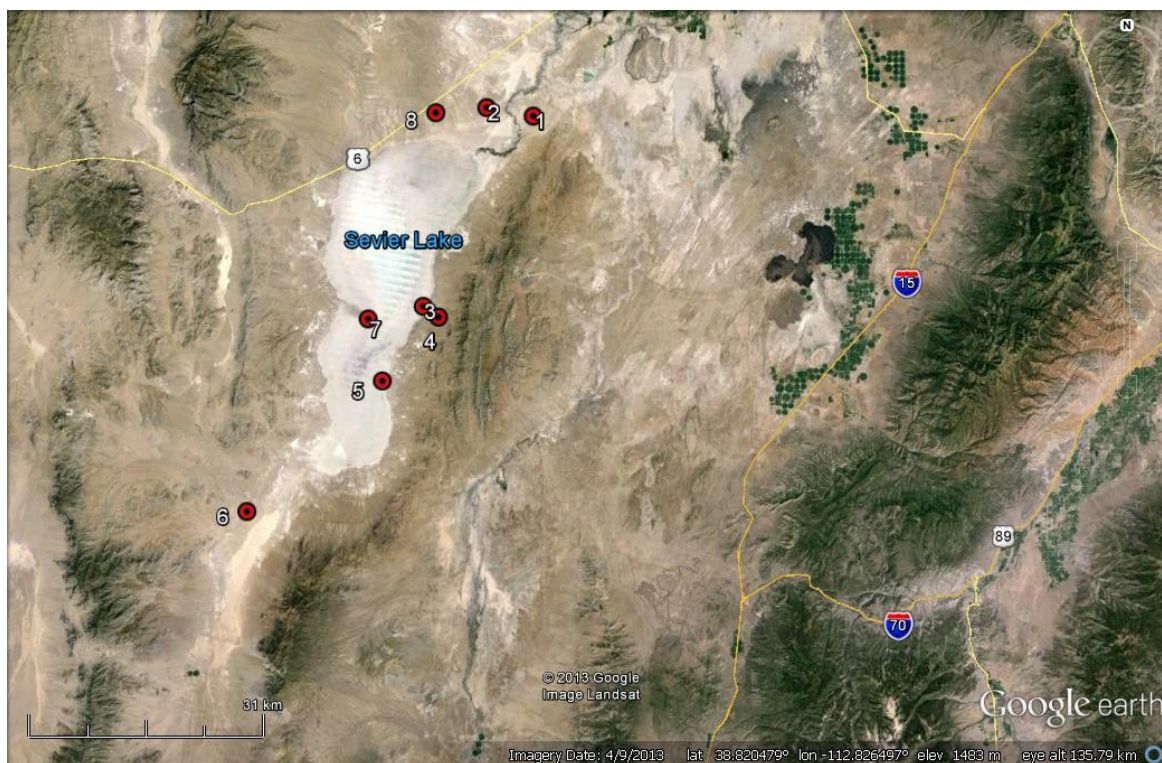


Figure 4.1: Map of the Sevier Dry Lake region with BSNE dust and soil sample sites indicated. See Table 4.1 for descriptions and locations of sample sites.



Figure 4.2: Photo taken from Needle Point (Site Number 7, see Fig. 4.1 and Table 4.1) on the Sevier Dry Lake looking east on 19 March 2011. The BSNE sampler at this location is seen in the foreground as well as the salt crusted surface of the Sevier Dry Lake. A dust plume is seen in the background moving to the north and obscuring the view of the Cricket Mountains.

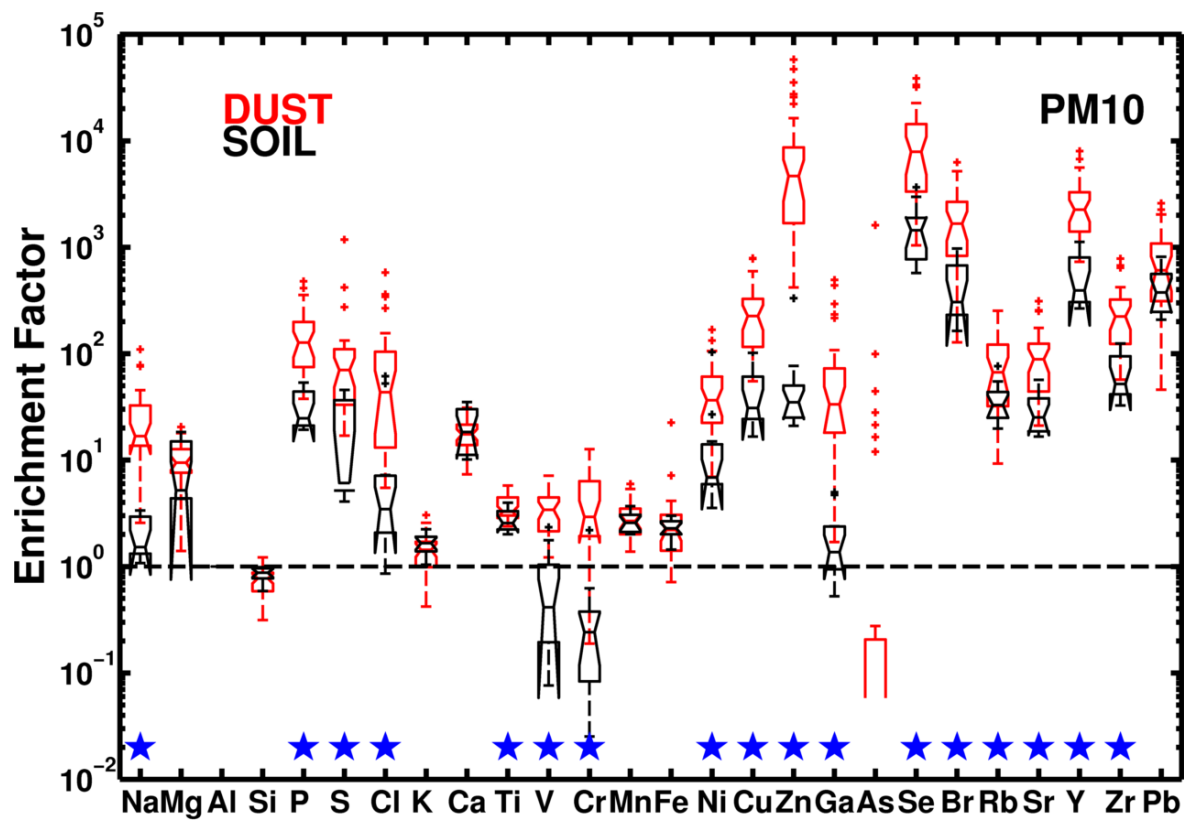


Figure 4.3: Box plot of dust and soil enrichment factor for each element for all sizes less than $10\ \mu\text{m}$ (PM10). Stars indicate where dust and soil distributions were found to be different to a 5% confidence level ($p < 0.05$) (Table 4.2).

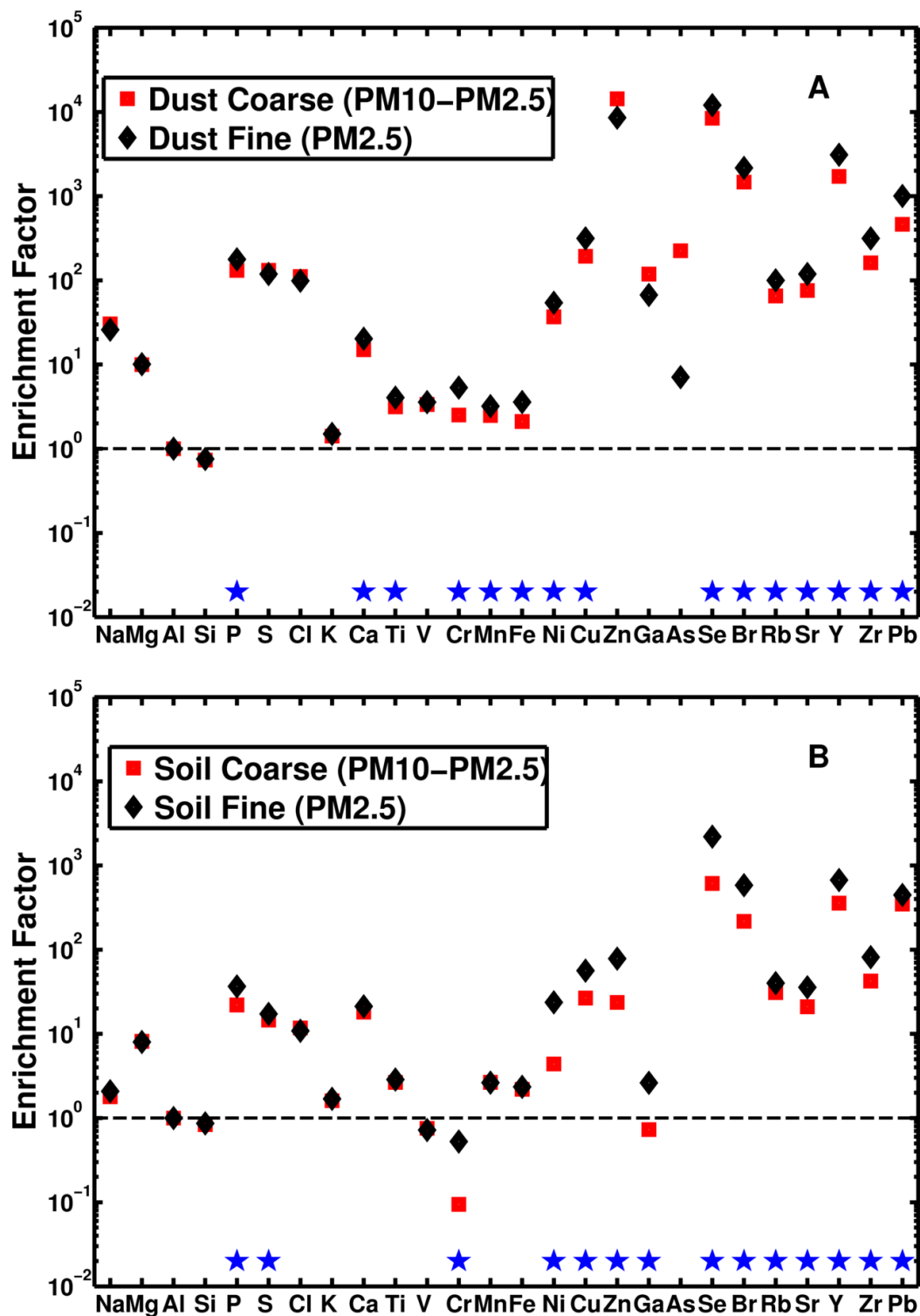


Figure 4.4: Mean values of the enrichment factor for dust (A) and soil (B) for the coarse (2.5 to 10 μm) (squares) and fine (less than 2.5 μm) (diamonds) fractions. Stars indicate where coarse and fine distributions were found to be different to a 5% confidence level ($p < 0.05$) (Table 4.2).

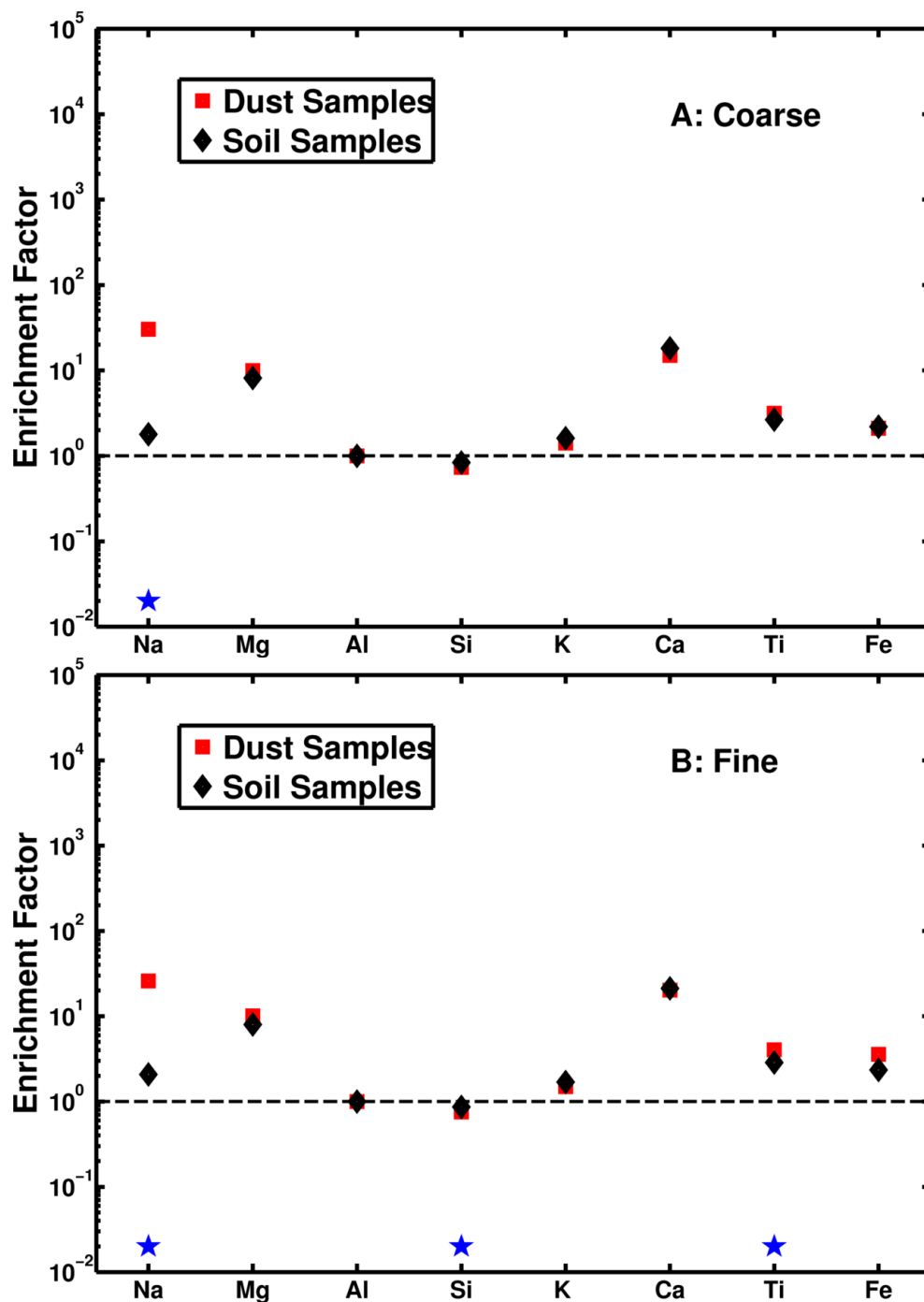


Figure 4.5: Mean values of the enrichment factor for the major elements for coarse (2.5 to 10 μm) (A) and fine (less than 2.5 μm) (B) fractions for dust (squares) and soil (diamonds) samples. Stars indicate where dust and soil distributions were found to be different to a 5% confidence level ($p < 0.05$) (Table 4.2).

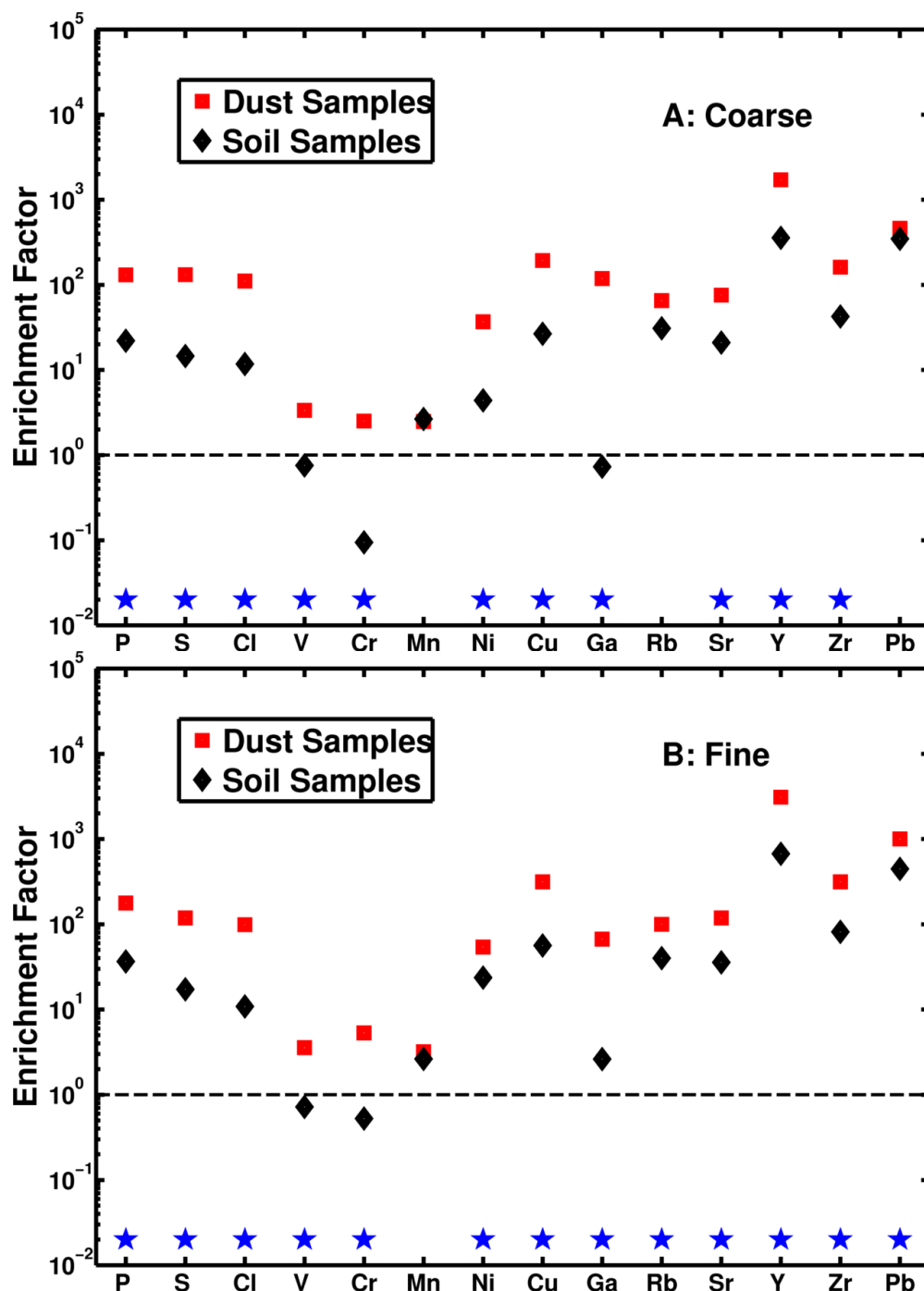


Figure 4.6: Mean values of the enrichment factor for selected trace elements for coarse (2.5 to 10 μm) (A) and fine (less than 2.5 μm) (B) fractions for dust (squares) and soil (diamonds) samples. Stars indicate where dust and soil distributions were found to be different to a 5% confidence level ($p < 0.05$) (Table 4.2).

4.7 References

Ballantyne, A.P., Brahney, J., Fernandez, D., Lawrence, C.L., Saros, J., Neff, J.C., 2011. Biogeochemical response of alpine lakes to a recent increase in dust deposition in the Southwestern, US. *Biogeosciences*, 8, 2689-2706. doi:10.5194/bg-8-2689-2011

Carling, G.T., Fernandez, D.P., Johnson, W.P., 2012. Dust-mediated loading of trace and major elements to Wasatch Mountain snowpack. *Science of the Total Environment*, 432, 65-77. doi: 10.1016/j.scitotenv.2012.05.077

Custom Products and Consulting, cited 2010: BSNE Wind Aspirated Dust Sampler. [Available online at <http://www.fyreardustsamplers.com/bsne.html>.]

Fryear, D.W., 1986. A field dust sampler. *Journal of Soil and Water Conservation*, 41, 117-120.

Gilbert, G.K., 1890. Lake Bonneville. U.S. Geological Survey Monograph, v. 1, 438 p.

Gill, T.E., Zobeck, T.M., Stout, J.E., 2006. Technologies for laboratory generation of dust from geological materials. *Journal of Hazardous Materials*, 132, 1-13. doi: 10.1016/j.hazmat.2005.11.083

Glanzman, R.K., 1977. Geochemical and mineralogical comparison of surficial materials in the Great Salt Lake Desert, Pilot Valley, and Sevier Lake, Utah. In Greer, D.C., editor, *Desertic terminal lakes*. Logan, Utah, Water Research Laboratory, Utah State University, p. 183-196.

Goudie, A.S., 2014. Desert dust and human health disorders. *Environmental International*, 63, 101-113. doi: 10.1016/j.envint.2013.10.011

Grayson, D.K., 1993. *The Desert's Past: A Natural Prehistory of the Great Basin*. Smithsonian Institution Press, Washington, D.C.

Griffin, D.W., Kellogg, C.A., 2004. Dust storms and their impact on ocean and human health: dust in the earth's atmosphere. *EcoHealth*, 1, 284-295. doi: 10.1007/s10393-004-0120-8

Guven, N., Kerr, P.F., 1966. Selected Great Basin playa clays. *The American Mineralogist*, 51, 1056-1067.

Gwynn, J.W., 2006. History and mineral resource characterization of Sevier Lake, Millard County, Utah. Utah Geological Survey, Utah Department of Natural Resources, Miscellaneous Publication 06-6.

Hahnenberger, M., Nicoll, K., 2012. Meteorological characteristics of dust transport events in the Eastern Great Basin of Utah, U.S.A. *Atmospheric Environment*, 60, 601-

612. doi: 10.1016/j.atmosenv.2012.06.029

Hahnenberger, M., Nicoll, K., 2014. Geomorphic and land cover identification of dust sources in the eastern Great Basin of Utah, U.S.A. *Geomorphology*, 204, 657-672. doi: 10.1016/j.geomorph.2013.09.013

Hampton, D.A., 1978. Geochemistry of the saline and carbonate minerals of Sevier Lake playa, Millard County, Utah. Salt Lake City, University of Utah, M.S. Thesis, 75 p.

Jickells, T.D., An, Z.S., Andersen, K.K., Baker, A.R., Bergametti, G., Brooks, N., Cao, J.J., Boyd, P.W., Duce, R.A., Hunter, K.A., Kawahata, H., Kubilay, N., laRoche, J., Liss, P.S., Mahowald, N., Prospero, J.M., Ridgeway, A.J., Tegen, I., Torres, R., 2005. Global iron connections between desert dust, ocean biogeochemistry, and climate. *Science*, 308, 67-71. doi: 10.1126/science.1105959

Jones, K.W., Gordon, B.M., Hanson, A.L., Kwiatek, W.M., Pounds, J.G., 1988. X-ray fluorescence with synchrotron radiation. *Ultramicroscopy*, 24, 313-328. doi: [10.1016/0304-3991\(88\)90318-X](https://doi.org/10.1016/0304-3991(88)90318-X)

Lawrence, C.R., Neff, J.C., 2009. The contemporary physical and chemical flux of aeolian dust: a synthesis of direct measurements of dust deposition. *Chemical Geology*, 267, 46-63. doi: 10.1016/j.chemgeo.2009.02.005

Malek, E., Davis, T., Martin, R.S., Silva, P.J., 2006. Meteorological and environmental aspects of one of the worst national air pollution episodes (January, 2004) in Logan, Cache Valley, Utah, USA. *Atmospheric Research*, 79, 108-122. doi: [10.1016/j.atmosres.2005.05.003](https://doi.org/10.1016/j.atmosres.2005.05.003)

McTainsh, G.H., Nickling, W.G., Lynch, A.W., 1997. Dust deposition and particle size in Mali, West Africa. *CATENA*, 29, 307-322. doi: 10.1016/S0341-8162(96)00075-6

Mendez, M.J., Funk, R., Buschiazzi, D.E., 2011. Field wind erosion measurements with Big Spring Number Eight (BSNE) and Modified Wilson and Cook (MWAC) samplers. *Geomorphology*, 129, 43-48. doi: 10.1016/j.geomorph.2011.01.011

Miller, M.E., Bowker, M.A., Reynolds, R.L., Goldstein, H.L., 2012. Post-fire land treatments and wind erosion – Lessons from the Milford Flat Fire, UT, USA. *Aeolian Research*, 7, 29-44. doi: [10.1016/j.aeolia.2012.04.001](https://doi.org/10.1016/j.aeolia.2012.04.001)

Mori, I., Nishikawa, M., Tanimura, T., Quan, H., 2003. Change in size distribution and chemical composition of kosa (Asian dust) aerosol during long-range transport. *Atmospheric Environment*, 37, 4253-4263. doi: 10.1016/S1352-2310(03)00535-1

Okin, G.S., Mahowald, N., Chadwick, O.A., Artaxo, P., 2004. Impact of desert dust on the biogeochemistry of phosphorus in terrestrial ecosystems. *Global Biogeochemical Cycles*, 18, GB2005. doi: [10.1029/2003GB002145](https://doi.org/10.1029/2003GB002145)

- Perry, K.D., Cliff, S.S., Jimenez-Cruz, M.P., 2004. Evidence for hygroscopic mineral dust particles from the Intercontinental Transport and Chemical Transformation Experiment. *Journal of Geophysical Research*, 109, D23S28. doi: [10.1029/2004JD004979](https://doi.org/10.1029/2004JD004979)
- Reheis, M.C., 2003. Dust deposition in Nevada, California and Utah, 1984-2002. U.S. Geological Survey Open-File Report 03-138. http://pubs.usgs.gov/of/2003/ofr-03-138/ofr_03_138_508.pdf
- Reheis, M.C., 2006. A 16-year record of eolian dust in Southern Nevada and California, USA: controls on dust generation and accumulation. *Journal of Arid Environments*, 67, 487-520. doi:[10.1016/j.jaridenv.2006.03.006](https://doi.org/10.1016/j.jaridenv.2006.03.006)
- Reynolds, R., Neff, J., Reheis, M., Lamothe, P., 2006. Atmospheric dust in modern soil on aeolian sandstone, Colorado Plateau (USA): variation with landscape position and contribution to potential plant nutrients. *Geoderma*, 130, 108-123. doi: [10.1016/j.geoderma.2005.01.012](https://doi.org/10.1016/j.geoderma.2005.01.012)
- Reynolds, R.L., Yount, J.C., Reheis, M.C., Goldstein, H., Chavez Jr., P., Fulton, R., Whitney, J., Fuller, C., Forester, R.M., 2007. Dust emission from wet and dry playas in the Mojave Desert. *Earth Surface Processes and Landforms*, 32, 1811-1827. doi: [10.1002/esp](https://doi.org/10.1002/esp)
- Reynolds, R.L., Goldstein, H.L., Moskowitz, B.M., Bryant, A.C., Skiles, S.M., Kokaly, R.F., Flagg, C.B., Yauk, K., Berquo, T., Breit, G., Ketterer, M., Fernandez, D., Miller, M.E., Painter, T.H., 2013. composition of dust deposited to snow cover in the Wasatch Range (Utah, USA): controls on radiative properties of snow cover and comparison to some dust-source sediments. *Aeolian Research*, In Press. doi: [10.1016/j.aeolia.2013.08.001](https://doi.org/10.1016/j.aeolia.2013.08.001)
- Rosenfeld, D., Rudich, Y., Lahav, R., 2001. Desert dust suppressing precipitation: a possible desertification feedback loop. *Proceedings of the National Academy of Sciences*, 98, 5975-5980. doi: [10.1073/pnas.101122798](https://doi.org/10.1073/pnas.101122798)
- Wilks, D.S., 2006. *Statistical Methods in the Atmospheric Sciences*, Second Edition. Burlington, MA: Academic Press.

CHAPTER 5

CONCLUSIONS

This study is the first detailed analysis of the meteorological, source, and chemical characteristics of dust storm events in the eastern Great Basin. This analysis is unique as it is interdisciplinary and delves into a variety of scientific expertise in order to fully describe this complex process. Dust transport is by its nature an interdisciplinary process whose production, transport, and deposition are interrelated with earth, atmosphere, and life science. It is critical, therefore, to develop research programs that involve researchers across disciplines who are open minded to the variety of implications of their work.

This study is described in the sections, which each characterize part of the dust production and transport process in the eastern Great Basin; the first describes meteorological characteristics and drivers, the second analyzes source areas that produce this dust, and the third provides chemical analysis of dust from this region and puts this in a global and regional context. While each of these studies on its own provide a new and valid insight into dust transport in the eastern Great Basin, together they provide a much more robust and complete description of these processes and how they fit into the global dust production complex.

First, an understanding the meteorological drivers of dust storms in this region is developed. We assess the climatology of dust storm events affecting Salt Lake City, Utah (SLC), and documented the controls on atmospheric dust generation and transport. Since 1930, SLC had 379 dust event days (DEDs), averaging 4.7 per year, with elevated PM₁₀ exceeding NAAQS on 16 days since 1993, or 0.9 per year. Dust storms typically occur in spring months during the afternoon. This pattern is associated with strengthening cyclonic systems, which are the primary producer of these dust storms. The Great Basin Confluence Zone (GBCZ) acts to strengthen these storms just prior to their arrival in the eastern Great Basin, located in western Utah.

Next, source locations producing dust during these high wind events were analyzed. Anthropogenically disturbed areas and barren playa surfaces were identified as the primary dust source types that contribute to dust storms in the region. MODIS satellite imagery provided a high resolution picture over the region about two times each day; on DEDs we analyzed the MODIS data to identify dust plumes, and assessed the characteristics of dust source areas. The largest plumes are generally seen during the spring and fall months and during moderate or greater drought. Most plumes originate from playas, classified as Barren land cover, with a silty clay soil surface. However, playa surfaces, while often considered natural dust sources, often have anthropogenic disturbances in the eastern Great Basin, including military operations and water withdrawal. Disturbance is necessary to produce dust from vegetated landscapes in the region, evidenced by the new dust source active from 2008-2010 in the area burned by the 2007 Milford Flat fire, which spread rapidly due to high winds, dry vegetation, and extensive cover of invasive cheat grass. This area was further disturbed by postfire land

treatments like chaining and drilling that actually exacerbated dust production instead of abating it.

Finally, the elemental composition of dust in the region was characterized. Surface soil and dust samples, using passive BSNE samplers, were collected, resuspended, and analyzed with SXRF. Dust and soil from the eastern Great Basin are distinctly different, and identifiable. Within the dust and soil groups, however, large differences are not seen, meaning that specific sample locations cannot be identified by their element compositions. Dust and soil from the eastern Great Basin tends to not be enriched in most major soil elements, excepting the large enrichment of Na seen only in dust. This high amount of Na in dust is likely a result of sodium containing evaporate minerals forming on the surface of the Sevier Dry Lake and then eroding from the surface. In trace elements, however, very large enrichment values for both dust and soil are observed. The enrichment of dust samples in certain elements has particular importance for both ecosystem functioning and human health.

This work provides an outline for developing improved forecasting and warning of dust storms in this region. Elevated particulate levels have direct impacts on human health, which may be exacerbated by the presence of elevated levels of toxic minerals and elements. While dust storms in the region are generally considered natural phenomena, this work purports that most dust sources have distinct anthropogenic influences that may act to increase dust production from the region.

The first step forward for alleviating human health impacts is to forecast and warn for these dust events. The synoptic systems producing this dust can be forecast days in advance, and nowcasting of storms can be aided with webcams, visibility sensors, and

real time satellite data. The second step for dust storm alleviation is improved land management. The most applicable case is to take both climatological and surface characteristics into account during postfire land treatments. Current methodologies use a “one size fits all” approach that can be catastrophic in certain landscapes, particularly when exacerbated by drought conditions. A more dynamic approach is necessary. Other land management strategies could include limiting military operations on known dust producing areas to alleviate disturbance, revising grazing plans to allow for vegetation maintenance, and possibly allowing more water flow into some anthropogenically dried playa areas.

This holistic and interdisciplinary view of dust transport allows for more comprehensive understanding of dust storms in the eastern Great Basin. This study, therefore, provides operational personnel, decision makers, and land managers with improved guidelines on forecasting, warning, and managing dust storms in this region. With improved understanding of these events we can now limit human exposure to elevated levels of particulate matter and, therefore, improve human health in the populated regions of Utah.

APPENDIX

TABLE OF DUST SOURCE LOCATIONS

Index	Date	Sensor	Number	Latitude (deg)	Longitude (deg)	Location	Land Cover	Soil Texture	Salinity (mmhos/cm)
1	20040510	Aqua	1	39.39366944	-113.4221222	Tule Dry Lake	Barren Land	Silty clay	16
2	20040510	Aqua	2	38.48668889	-113.4384639	Wah Wah Valley	Shrub/Scrub	Gravelly Loam	0.0 to 4.0
3	20040510	Aqua	3	38.50780556	-113.4091639	Wah Wah Valley	Shrub/Scrub	Gravelly sandy loam	2.0 to 4.0
4	20040510	Terra	1	37.83545278	-113.6742639	Beryl/Zane	Shrub/Scrub	Loam	0.0 to 4.0
5	20041016	Terra	1	40.18468889	-113.4155333	Great Salt Lake Desert/Dugway	Barren Land	Silty clay	16
6	20080415	Terra	1	38.81068333	-112.6150722	Milford Flat Burned Area	Grassland/Herbaceous	Very cobbly loam	N/A
7	20080415	Terra	2	38.82871389	-112.6984944	Milford Flat Burned Area	Shrub/Scrub	Very gravelly sandy loam	0.0 to 2.0
8	20080415	Terra	3	38.74794444	-113.2079667	Sevier Dry Lake	Barren Land	Silty clay	16
9	20080419	Terra	1	38.781275	-113.1372028	Sevier Dry Lake	Barren Land	Silty clay	16
10	20080419	Terra	2	38.7758	-113.1694694	Sevier Dry Lake	Barren Land	Silty clay	16
11	20080419	Terra	3	38.80124722	-113.1888	Sevier Dry Lake	Barren Land	Silty clay	16
12	20080419	Terra	4	38.85873889	-113.1803694	Sevier Dry Lake	Barren Land	Silty clay	16
13	20080419	Terra	5	38.82678611	-112.6414722	Milford Flat Burned Area	Shrub/Scrub	Loamy fine sand	0.0 to 2.0
14	20080419	Terra	6	38.801675	-112.6950917	Milford Flat Burned Area	Shrub/Scrub	Very gravelly sandy loam	0.0 to 2.0
15	20080419	Terra	7	38.76719167	-112.7856528	Milford Flat Burned Area	Grassland/Herbaceous	Very gravelly sandy loam	0.0 to 2.0
16	20080419	Terra	8	38.93625278	-112.738825	Milford Flat Burned Area	Shrub/Scrub	Gravelly sandy loam	2.0 to 4.0
17	20080419	Terra	9	39.38899444	-113.4324472	Tule Dry Lake	Barren Land	Silty clay	16
18	20080419	Terra	10	39.41781111	-113.4490722	Tule Dry Lake	Barren Land	Silty clay	16
19	20080419	Terra	11	39.50100556	-113.4615028	Tule Dry Lake	Barren Land	Silty clay	16
20	20080419	Terra	12	39.98640278	-113.3253528	Great Salt Lake Desert/Dugway	Barren Land	Silty clay	16
21	20080419	Terra	13	40.01591111	-113.3448111	Great Salt Lake Desert/Dugway	Barren Land	Silty clay	16
22	20080419	Terra	14	40.03807778	-113.3449417	Great Salt Lake Desert/Dugway	Barren Land	Silty clay	16
23	20080419	Terra	15	40.06756111	-113.3805278	Great Salt Lake Desert/Dugway	Barren Land	Silty clay	16
24	20080419	Terra	16	40.14615833	-113.481	Great Salt Lake Desert/Dugway	Barren Land	Silty clay	16
25	20080419	Terra	17	40.17813611	-113.5070861	Great Salt Lake Desert/Dugway	Barren Land	Silty clay	16
26	20080419	Aqua	1	38.83189722	-112.6463417	Milford Flat Burned Area	Shrub/Scrub	Loamy fine sand	0.0 to 2.0
27	20080419	Aqua	2	38.74984722	-112.7891444	Milford Flat Burned Area	Shrub/Scrub	Loam	2.0 to 4.0
28	20080419	Aqua	3	38.78856111	-113.1337611	Sevier Dry Lake	Barren Land	Silty clay	16
29	20080419	Aqua	4	38.77052222	-113.1752778	Sevier Dry Lake	Barren Land	Silty clay	16
30	20080419	Aqua	5	39.42435	-113.4395444	Tule Dry Lake	Barren Land	Silty clay	16
31	20080419	Aqua	6	39.481325	-113.4537472	Tule Dry Lake	Barren Land	Silty clay	16
32	20080420	Terra	1	40.05326944	-113.4506	Great Salt Lake Desert/Dugway	Barren Land	Silty clay	16
33	20080420	Terra	2	40.07828333	-113.4050028	Great Salt Lake Desert/Dugway	Barren Land	Silty clay	16
34	20080420	Terra	3	39.48924444	-113.4462444	Tule Dry Lake	Barren Land	Silty clay	16
35	20080420	Terra	4	39.44050556	-113.4459583	Tule Dry Lake	Barren Land	Silty clay	16
36	20080420	Terra	5	38.76464444	-113.1562917	Sevier Dry Lake	Barren Land	Silty clay	16
37	20080420	Aqua	1	38.78153056	-113.1603139	Sevier Dry Lake	Barren Land	Silty clay	16
38	20080429	Aqua	1	38.81846944	-112.7881111	Milford Flat Burned Area	Shrub/Scrub	Very gravelly sandy loam	0.0 to 2.0
39	20080429	Aqua	2	38.76718611	-112.7714278	Milford Flat Burned Area	Shrub/Scrub	Very gravelly sandy loam	0.0 to 2.0
40	20080429	Aqua	3	38.79832778	-112.6970917	Milford Flat Burned Area	Shrub/Scrub	Very gravelly sandy loam	0.0 to 2.0
41	20090303	Terra	1	38.79753056	-113.1581139	Sevier Dry Lake	Barren Land	Silty clay	16
42	20090303	Terra	2	38.95943056	-113.1930806	Sevier Dry Lake	Barren Land	Silty clay	16
43	20090303	Terra	3	38.84207222	-112.6738667	Milford Flat Burned Area	Shrub/Scrub	Very gravelly sandy loam	0.0 to 2.0
44	20090303	Terra	4	38.83479722	-112.7570806	Milford Flat Burned Area	Shrub/Scrub	Very gravelly sandy loam	0.0 to 2.0
45	20090303	Terra	5	38.94373611	-112.7370306	Milford Flat Burned Area	Shrub/Scrub	Gravelly sandy loam	2.0 to 4.0
46	20090303	Terra	6	39.15911944	-112.7474889	Pot Playas	Barren Land	Very gravelly sandy loam	0.0 to 2.0
47	20090303	Terra	7	39.189025	-112.7985111	Pot Playas	Barren Land	Very gravelly sandy loam	0.0 to 2.0
48	20090303	Terra	8	39.34196111	-113.4655861	Tule Dry Lake	Barren Land	Silty clay	16

49	20090303	Terra	9	39.38369167	-113.4639278	Tule Dry Lake	Barren Land	Silty clay	16
50	20090303	Terra	10	39.44408056	-113.449925	Tule Dry Lake	Barren Land	Silty clay	16
51	20090303	Terra	11	39.54129722	-113.4575778	Tule Dry Lake	Barren Land	Silty clay	16
52	20090303	Terra	12	39.49738333	-113.4478111	Tule Dry Lake	Barren Land	Silty clay	16
53	20090303	Terra	13	40.01364722	-113.3179167	Great Salt Lake Desert/Dugway	Barren Land	Silty clay	16
54	20090303	Terra	14	40.04360556	-113.3365417	Great Salt Lake Desert/Dugway	Barren Land	Silty clay	16
55	20090303	Terra	15	40.10128056	-113.5889694	Great Salt Lake Desert/Dugway	Barren Land	Silty clay	16
56	20090303	Terra	16	40.22119167	-113.6367972	Great Salt Lake Desert/Dugway	Barren Land	Silty clay	16
57	20090303	Terra	17	40.30676667	-113.6476444	Great Salt Lake Desert/Dugway	Barren Land	Silty clay	16
58	20090303	Terra	18	40.25171389	-113.4068917	Great Salt Lake Desert/Dugway	Barren Land	Silty clay	16
59	20090303	Terra	19	40.30586667	-113.3225694	Great Salt Lake Desert/Dugway	Barren Land	Silty clay	16
60	20090303	Terra	20	40.1569	-113.5366278	Great Salt Lake Desert/Dugway	Barren Land	Silty clay	16
61	20090303	Terra	21	40.17400556	-113.6148056	Great Salt Lake Desert/Dugway	Barren Land	Silty clay	16
62	20090303	Terra	22	39.97218333	-113.2900667	Great Salt Lake Desert/Dugway	Barren Land	Silty clay	16
63	20090303	Terra	23	40.23933056	-113.4827417	Great Salt Lake Desert/Dugway	Barren Land	Silty clay	16
64	20090303	Aqua	1	38.88870556	-112.6340972	Milford Flat Burned Area	Shrub/Scrub	Loamy fine sand	0.0 to 2.0
65	20090303	Aqua	2	38.9198	-112.6494278	Milford Flat Burned Area	Shrub/Scrub	Loamy fine sand	0.0 to 2.0
66	20090303	Aqua	3	38.91576667	-112.6989806	Milford Flat Burned Area	Shrub/Scrub	Loamy fine sand	0.0 to 2.0
67	20090303	Aqua	4	38.98745556	-112.6964167	Milford Flat Burned Area	Shrub/Scrub	Gravelly sandy loam	2.0 to 4.0
68	20090303	Aqua	5	38.867125	-113.1337139	Sevier Dry Lake	Barren Land	Silty clay	16
69	20090303	Aqua	6	39.98478056	-113.3044639	Great Salt Lake Desert/Dugway	Barren Land	Silty clay	16
70	20090303	Aqua	7	40.01594722	-113.3304083	Great Salt Lake Desert/Dugway	Barren Land	Silty clay	16
71	20090303	Aqua	8	40.04455	-113.35645	Great Salt Lake Desert/Dugway	Barren Land	Silty clay	16
72	20090303	Aqua	9	40.12993056	-113.5823278	Great Salt Lake Desert/Dugway	Barren Land	Silty clay	16
73	20090303	Aqua	10	40.16865556	-113.6014972	Great Salt Lake Desert/Dugway	Barren Land	Silty clay	16
74	20090303	Aqua	11	40.19697222	-113.4296778	Great Salt Lake Desert/Dugway	Barren Land	Silty clay	16
75	20090303	Aqua	12	40.21824167	-113.4795611	Great Salt Lake Desert/Dugway	Barren Land	Silty clay	16
76	20090303	Aqua	13	40.18285278	-113.6239583	Great Salt Lake Desert/Dugway	Barren Land	Silty clay	16
77	20090304	Terra	1	38.54304167	-112.9013222	Beaver Bottom	Shrub/Scrub	Coarse sandy loam	0.0 to 2.0
78	20090304	Terra	2	38.8864	-112.6414528	Milford Flat Burned Area	Shrub/Scrub	Loamy fine sand	0.0 to 2.0
79	20090304	Terra	3	38.88759167	-112.6785667	Milford Flat Burned Area	Shrub/Scrub	Loamy fine sand	0.0 to 2.0
80	20090304	Terra	4	38.96433889	-112.7117444	Milford Flat Burned Area	Shrub/Scrub	Gravelly sandy loam	2.0 to 4.0
81	20090304	Terra	5	38.77672778	-113.1417639	Sevier Dry Lake	Barren Land	Silty clay	16
82	20090304	Terra	6	38.78808611	-113.1498528	Sevier Dry Lake	Barren Land	Silty clay	16
83	20090304	Terra	7	38.85471389	-113.1412028	Sevier Dry Lake	Barren Land	Gravelly loam	0.0 to 4.0
84	20090304	Terra	8	38.92715	-113.1810583	Sevier Dry Lake	Barren Land	Silty clay	16
85	20090304	Terra	9	38.96929722	-113.1734444	Sevier Dry Lake	Barren Land	Silty clay	16
86	20090304	Terra	10	39.39521389	-113.4406861	Tule Dry Lake	Barren Land	Silty clay	16
87	20090304	Terra	11	39.45753333	-113.4409361	Tule Dry Lake	Barren Land	Silty clay	16
88	20090304	Terra	12	39.51570556	-113.4529083	Tule Dry Lake	Barren Land	Silty clay	16
89	20090304	Terra	13	39.01813611	-113.16975	Sevier Dry Lake	Barren Land	Silty clay	16
90	20090304	Terra	14	39.98380833	-113.2834722	Great Salt Lake Desert/Dugway	Barren Land	Silty clay	16
91	20090304	Terra	15	40.006925	-113.3144528	Great Salt Lake Desert/Dugway	Barren Land	Silty clay	16
92	20090304	Terra	16	40.02481389	-113.3165694	Great Salt Lake Desert/Dugway	Barren Land	Silty clay	16
93	20090304	Terra	17	40.04991944	-113.3387528	Great Salt Lake Desert/Dugway	Barren Land	Silty clay	16
94	20090304	Terra	18	40.11286944	-113.3593	Great Salt Lake Desert/Dugway	Barren Land	Silty clay	16
95	20090304	Terra	19	40.14909722	-113.3810444	Great Salt Lake Desert/Dugway	Barren Land	Silty clay	16
96	20090304	Terra	20	40.15791944	-113.4652222	Great Salt Lake Desert/Dugway	Barren Land	Silty clay	16
97	20090304	Terra	21	40.12826389	-113.527675	Great Salt Lake Desert/Dugway	Barren Land	Silty clay	16

98	20090304	Terra	22	40.11808611	-113.5659778	Great Salt Lake Desert/Dugway	Barren Land	Silty clay	16
99	20090304	Terra	23	40.112425	-113.6040722	Great Salt Lake Desert/Dugway	Barren Land	Silty clay	16
100	20090304	Terra	24	40.13722222	-113.63355	Great Salt Lake Desert/Dugway	Barren Land	Silty clay	16
101	20090304	Terra	25	40.187625	-113.6139139	Great Salt Lake Desert/Dugway	Barren Land	Silty clay	16
102	20090304	Terra	26	40.21599167	-113.6246222	Great Salt Lake Desert/Dugway	Barren Land	Silty clay	16
103	20090304	Terra	27	40.24579444	-113.6352611	Great Salt Lake Desert/Dugway	Barren Land	Silty clay	16
104	20090304	Terra	28	40.43469722	-113.6518806	Great Salt Lake Desert/Dugway	Barren Land	Silty clay	16
105	20090304	Terra	29	40.45110278	-113.67995	Great Salt Lake Desert/Dugway	Barren Land	Silty clay	16
106	20090304	Terra	30	40.46583611	-113.7283361	Great Salt Lake Desert/Dugway	Barren Land	Silty clay	16
107	20090304	Terra	31	40.52135278	-113.7559972	Great Salt Lake Desert/Dugway	Barren Land	Silty clay	16
108	20090304	Terra	32	40.14160278	-113.4986417	Great Salt Lake Desert/Dugway	Barren Land	Silty clay	16
109	20090304	Terra	33	40.24983889	-113.0437972	Great Salt Lake Desert/Dugway	Barren Land	Silty clay	16
110	20090304	Aqua	1	38.42194444	-112.9791667	Beaver Bottom	Shrub/Scrub	Coarse sandy loam	0.0 to 2.0
111	20090304	Aqua	2	38.945575	-112.726325	Milford Flat Burned Area	Shrub/Scrub	Gravelly sandy loam	2.0 to 4.0
112	20090304	Aqua	3	38.96226111	-112.7548056	Milford Flat Burned Area	Shrub/Scrub	Gravelly sandy loam	2.0 to 4.0
113	20090304	Aqua	4	38.64611111	-113.0537944	Beaver Bottom	Shrub/Scrub	Very gravelly sandy loam	0.0 to 2.0
114	20090304	Aqua	5	38.76243611	-113.1499833	Sevier Dry Lake	Barren Land	Silty clay	16
115	20090304	Aqua	6	38.80678889	-113.1821778	Sevier Dry Lake	Barren Land	Silty clay	16
116	20090304	Aqua	7	38.86539444	-113.1931222	Sevier Dry Lake	Barren Land	Silty clay	16
117	20090304	Aqua	8	40.21228611	-113.3936833	Great Salt Lake Desert/Dugway	Barren Land	Silty clay	16
118	20090304	Aqua	9	40.19675278	-113.4699833	Great Salt Lake Desert/Dugway	Barren Land	Silty clay	16
119	20090304	Aqua	10	40.18416667	-113.6102583	Great Salt Lake Desert/Dugway	Barren Land	Silty clay	16
120	20090321	Aqua	1	40.04143333	-113.3615222	Great Salt Lake Desert/Dugway	Barren Land	Silty clay	16
121	20090321	Aqua	2	40.09068056	-113.3959028	Great Salt Lake Desert/Dugway	Barren Land	Silty clay	16
122	20090321	Aqua	3	40.12585278	-113.4372278	Great Salt Lake Desert/Dugway	Barren Land	Silty clay	16
123	20090321	Aqua	4	40.17856667	-113.485475	Great Salt Lake Desert/Dugway	Barren Land	Silty clay	16
124	20090321	Aqua	5	40.22600556	-113.5130889	Great Salt Lake Desert/Dugway	Barren Land	Silty clay	16
125	20090321	Aqua	6	40.26289444	-113.5660778	Great Salt Lake Desert/Dugway	Barren Land	Silty clay	16
126	20090321	Aqua	7	40.31083611	-113.5949972	Great Salt Lake Desert/Dugway	Barren Land	Silty clay	16
127	20090322	Terra	1	38.64641944	-113.0500528	Beaver Bottom	Shrub/Scrub	Very gravelly sandy loam	0.0 to 2.0
128	20090322	Terra	2	38.80891667	-112.6523917	Milford Flat Burned Area	Grassland/Herbaceous	Very gravelly sandy loam	0.0 to 2.0
129	20090322	Terra	3	38.81510833	-112.6890417	Milford Flat Burned Area	Shrub/Scrub	Very gravelly sandy loam	0.0 to 2.0
130	20090322	Terra	4	38.94171389	-112.7199278	Milford Flat Burned Area	Shrub/Scrub	Gravelly sandy loam	2.0 to 4.0
131	20090806	Aqua	1	38.52399167	-113.3583167	Wah Wah Valley	Shrub/Scrub	Gravelly sandy loam	2.0 to 4.0
132	20090806	Aqua	2	38.848075	-112.7105528	Milford Flat Burned Area	Shrub/Scrub	Very gravelly sandy loam	0.0 to 2.0
133	20090806	Aqua	3	38.83050833	-112.6721417	Milford Flat Burned Area	Shrub/Scrub	Very gravelly sandy loam	0.0 to 2.0
134	20090806	Aqua	4	38.64780556	-113.0385056	Beaver Bottom	Shrub/Scrub	Very gravelly sandy loam	0.0 to 2.0
135	20090806	Aqua	5	38.866875	-112.5446722	Milford Flat Burned Area	Shrub/Scrub	Very cobbly loam	N/A
136	20090806	Aqua	6	38.85925	-112.5856028	Milford Flat Burned Area	Shrub/Scrub	Loamy fine sand	0.0 to 2.0
137	20091004	Terra	1	37.88531667	-113.5757222	Beryl/Zane	Shrub/Scrub	Loam	0.0 to 4.0
138	20091004	Aqua	1	37.88309444	-113.5750917	Beryl/Zane	Shrub/Scrub	Loam	0.0 to 4.0
139	20100330	Terra	1	38.82498056	-112.61995	Milford Flat Burned Area	Shrub/Scrub	Loamy fine sand	0.0 to 2.0
140	20100330	Terra	2	38.82722222	-112.6408361	Milford Flat Burned Area	Shrub/Scrub	Loamy fine sand	0.0 to 2.0
141	20100330	Terra	3	38.84116944	-112.6696056	Milford Flat Burned Area	Shrub/Scrub	Very gravelly sandy loam	0.0 to 2.0
142	20100330	Terra	4	38.84219722	-112.7052889	Milford Flat Burned Area	Shrub/Scrub	Very gravelly sandy loam	0.0 to 2.0
143	20100330	Terra	5	38.95470278	-112.7178583	Milford Flat Burned Area	Shrub/Scrub	Gravelly sandy loam	2.0 to 4.0
144	20100330	Terra	6	38.96808333	-112.7090778	Milford Flat Burned Area	Shrub/Scrub	Gravelly sandy loam	2.0 to 4.0
145	20100330	Terra	7	38.99684722	-112.7297333	Milford Flat Burned Area	Shrub/Scrub	Very gravelly sandy loam	0.0 to 2.0
146	20100330	Terra	8	38.81448056	-112.7674667	Milford Flat Burned Area	Shrub/Scrub	Very gravelly sandy loam	0.0 to 2.0

147	20100330	Aqua	1	38.61793056	-113.0570389	Beaver Bottom	Shrub/Scrub	Gravelly Loam	0.0 to 4.0
148	20100330	Aqua	2	38.79448056	-112.6893944	Milford Flat Burned Area	Shrub/Scrub	Very gravelly sandy loam	0.0 to 2.0
149	20100330	Aqua	3	38.84526111	-112.7022667	Milford Flat Burned Area	Shrub/Scrub	Very gravelly sandy loam	0.0 to 2.0
150	20100330	Aqua	4	38.80837222	-112.7608861	Milford Flat Burned Area	Shrub/Scrub	Very gravelly sandy loam	0.0 to 2.0
151	20100330	Aqua	5	38.95228611	-112.7163972	Milford Flat Burned Area	Shrub/Scrub	Gravelly sandy loam	2.0 to 4.0
152	20100330	Aqua	6	39.48166944	-113.4341889	Tule Dry Lake	Barren Land	Silty clay	16
153	20100330	Aqua	7	39.532725	-113.4670556	Tule Dry Lake	Barren Land	Silty clay	16
154	20100330	Aqua	8	39.02846389	-113.0349583	Sevier Dry Lake	Barren Land	Silty clay	16
155	20100330	Aqua	9	38.57339444	-113.3649944	Wah Wah Valley	Shrub/Scrub	Gravelly sandy loam	2.0 to 4.0
156	20100405	Aqua	1	38.80655833	-112.6854972	Milford Flat Burned Area	Shrub/Scrub	Very gravelly sandy loam	0.0 to 2.0
157	20100405	Aqua	2	38.8374	-112.7074389	Milford Flat Burned Area	Shrub/Scrub	Very gravelly sandy loam	0.0 to 2.0
158	20100405	Aqua	3	38.81879444	-112.7574444	Milford Flat Burned Area	Shrub/Scrub	Very gravelly sandy loam	0.0 to 2.0
159	20100427	Aqua	1	40.43871389	-112.852075	Skull Valley	Grassland/Herbaceous	Fine sandy loam	2.0 to 4.0
160	20100427	Aqua	2	40.57859722	-112.7681306	Skull Valley	Barren Land	Silty clay	16
161	20100528	Terra	1	38.83620556	-112.6779028	Milford Flat Burned Area	Shrub/Scrub	Very gravelly sandy loam	0.0 to 2.0
162	20100528	Terra	2	38.85320556	-112.7049917	Milford Flat Burned Area	Shrub/Scrub	Very gravelly sandy loam	0.0 to 2.0
163	20100528	Terra	3	38.94587778	-112.7252083	Milford Flat Burned Area	Shrub/Scrub	Gravelly sandy loam	2.0 to 4.0
164	20100528	Aqua	1	38.64337222	-113.0459694	Beaver Bottom	Shrub/Scrub	Very gravelly sandy loam	0.0 to 2.0
165	20100528	Aqua	2	38.80500556	-112.6953833	Milford Flat Burned Area	Shrub/Scrub	Very gravelly sandy loam	0.0 to 2.0
166	20100528	Aqua	3	38.8354	-112.6823917	Milford Flat Burned Area	Shrub/Scrub	Very gravelly sandy loam	0.0 to 2.0
167	20100528	Aqua	4	38.85120278	-112.7054333	Milford Flat Burned Area	Shrub/Scrub	Very gravelly sandy loam	0.0 to 2.0
168	20100528	Aqua	5	38.93764167	-112.7299222	Milford Flat Burned Area	Shrub/Scrub	Gravelly sandy loam	2.0 to 4.0